



POLITECNICO

MILANO 1863

Department of Aerospace Science and Technology
Space System Engineering and Operations Course
Academic Year 2023/2024

Preliminary mission and system requirements for the Juno Mission

Group - 27

Gianluca Scudier - PC 10697668

Alessandro Massini - PC 10990413

Luca Frassinella - PC 10795356

Edoardo Mensi Weingrill - PC 10706185

Jonathan Alexandus - PC 11030445

Marvin Ahlborn - PC 11008162

Nomenclature

| | |
|----------|-----------------------------------------------------|
| I_{sp} | Gravimetric Specific Impulse |
| ACS | Attitude Control System |
| ADCS | Attitude Determination and Control System |
| ASC | Advanced Stellar Compass |
| cPCI | compact Peripheral Component Interconnect |
| CPU | Central Processor Unit |
| DNS | Deep Space Network |
| DSM | Deep Space Maneuver |
| DSM | Deep Space Manoeuvre |
| EEPROM | Electrically Erasable Programmable Read-Only Memory |
| EFB | Earth Fly-by |
| EGA | Earth Gravity Assist |
| EPS | Electric Power Subsystem |
| FGM | Flux Gate Magnetometer |
| FPGA | Field Programmable Gate Array |
| GS | Gravity Science |
| HGA | High Gain Antenna |
| JADE | Jovian Auroral Distribution Experiment |
| JEDI | Jupiter Energetic Particle Detector Instrument |
| JIRAM | Jovian Infrared Auroral Mapper |
| JOI | Jupiter Orbit Insertion |
| KIPS | Kilo Instructions per Seconds |
| LGA | Low Gain Antenna |
| MAG | Magnetometer |
| ME | Main Engine |
| MGA | Medium Gain Antenna |
| MLI | Multi-Layer Insulation |

| | |
|------|-----------------------------------------------|
| MR | Mass Ratio |
| MWR | Microwave Radiometer |
| NASA | National Aeronautics and Space Administration |
| OF | Oxidizer Fuel ratio |
| OTM | Orbit Trim Manoeuvre |
| OTM | Orbital Trim Maneuver |
| PDDU | Power Distribution and Drive Unit |
| PMD | Propellant Management Device |
| PPM | Primary Propulsion Unit |
| PRM | Period Reduction Manoeuvre |
| PROM | Programmable Read-Only Memory |
| RCS | Reaction Control System |
| RCT | Reaction Control Thruster |
| REM | Rocket Engine Module |
| RTG | Radioisotope Thermal Generator |
| SEU | Single Event Upset |
| SRAM | Static Random Access Memory |
| TCM | Trajectory Correction Manoeuvre |
| TCS | Thermal Control System |
| TCS | Thermal control system |
| TWR | Thrust to Weight Ratio |
| UVS | Ultraviolet Imaging Spectrograph |

Contents

| | |
|-------------------------------------------------------------------------|-----------|
| 1 Mission Understanding | 1 |
| 1.1 Introduction | 2 |
| 1.2 High-Level Goals | 2 |
| 1.3 Mission Drivers | 2 |
| 1.4 Functional Analysis | 3 |
| 1.5 Mission Phases and ConOps | 3 |
| 1.5.1 Mission Phases | 3 |
| 1.5.2 ConOps | 5 |
| 1.6 Instruments and Payload Correlations | 6 |
| 1.6.1 Scientific Instruments | 6 |
| 1.6.2 Payload Correlations | 7 |
| 1.7 Mission Analysis | 7 |
| 1.7.1 Mission Constraints | 7 |
| 1.7.2 Trajectory Design | 8 |
| 2 Propulsion System | 9 |
| 2.1 Mission Analysis | 10 |
| 2.1.1 Trajectory Overview | 10 |
| 2.1.2 Trajectory Simulation | 11 |
| 2.1.3 Station Keeping | 11 |
| 2.2 Propulsion Subsystem | 12 |
| 2.2.1 Selection of the Primary and Secondary Propulsion Units | 12 |
| 2.2.2 Understanding of the Propulsion System Architecture | 12 |
| 2.2.3 Reverse Sizing | 14 |
| 3 TTMTTC System | 17 |
| 3.1 TTMTTC subsystem overview | 18 |
| 3.1.1 Antennas Configuration and Analysis | 18 |
| 3.1.2 Ground Stations | 19 |
| 3.1.3 TTMTTC subsystem architecture | 20 |
| 3.2 Reverse sizing | 20 |
| 3.2.1 Frequency Band selection | 20 |
| 3.2.2 Antenna selection | 21 |
| 3.2.3 Link Budget | 21 |
| 3.2.4 Results | 22 |
| 3.3 Input Data and Results Table | 23 |
| 4 Attitude Determination and Control System | 24 |
| 4.1 AOCS architecture | 25 |
| 4.1.1 Selection of the Actuators | 25 |
| 4.1.2 Selection of the Attitude Sensors | 26 |
| 4.1.3 Stabilization | 26 |
| 4.2 Control modes | 27 |
| 4.3 Pointing budget | 28 |

| | | |
|----------|-------------------------------------------------------|-----------|
| 4.4 | Reverse sizing | 28 |
| 4.4.1 | Model of the Disturbances | 29 |
| 4.4.2 | Attitude actuator sizing | 29 |
| 4.4.3 | Orbital Control | 29 |
| 4.4.4 | Final comments | 31 |
| 5 | Thermal Control System | 32 |
| 5.1 | TCS Architecture and Design Rationale | 33 |
| 5.1.1 | TCS Main Components | 33 |
| 5.1.2 | Peculiar Solutions | 34 |
| 5.2 | Heat Sources along the mission phases | 35 |
| 5.3 | Reverse sizing | 36 |
| 5.3.1 | Worst cases | 36 |
| 5.3.2 | Sizing MLI | 37 |
| 5.3.3 | Hot Case | 37 |
| 5.3.4 | Cold Case | 38 |
| 5.3.5 | Mass, Power, and Data Budgets | 38 |
| 6 | Electric Power System | 39 |
| 6.1 | EPS Architecture and Design Rationale | 40 |
| 6.1.1 | Primary Source: Solar Arrays | 40 |
| 6.1.2 | Secondary Source: Li-ion Batteries | 41 |
| 6.1.3 | Power Distribution | 41 |
| 6.2 | Power Budget | 41 |
| 6.3 | Reverse Sizing | 43 |
| 6.3.1 | Solar Arrays | 43 |
| 6.3.2 | Batteries | 45 |
| 6.3.3 | Mass, Power, Volume and Data Budgets | 45 |
| 7 | CONF & OBDH System | 46 |
| 7.1 | Configuration | 47 |
| 7.1.1 | Structural Design | 47 |
| 7.1.2 | Launcher Interface and Launch Configuration | 47 |
| 7.1.3 | Subsystems Configuration | 47 |
| 7.1.4 | Payload Configuration | 49 |
| 7.2 | On Board Data Handling Subsystem | 50 |
| 7.2.1 | Architecture and Design Rationale | 50 |
| 7.2.2 | Components | 50 |
| 7.2.3 | Reverse Sizing | 52 |
| .1 | Appendix A: Configuration Figures | i |
| .2 | Appendix B: RAD750 | iv |

Chapter 1

Mission Understanding

Change Log H1

| Paragraph number | Changes made |
|------------------|---------------------------------------------------------------------|
| § 1.3 | pp. 2: changed Driver # 2 |
| § 1.4 | pp. 3: fig. 1.1 revised |
| § 1.5.2 | pp. 5: text added to explain ConOps |
| § 1.5.2 | pp. 5: fig. 1.4 revised adding Antenna activities |
| § 1.5.2 | pp. 6: fig. 1.5 added to explain ConOps of Instruments during Orbit |

1.1 Introduction

Juno is a NASA space mission launched in August 5th, 2011 to explore the biggest planet of the Solar System, Jupiter. Juno's goal is to understand the origin and evolution of Jupiter. Its investigation focuses on four themes, the planet's origin, interior structure, atmospheric composition and dynamics and the polar magnetosphere [14]. The overall mission was initially supposed to end on February 20th, 2018, after the de-orbit phase, but it was extended, in order to collect data about the full Jovian system, through September 2025, or spacecraft's end of life.[23]

In this brief paper, the overview of the initial designed mission (2018) will be presented, including the mission's goals, drivers, phases and functional analysis, as well as the scientific instruments and payload.

1.2 High-Level Goals

The overall goal of the Juno Mission is to perform an in-depth study of Jupiter, which will be useful not only to have a better knowledge of the planet but of the whole Solar System. In this section, the high-level goals of the mission will be briefly presented.[8][44]

Jupiter's Magnetic Field: The main goal of the Juno Mission is to study Jupiter's magnetic field, which is the strongest among any planet in the solar system, dominating the magnetosphere, an extensive region which is almost 150 times wider than the planet.

Studying the magnetosphere – which is directly linked to the planet's interior – the mission will be able to measure how fast Jupiter spins, since the spinning clouds of the planet all rotate at varying speeds and therefore do not provide any reliable information on the planet's spin rate.

It will also be possible to study in great detail the interaction between the magnetosphere and the planet's atmosphere, which produces the so-called auroras.

Jupiter's composition: Another high-level goal of the Juno Mission is to study Jupiter's atmosphere and its composition, as well as the mass distribution.

One of the main tasks of Juno is to scan the atmosphere with a Microwave Radiometer and infrared cameras to measure how much of the atmosphere is composed by water, as well as the temperature, structure and motion of the layers. Particular attention is to be brought to the Great Red Spot on the planet's surface to study if this feature is related to the structure and motion of gas deep in the interior of Jupiter or to shallow patterns of the external layers of the planet.

Another aspect of high interest is studying the planet's internal core and possible presence of ice.

Jupiter's genesis: The Juno Mission also has the high-level goal of better understanding the genesis of the gas giant, which is strictly linked to the genesis of our solar system.

By studying Jupiter's composition, as well as the heavy elements contained in the planet, the goal is to have a better understanding of the planet's formation and also to record information about the composition of the solar system at the time.

1.3 Mission Drivers

The mission drivers are critical requirements that lead either completely or partly the system design process. The mission drivers identified for the Juno Mission are: Surviving to the extreme conditions in Jupiter's environment, Ensuring the electric power needed through Solar Arrays, Communicating with Earth.[44]

Surviving to the extreme conditions in Jupiter's environment: Jupiter's environment is extremely challenging in terms of spacecraft design in several ways. Its intense magnetosphere (it extends out 100 Jupiter's radii on the sun-facing side - Earth's one only for 10 radii to draw a comparison) traps high-energy particles, as ions and electrons, creating intense radiation belts forming a torus around Jupiter. The most critical zone is at the equator.

Since the incoming radiations damage the sensitive electronics and scientific instruments, the design of the structure of the spacecraft has to be carefully engineered, as they need to be shielded. Also Juno's orbit need to be designed taking into account the harsh environment of Jupiter, in order to closely examine the planet while avoiding its potentially destroying radiations.

paragraph Plutonium Shortage, how to provide Electrical Power to the Spcecraft: Until now, missions to Jupiter and beyond (Cassini, Voyager 1 and 2) have relied on spacecrafts with the use of nuclear-powered electrical generators called Radioisotope Thermal Generators (RTGs), as primary power source for the Electric Power Subsystem (EPS); typically the radio-isotope used is Plutonium. Due to the plutonium shortage that United States was and is still facing today, it was mandatory to design an alternative [22].

In addition to this, the great distance that Juno must reach imposed constraints on the solar arrays choice too. For these reasons, the choice and the design of the primary energy source for the EPS, was a main driver for Juno mission affecting the whole S/C, Trajectory and Orbit design.

Communicating with Earth: Another crucial task for the success of the mission is communicating with Earth, both for command uplink and science data and telemetry downlink.

To keep in touch with Juno from ground station, we need to use the 3 radio antennas of NASA's Deep Space Network (DSN) dislocated around the Earth. Because of the massive distance of the spacecraft from Earth during its mission, we are not able to communicate with it in real time. This is due to the fact that a signal sent from Earth would take approximately 45 minutes to reach Jupiter, and another 45 minutes would be required to receive the spacecraft's reply. This is why Juno must be able to carry out tasks automatically, following lists of instructions from Earth, and reporting its current status and the data gathered by its science instruments.[44] So it is convenient to implement a standby condition known as safe mode, useful when some errors arise and there are no communications with Earth. In this situation, the spacecraft will automatically reorient itself in order to point the solar arrays towards the Sun, and waits until the link with Earth is restored and receive new instructions.

In addition, in order to communicate with Earth at such distance, the Juno's Communication System must be equipped with multiple antennas, and especially with an High Gain Antenna (HGA) capable of transmitting data with Earth at a very high rate. Obviously, Earth (in particular one of the three antennas of NASA's DSN) should be in view of the Antenna to be able to establish the link between the spacecraft and the ground station. This clearly affects the Mission Analysis and the ACDS again, as the spacecraft has to point towards the Earth throughout the mission.

1.4 Functional Analysis

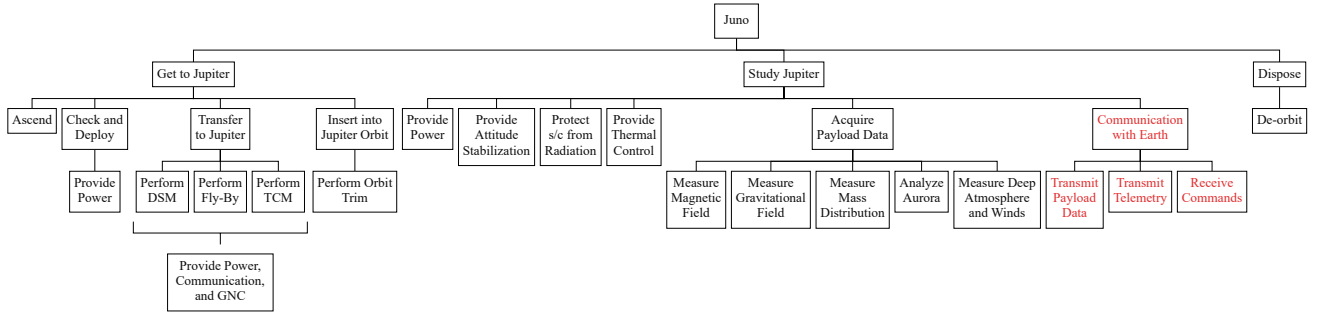


Figure 1.1: Functional Analysis for the Juno mission.

1.5 Mission Phases and ConOps

1.5.1 Mission Phases

The Juno mission was planned to have 6 mission phases divided in 13 mission sub-phases. In this section each of them will be briefly analyzed.[31][60]

Launch

Pre-Launch: This phase had the objective of health check and final testing of the launch base and the Juno vehicle. It went from Launch-minus-(L-) 3 days to the final configuration at L-45 min.

Launch: The launch was performed on August 5th, 2011 through an Atlas V551 rocket at 16:25 UTC. The Atlas V551 had an engine with five solid rocket boosters in the first stage and a Centaur upper stage which also provided the spin to the spacecraft before the separation. The spinning is extremely important in terms of stabilization and pointing. A critical activity during this phase was the deployment of the three solar arrays.

The total duration of the launch phase was of 55 hours at the end of which the spacecraft had been inserted in the heliocentric trajectory.

Cruise

The cruise phase began roughly at L+3 days and continued for five years; in this period of time two deep space manoeuvres (DSMs) and an Earth fly-by (EFB) were performed. Juno's path is subdivided into four different phases: the inner cruise phases, which take place mostly inside Mars orbit, and the outer cruise phase which is the longest phase of the mission.

Inner cruise 1: It went from L+3 days to L+66 days and it was a junction between the launch and cruise phases. The instruments were powered up and checked and the two Waves Antennas were deployed; moreover a first Trajectory Correction Manoeuvre (TCM) was performed.

Inner cruise 2: In this long phase (598 days) Juno performed two DSMs. During this phase the HGA was used to send communications to Earth, the instruments were checked, calibrated and activated for science data acquisition. Before the manoeuvres, the spin rate was increased to 2 RPM.

Inner cruise 3: This phase lasted 161 days and it was characterized by the Earth Gravity Assist (EGA). This phase was exploited to acquire Earth's environment data and to allow mission controllers to practice operating the spacecraft's instruments, preparing them for the upcoming science mission. Following the EFB, the spin rate returned to 1 RPM.

Outer cruise: It began just after the EGA at L+822 days and had a duration of 2.2 years. During this phase the spacecraft approached Jupiter with no special operation other than maintenance and data acquisition.

Jupiter Approach

This phase lasted 178 days of the cruise phase and was characterized by several TCMs in order to prepare for the orbit insertion. The instruments in this phase started to carry out early observation of Jupiter environment and continued the calibration preparing the Juno team for successfully returning Jupiter science data.

Jupiter Orbit Insertion

The Jupiter Orbit Insertion (JOI) phase was the most critical event following the launch, meaning that the coverage from the DSN had to be guaranteed for all its duration. The main goal of the JOI is to place the spacecraft into the designed Jovocentric orbit, fulfilling the scientific requirements. The operation was conducted through a series of different manoeuvres.

Orbit Insertion: This critical manoeuvre occurred on July 5th, 2016 and was performed on the closest Jupiter approach. All the instruments were turned off 4 days before JOI and stayed off for all the phase due to the critical environment in which the manoeuvre happened. Before the JOI burn, it was necessary an attitude change in order to point the HGA away from the Earth. Once the JOI burn was completed, Juno, through its Reaction Control System, re-oriented itself to its nominal attitude.

Capture Orbit: The JOI put the spacecraft in a 53.5 days period capture orbit decreasing substantially the Δv needed for the insertion. During the coasting, all the instruments were turned back on and calibrated in Jupiter environment in order to start the operations as soon as the Science Phase had begun.

Period Reduction Manoeuvre (PRM): The manoeuvre had the task to put the spacecraft in the 14 days (precisely 13 days, 23 hours and 41 minutes) period orbit. It was the last Main Engine (ME) burn of Juno mission. The burn was performed around the perijove and had a duration of 22 minutes, at the end of which the spacecraft was slowed enough to bring down the apojove altitude and reduce the period.

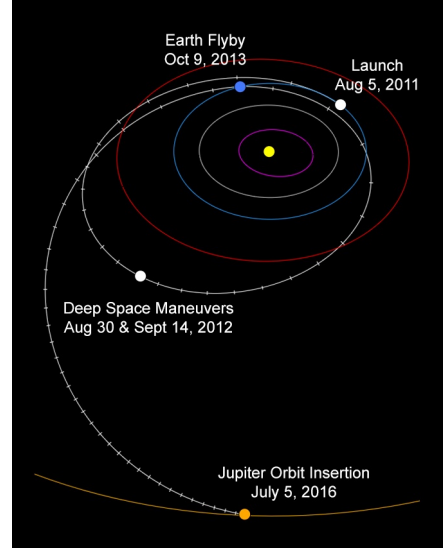


Figure 1.2: Juno's trajectory.¹

¹Credit: NASA/JPL-Caltech

Science Phase

After the PRM the spacecraft was in the Science Phase of the mission; the first orbit (#3) was designed to clean-up the trajectory, while from #4 to #36 Juno performed scientific operations. Juno orbits are highly elliptical, polar orbits. During the passage at the perijove, the measurements would have been performed while the rest of the orbit is mainly used to communicate with DSN, to transmit the data and to perform spacecraft operations. The trajectory is designed to maximize the coverage of Jupiter, in the earliest orbits, while the later ones focused on increasing the resolution of the measurements. After 36 orbits, in which all the science data were acquired the spacecraft enters in the Deorbit phase.

Deorbit phase

The Deorbit of Juno has to be controlled following the NASA's Planetary Protection Guidelines in order to not collide or contaminate the Galilean moons, believed to have liquid water oceans beneath their icy surfaces. The deorbit phase, as originally designed, was supposed to start several days after the 37th orbit using Juno's Reaction Control Thruster (RCT) to slow down the spacecraft until the perijove would have fallen into Jupiter atmosphere. The high density would have caused the disintegration of the vehicle.

1.5.2 ConOps

In Figure 1.4 a schematic view of the mission's ConOps is represented, while a more detailed scheme of the activity of the instruments is showcased in Figure 1.5.

The scheme summarizes a typical activity period in terms of instruments' data rate in the proximity of the Perijove of GRAV orbit 10. As can be seen, the GS instrument uses the entire 6 hour window to acquire science data and observe the internal gravity field of Jupiter. MWR, JIRAM and the JunoCam are all able to view Jupiter during the perijove passage, although MWR is not in the preferred orientation and requires to be turned on about 10 hours before the passage to stabilize thermally. Finally UVS, JEDI, MAG, JADE and Waves take high-rate data during the passage [60].

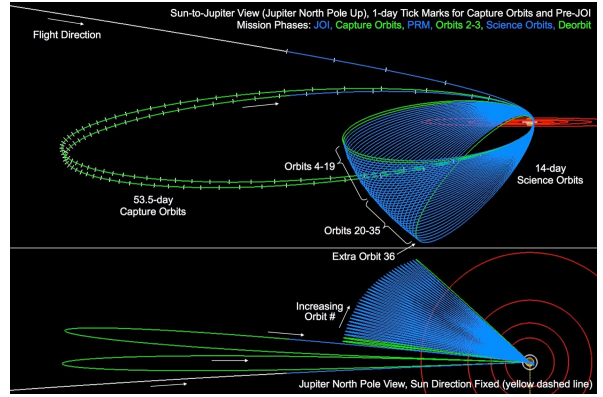


Figure 1.3: Juno's orbits around Jupiter.²

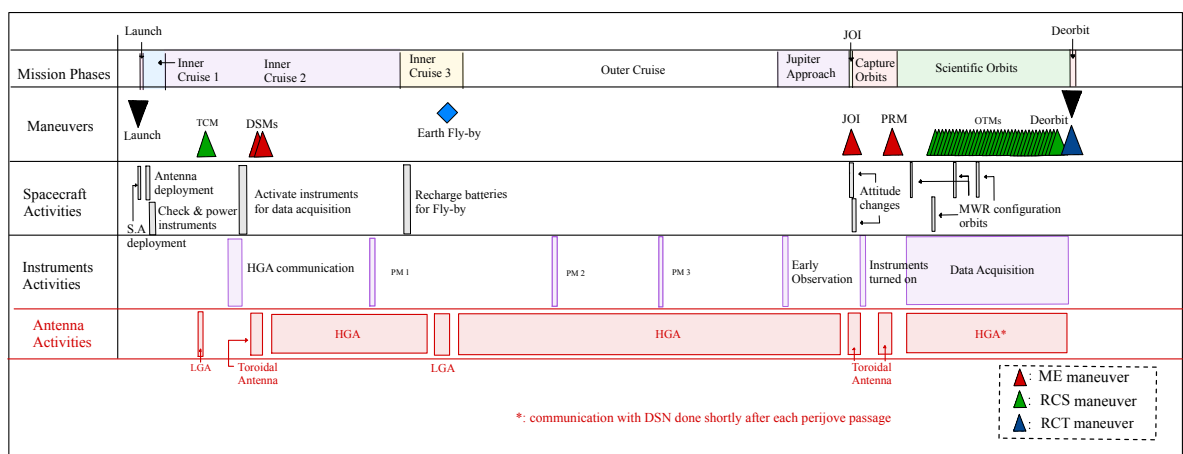


Figure 1.4: Conceptual Operations for Juno Mission

²Credit: NASA/JPL-Caltech

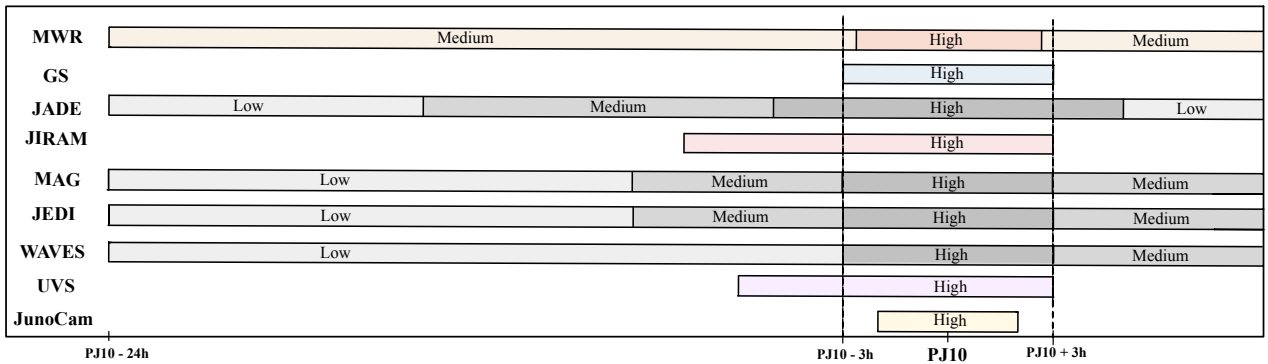


Figure 1.5: Conceptual Operations for Juno Instruments during Perijove Passage of GRAV Orbit 10

1.6 Instruments and Payload Correlations

This section will provide a brief overview of Juno’s main payload – the nine scientific instruments intended to study Jupiter – as well as how they relate to the main mission objectives and phases.[12][14][24]

1.6.1 Scientific Instruments

Microwave Radiometer (MWR): The MWR comprises six radiometers designed for different wavelengths, measuring the radiation emitted at six different depths of Jupiter’s atmosphere. Its clouds radiate microwaves of all kinds of frequencies. The depth from which the microwave radiation can reach space is dependent on its frequency, which allows MWR to observe radiation from different clouds layers.

This instrument allows to measure Jupiter’s deep water content as well as determine how far inward atmospheric features – such as its Great Red Spot – reach.

Jovian Infrared Auroral Mapper (JIRAM): JIRAM consists of a camera and a spectrometer designed to study the atmosphere around Jupiter’s auroras. By analyzing the absorption lines measured by the spectrometer, scientist are able to determine the composition of the observed gas. Furthermore, the infrared camera can be used to study clouds circulation.

JIRAM is supposed to reveal the interaction between Jupiter’s atmosphere and its auroras, while the clouds circulation can provide information about its atmosphere’s water content.

Magnetometer (MAG): It consists of two instruments: The Flux Gate Magnetometer (FGM) and the Advanced Stellar Compass (ASC). FGM measures the strength and orientation of the magnetic field while ASC determines the Magnetometer’s orientation in space. To reduce EM contamination from onboard instruments, there are two sets of MAG instruments, one of which is placed at 10m and the other one at 12m from Juno’s center. Both of them are on a boom at the end of one of Juno’s solar arrays.

This instrument helps to determine the depth, inner structure, and flow of electrically charged material inside Jupiter.

Gravity Science (GS): It measures Jupiter’s gravitational field by determining Juno’s displacement and velocity change close to Jupiter using signal runtime and doppler-shift measurements. X- and Ka-band signals are sent from Earth to Juno where they are immediately returned back to earth. The delay and frequency of the incoming wave at earth allow measuring Juno’s distance and relative velocity.

This instrument plays a crucial role in determining Jupiter’s material composition, dynamics, and internal structure.

Jupiter Energetic Particle Detector Instrument (JEDI): It measures the energy, type and direction of energetic particles consisting of electrons, protons, and heavier ions.

JEDI allows to observe how the particles interact with the magnetic field and how they are redirected – mainly to Jupiter’s poles – to create its auroras.

Jovian Auroral Distribution Experiment (JADE): JADE is responsible for the analysis and identification of the particles emitted by the Jovian aurora, and for the creation of a three-dimensional map of Jupiter’s magnetosphere.

In order to do so it is equipped with three sensors detecting electrons, and one sensor perceiving positive ions, hydrogen, helium and oxygen.

The measurements include the attitude of incoming electrons as well as the composition and velocity-space distribution of ions.

Ultraviolet Imaging Spectrograph (UVS): UVS works in parallel with JEDI and JADE in order to help creating a whole view of the relationship between magnetosphere, auroras and streaming particles.

Through its wavelength range from 70 to 205 nanometers, it is able to take pictures in ultraviolet light of the auroras observing them directly from above, spanning across the North and South Poles.

Waves: Waves measures radio and plasma waves generated in Jupiter's magnetosphere.

The magnetosphere is a region, created by Jupiter's magnetic field, which traps plasma and electrically charged gas. Due to the fact that plasma surrounds the entire planet and conduct electricity, Waves, monitoring one region, is able to record the entire magnetosphere.

Waves instrument is a four meters span, V-shaped antenna whose two tips are responsible for two different wave detection: the first has the task to pick up the electric component of the plasma waves, while the other one receives the magnetic part.

JunoCam: Less directly pertinent to the mission goals is the JunoCam, which mostly facilitates education and public outreach. It is designed to provide high resolution full color images of Jupiter exploiting a so-called "push-broom imager", which take just a thin strip of image when the spacecraft faces Jupiter and then reconstructs the whole picture.

JunoCam is eaten away by the high-energy particles emitted from Jupiter, because of that it has been designed to resist at least for seven orbits.

1.6.2 Payload Correlations

In Table 1.1a is shown the relationship between each High-Goal reported in Section 1.2 and the scientific instruments, while in Table 1.1b are reported the activities that the scientific instruments need to perform during each mission phase.

| Payloads | Goals |
|--------------|-------------------------|
| MWR, JIRAM | Characterize Atmosphere |
| MAG | Map Magnetic Field |
| GS | Map Gravitational Field |
| JEDI, JADE,— | Characterize Polar— |
| UVS, Waves | Magnetosphere |
| JunoCam | Photograph Jupiter |

(a)

| Phase | Payloads |
|-------------------------|----------------------------------------------------|
| Earth Fly-by | Check |
| Jupiter approach | Early observation, calibration |
| Jupiter Insertion Orbit | Switch off |
| Science Phase | Observation (MWR and GS only in respective orbits) |

(b)

Table 1.1: (a) Correlation goal to payloads functions. (b) Correlation phases to payloads.

1.7 Mission Analysis

1.7.1 Mission Constraints

Juno's trajectory has been designed carefully taking into account some critical constraints. The key points considered are:

- to minimize the total Δv needed
- while getting to Jupiter, to avoid solar conjunction during DSMs
- to avoid, as much as possible, the radiation belts of Jupiter
- to guarantee maximum exposition to sunlight, to maximize power availability throughout the mission
- to maximize Jupiter coverage during Science Phase
- to facilitate an enduring connection with the NASA's DSN

1.7.2 Trajectory Design

Launch and Cruise: The launch and the cruise trajectory are critical, during design process, in terms of minimization of Δv . The launch window (from 05/08/2011 to 26/08/2011) was accurately selected in order to maximize the injected mass into Jupiter science orbit and to ensure sufficient contingency days for the DSMs during the entire launch period.[47]

Juno used a Δv -EGA 2+ trajectory, which means two manoeuvres and an Earth Gravity Assist, to reach Jupiter in 59 months. After the launch, the spacecraft was injected in an heliocentric orbit heading for the correct time, selected to avoid the Solar conjunction shadowing the coverage from DSN, to perform the manoeuvres. Two DSMs were planned to take place 13 months after the launch targeting the path back to the Earth; theoretically the burn could have been performed in a single manoeuvre but, since the ME was not certified for a 60-minutes burn, it was cut in two different 30-minute burns. A side benefit of the DSMs was the characterization of the ME and coverage from DSN in preparation for the JOI. [31][47]

The EFB occurred 26 months after the launch; it provided the gravity assist, resulting $\Delta v = 7.3[\frac{km}{s}]$, necessary to reach Jupiter. During the EFB Juno was inside a full eclipse zone that lasted about 20 minutes. The electrical power issue, arising from the shadowing of Solar Arrays, was solved using Juno's lithium-ion batteries that had to be charged in advance. One of the reasons why the Earth was chosen for the fly-by was that during the EFB we could collect data and prepare the instruments for the Science Phase. [47][60]

After the EFB the spacecraft is heading to Jupiter and no other critical manoeuvres, apart for TCMs, were performed in this last phase of the cruise.

Jupiter Orbit Insertion, Capture Orbits and Period Reduction Manoeuvre: JOI was the 2nd critical event of the mission, after the launch. The point of ignition had to be aimed very precisely in order to not result in an unnecessary fuel consumption, reason why several TCMs were performed to fine-tuning the trajectory. Additionally, the constraints highlighted in Section 1.7.1 required a specific design, and a full and redundant coverage from DSN. The manoeuvre was performed through the ME, providing a $\Delta v = 0.542[\frac{km}{s}]$ [31], with a 35-minutes burn. During this sensitive operation, it was required an attitude change in order to point the HGA away from the Earth.

Through the JOI, Juno was injected in the 53.5-days-period capture orbit; this intermediate step between the cruise and the Science Phase was crucial in term of fuel consumption and it allowed to perform the many instruments activities and calibrations. [31]

The last operation, before the begins of the Science Phase, was a PRM, in order to move the spacecraft from the capture orbit to the right one. The manoeuvre, performed through the ME, lasted 22 minutes and cost $0.350[\frac{km}{s}]$ in term of Δv . The modalities on which the PRM happened were similar to the JOI's ones. After the successful outcome of the operation, the spacecraft was in a 13.965-days-period orbit ready to perform two set up orbits (#2 and #3) before the start of the proper Science Phase. [47]

Science Phase: For the Science Phase, one of the main constraint was to avoid the radiation belts forming a torus around the planet. Therefore a highly elliptical, polar orbit of around 90 degrees, characterized by a perijove of 1.06 Jupiter radii and an apojove of 39 Jupiter radii, has been selected in such a way to move from pole to pole in about two hours.

Indeed the orbit had an initial perijove passage at a latitude of 3 degrees on Jupiter, followed by the descending node of its orbit. In the following passages, the argument of perijove is increased about 0.9 degrees each orbit, moving the latitude of perijove further from equator and forcing the apse line to rotate.

The design of the mission aimed to maximize the coverage of Jupiter, therefore after every orbit an Orbit Trim Manoeuvre allowed to change the longitude of the following orbit. A total coverage was reached thanks to 36 orbits with a shift of 90 degrees for each of the first four orbits, of 45 degrees for the following four, of 22.5 degrees for the successive eight and of 11.25 degrees for the remaining ones. As the shifting in the longitude decreased, the resolution of measurements was increased matching the requirements for scientific instruments.

During the science mission Juno performed two types of orbit differing for spacecraft orientation: MWR Orbits and GS Passes. For the MWR passes Juno's spin plane needed to point towards Jupiter's core in order to allow the Radiometers to scan the surface of the Planet from a direct angle. These orbits are #2 (for set up), from #6 to #9 and #14. On the other hand in the GS passes HGA required to be pointed directly to the Earth, so that Ka-band Signals and X-Band Signals can be sent and received. All other instruments can acquire science data during these two different attitude passes.[31]

Chapter 2

Propulsion System

2.1 Mission Analysis

2.1.1 Trajectory Overview

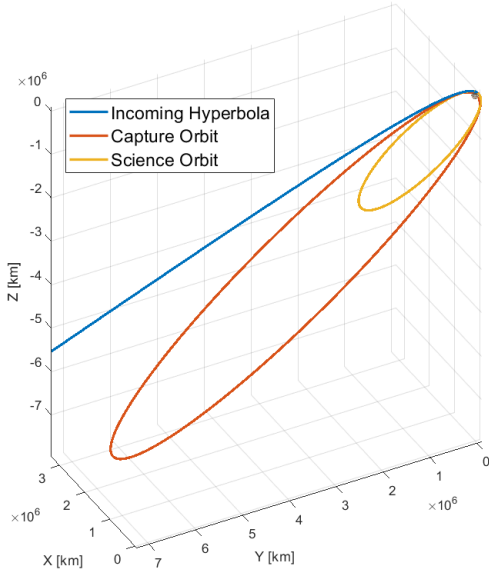
The following section will relate Juno's trajectory to the mission's functionalities and give an overview of the requirements posed to the propulsion system. The detailed Δv budget breakdown is given in Table 2.2. The analysis is structured according to the planned mission phases. [48][26]

Transfer to Jupiter: The transfer to Jupiter begins after launching from Earth into a heliocentric orbit with a period of around 2 years, Juno performs two DSMs at its apoapsis to target an Earth flyby. This flyby at an altitude of only 560 km gives it the necessary velocity to reach Jupiter after a 32 month long cruise. The purpose of this trajectory part is to get Juno to its Jupiter orbit to fulfill the mission objectives. Apart from that, it has to ensure power supply, pointing the solar arrays, and communication. Other than the two high Δv DSMs, this phase of the trajectory consisted only of TCMs in the order of 1 m/s. The transfer phase required a high thrust main engine to perform the DSMs as well as a precise RCS to perform the TCMs with the necessary precision.

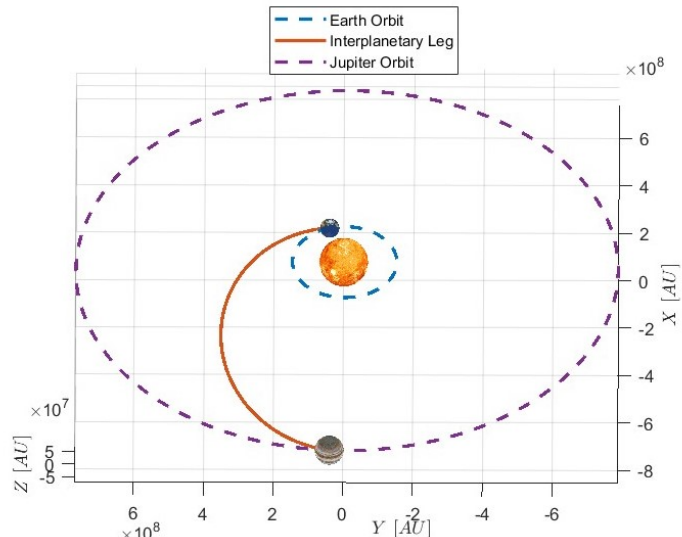
Insertion into Jupiter Orbit: This part of Juno's trajectory consisted of a JOI to get to an initial, highly elliptic Jupiter orbit, followed by a PRM as well as a precise cleanup. Note, that the PRM was not actually executed due to a broken valve. The authors decided to model it nonetheless because it was included in the final sizing of the mission. This phase shares its functionalities with the first phase. Juno's two highest Δv manoeuvres – the JOI and the PRM – are performed in this phase. These burns have to be performed in a short time. Therefore this part of the trajectory requires a high thrust main engine.

Science Orbits: In this phase all the scientific measurements are performed. It comprises 32 science orbits with the two configurations MWR and GS. Every revolution, Juno's orbit slightly shifts to study different areas of Jupiter requiring small manoeuvres. The main functionality of these science orbits is to acquire data from Juno's scientific payloads and making sure to study all parts of Jupiter during the course of the 32 orbits. In addition to also providing power and communication, these science orbits were specifically designed to withstand Jupiter's intense radiation. Their high eccentricity allow staying close to Jupiter only for a brief period and being out of the radiation belts for the rest of the time. From this time in the mission onward, the main engine was not used as all the manoeuvres could be performed with the RCS.

De-orbit: This phase consists of a de-orbit burn with the intention of the disposing of the spacecraft in a safe way after the mission is over and is performed by the RCS thrusters.



(a) Simulated Juno's trajectory around Jupiter



(b) Simulated Juno's 2nd Interplanetary Leg after Earth GA

2.1.2 Trajectory Simulation

In this section, the authors decided to simulate the 2nd interplanetary leg (Figure 2.1b), the JOI and the PRM (Figure 2.1a) using MATLAB, in order to evaluate analytically the Δv required and to compare it with the impressed ones. The reason why these two manoeuvres were specifically chosen is that they are the most expensive maneuvers performed by the ME during the mission.

In order to simplify the calculations, it's been supposed that all the considered manoeuvres are impulsive and performed at the pericentre, additionally plane changes were not considered. Planets' positions were retrieved from the ephemeris.

| Real JOI | Sim JOI | Real PRM | Sim PRM |
|-----------|-----------|-----------|-----------|
| 541.7 m/s | 519.5 m/s | 395.2 m/s | 385.7 m/s |

Table 2.1: Comparison between real and simulated (Sim) Δv

As we can see in Table 2.1, the outcomes are very close. The differences between the results could be credited to the approximations done in order to simplify the computations.

2.1.3 Station Keeping

Since Juno is on a polar orbit, the only effect of Jupiter's oblateness (J_2 effect) is the rotation of the line of absides. This absidal rotation is about -0.95° per orbit, increasing the latitude of the perijove. Nevertheless, this rotation is leveraged during the science phase, hence no Δv is required for rectification.

The presence of Jupiter's satellites, and in particular the massive ones (Callisto, Io, Europa and Ganymede), generate a perturbation on Juno's spacecraft affecting orbit inclination and orbital period (semi-major axis). All the OTMs were planned to counterbalance these variations, in order to maintain the altitude of perijove and the period constant and to guarantee the proper equator-crossing longitude at the descending node of the next orbit for scientific investigation purposes. The variation of the orbit inclination is not controlled, as it is not changing significantly.

| Manoeuvre | Δv w/o Margin | | Δv w/ Margin | | # | Purp. | Δv | # | Purp. | Δv |
|--------------------|-----------------------|--------|----------------------|--------|----|--------|------------|----|-------|------------|
| | Manoeuvre | Margin | Margin | Margin | | | | | | |
| Launch— Correction | 0 | 30 m/s | 30 | | 0 | JOI | 541.7 | 18 | GS | 1.3 |
| DSM-1 | 360.1 | 5 % | 378.1 | | 1 | E. Sc. | 1.5 | 19 | GS | 6.4 |
| DSM-2 | 395.8 | 5 % | 415.6 | | 2 | PRM | 395.2 | 20 | GS | 3.8 |
| Earth— Flyby | 0 | 15 m/s | 15 | | 3 | Cl. Up | 0.0 | 21 | GS | 3.1 |
| Jupiter— Approach | 0 | 10 m/s | 10 | | 4 | MWR | 1.7 | 22 | GS | 2.4 |
| JOI | 541.7 | 5 % | 568.8 | | 5 | GS | 0.0 | 23 | GS | 3.8 |
| Early— Science | 1.5 | 5 % | 1.58 | | 6 | MWR | 2.4 | 24 | GS | 2.7 |
| PRM | 395.2 | 5 % | 415.0 | | 7 | MWR | 1.0 | 25 | GS | 2.5 |
| 32 Science— Orbits | 74.0 | 5 % | 77.7 | | 8 | GS | 7.9 | 26 | GS | 3.7 |
| De-orbit | 77.0 | 5 % | 80.9 | | 9 | MWR | 2.9 | 27 | GS | 0.5 |
| Total Δv | 1845.3 | — | 1992.7 | | 10 | GS | 1.8 | 28 | GS | 2.9 |
| | | | | | 11 | GS | 2.0 | 29 | GS | 0.4 |
| | | | | | 12 | GS | 3.8 | 30 | GS | 0.1 |
| | | | | | 13 | GS | 1.4 | 31 | GS | 1.8 |
| | | | | | 14 | MWR | 0.0 | 32 | GS | 2.0 |
| | | | | | 15 | GS | 4.2 | 33 | GS | 2.0 |
| | | | | | 16 | GS | 4.3 | 34 | GS | 0.4 |
| | | | | | 17 | GS | 0.1 | 35 | GS | 0.7 |

(a)

(b)

Table 2.2: **Detailed Δv budget breakdown** [48][26] including margins according to [3]. All Δv is deterministic in m/s. (a) Trajectory breakdown including margins. (b) Detailed breakdown of the Jupiter orbits. “Purp.”: Orbit's purpose; “E. Sc.”: Early Science; “Cl. Up”: Clean Up.

2.2 Propulsion Subsystem

Juno's Propulsion Subsystem is a dual-mode system, comprehending a LEROS 1b bi-propellant ME and 12 monopropellant RCS thruster. The ME uses hydrazine (N_2H_4) as fuel and nitrogen tetroxide (N_2O_4) as oxidizer and provides the correct thrust for the main manoeuvres. The RCS thrusters use hydrazine as fuel and they are employed not only for minor adjustments or trajectory maintenance but also for rotational adjustments and orientation control in space. In particular Juno carries six spherical propellant tanks, four holding the fuel and two holding the oxidizer. These tanks are pressurized through two tanks of liquid helium used as pressurant.

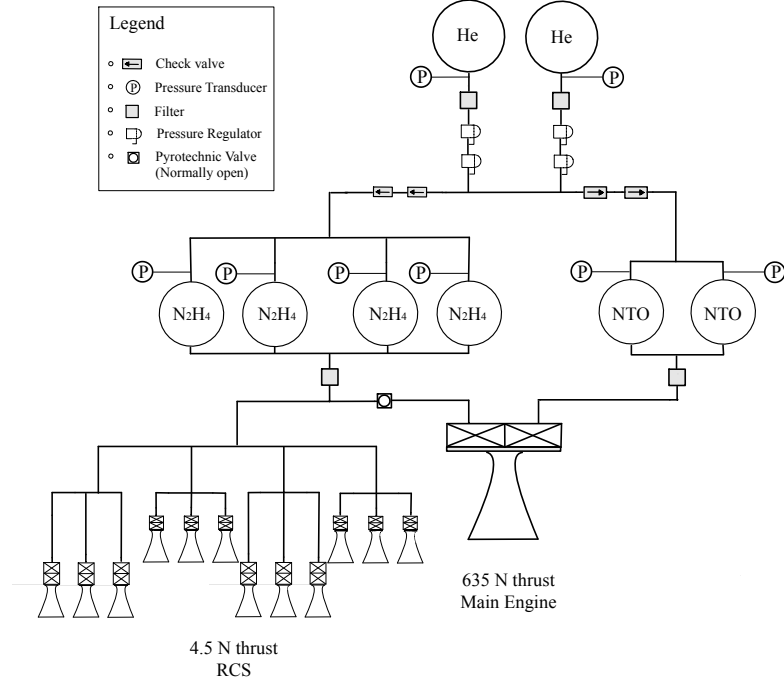


Figure 2.2: Juno's Propulsion System Architecture. Since the real scheme is not public, the authors implemented a simplified architecture based on the informations available.

2.2.1 Selection of the Primary and Secondary Propulsion Units

The primary propulsion unit is devoted to produce very large and Δv -for demanding manoeuvres, in particular all the orbital manoeuvres required to acquire the final orbit of the mission. Depending on the Δv required, in most of the missions the choice is between chemical or electrical propulsion. The first one guarantee high values of TWR ($10^{-2} - 100$ kN/Kg) but low specific impulse I_{sp} (200 - 410 sec), while electric propulsion instead means low TWR ($10^{-4} - 10^{-6}$) and high I_{sp} (1000 - 5000 sec). Both solutions present drawbacks, in particular electric propulsion needs a considered amount of power to work (around 1000 W). Juno's spacecraft, through its solar arrays, can't afford all that power for the propulsion Unit, due to the distance from the Sun of the operative orbit. Hence, the only alternative is to use chemical propulsion as PPM.

The same rationale can be applied in the choice of the secondary propulsion unit, whose main tasks are to perform station keeping, orbit adjustments and attitude control. Also in this case the issue of limited power budget emerges. Therefore, the adoption of chemical Propulsion is the sole viable alternative.

2.2.2 Understanding of the Propulsion System Architecture

The selection of a particular feed system and its components is governed primarily by the rocket applications, mission and by the general requirements of simplicity and minimum inert mass.[61]

For Juno mission a pressurized feed system has been chosen, since not only the total impulse and the propellant mass, but also the chamber pressure and the engine TWR required by the mission were relatively low. Because

of the significant increase in mass and complexity involved in the alternative, a turbo-pump feed system would have not been advantageous.

The propulsive system architecture consists of a biprop. system for the ME and a monopropellant system for the RCS. Since the ME need to perform the most Δv -demanding manoeuvres, a biprop. system is a suitable choice that guarantees high I_{sp} , even if its heavier than a monoprop system.

Monoprop. thrusters are used for the secondary propulsion Unit, as they are throttleable and they can perform pulsing operation, which are essential for attitude control.

Once defined the main architecture, in the next paragraphs we will analyze the single components of the subsystem.

Propellant: The Juno spacecraft uses a bipropellant mix of hydrazine and nitrogen tetroxide as fuel and oxidizer. The mixture is hypergolic, thus facilitating repeated ignition, which is simpler and more reliable as it eliminates the need for igniters. This propulsion couple also has a relatively low molecular weight and high flame temperature, contributing to increase the I_{sp} [9]. Furthermore, hydrazine is the most commonly used fuel in auxiliary control rockets. Therefore a lot of experience, data, and flight-proven parts are available. For the RCS it is decomposed using a catalyst, entailing modest complexity but higher performance than cold gas thrusters. The use of hydrazine for fuel allows a simpler fuel architecture, without the need to separate RCS and ME propellant tanks. Additionally, both hydrazine (N_2H_2) and nitrogen tetroxide [20] (N_2O_4) remain stable at room temperature, reducing the demand on TCS. They also possess long-term chemical stability and shock resistance, crucial for mitigating risks during launch and extended mission durations. Nitrogen tetroxide has the additional advantage of having a high density with 1.44 g/cm^3 .

Tanks: Juno features six main tanks: two for oxidizer and four for fuel. Due to nitrogen tetroxide's higher density compared to hydrazine and an oxidizer to fuel ratio of 0.8-0.9, there are twice as many fuel tanks. Consequently, the volume of fuel needed for propulsion is slightly less than double that of oxidizer. The excess of the volume is taken up by RCS fuel, as RCS does not need an oxidizer. They are spherical, because this shape fits well with the configuration and has the property of being geometrically strong, resulting in lower required wall thickness and therefore lower inert mass. The tanks' rotational symmetry aligns the center of gravity with Juno's axis of rotation, enhancing its stability. The tanks' mass increases Juno's moment of inertia, further stabilizing its rotation.

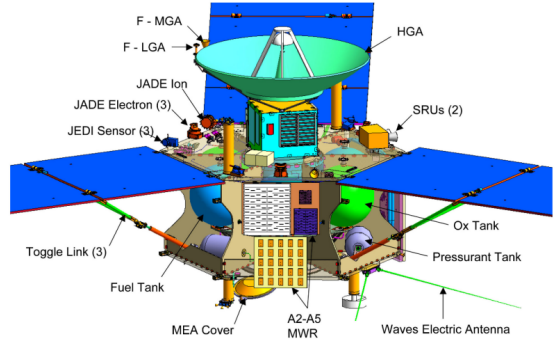


Figure 2.3: Tanks position.¹

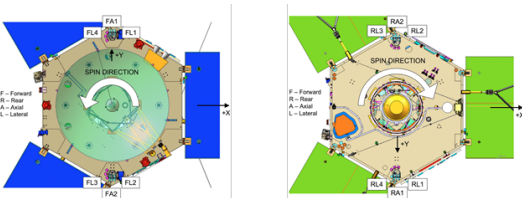


Figure 2.4: Forward and Aft view respectively of Juno Spacecraft.²

it is possible that the spacecraft is using the spinning of the craft as a PMD. This is further supported by the fact that the spacecraft spins up for ME maneuvers to 5 RPM from the usual 1 and 2 RPM during cruise and science phase respectively [32]. 5 RPM is close to the 6 RPM usually used to exploit centrifugal forces in spacecraft tanks [35].

²Credit: NASA JPL, *Maneuver Design for the Juno Mission: Inner Cruise*

Thrusters: Juno is equipped with only one main engine, a design choice that reduces both complexity and required space on the deck. Moreover, the utilization of a single engine simplifies the axial alignment of thrust, as ensuring the precise equality of thrust among multiple engines would have been necessary to prevent the generation of angular momentum and subsequent procession, imposing additional demands on the ACS. The ME was placed on the aft deck (Figure 2.4) along the spacecraft's z-axis, which is also the axis of rotation. This design allows a simpler control scheme, as the rotational symmetry makes the thrust direction independent from the rotation of Juno.

Additionally, Juno has 12 RCS thrusters, which are configured as 4 REMs on towers with 3 thrusters each. As the configuration of the spacecraft was largely dictated by its scientific instruments and power requirements, the thrusters as well as the control strategy had to be adapted accordingly. The 12 thrusters allow for translation and rotation about all three axes with balanced thrust coupling. A lower number of thrusters would have made the control strategy more complicated, while a larger number of thrusters would have led to a higher mass. The towers are placed along the y-axis with two pointing in the s/c's forward and two in the aft direction (Figure 2.4). This configuration was selected due to the relatively flattened core structure of Juno along the z-direction compared to its width in the x- and y-directions. The placement of the towers serves to augment the angular momentum that can be applied in the x- and y-directions as defined in Figure 2.5. Additionally, the thrusters could be placed further from the scientific instruments and the solar arrays, reducing possible disturbances due to

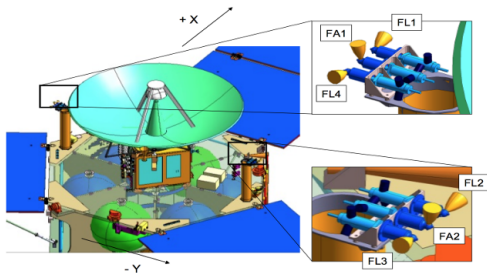


Figure 2.5: The location and orientation of the RCS-thruster clusters.²

like the placement on towers – help protect the instruments and solar arrays from thrust plumes.

exhaust plumes. On each of tower, three thrusters are mounted with two of them pointing lateral (positive and negative x-direction) as well as one pointing axially outward. The placement of twice as many thrusters pointing in the lateral direction is particularly significant as it enhances Juno's ability to control its spin rate effectively. This prioritization of thrusters in the lateral direction is logical, considering that the regular spin-up, spin-down, and control of the rotation period are crucial aspects of the mission. Furthermore, with this configuration no thrust can be generated in the y-direction. However, this is compensated by Juno's rotation, as the thrusters will eventually point into every direction along Juno's x-y-plane during one rotation period. The thrusters have cant angles, of 10° outward for the axial ones and 5° outward as well as 12.5° upward for the lateral ones. This –

2.2.3 Reverse Sizing

In this section the process of reverse sizing for the propellant and pressurizing gas tanks is presented.

The Juno spacecraft, as showcased in the previous sections, uses a dual-mode propulsion subsystem with a bi-propellant main engine (Leros 1-b) and mono-propellant reaction control system thrusters (MR-111C).

The following tables contain all the data that are used in order to do the calculations:

| (a) Spacecraft Properties | | | (b) Fuel, Oxidizer and Pressurizer Properties | | | |
|---------------------------|------------------|---------------|-----------------------------------------------|------------------------|-------------------------|---------------|
| Dry Mass | Fuel Mass | Oxidizer Mass | ρ_{Fuel} | ρ_{ox} | R_{He} | γ_{He} |
| 1593 kg | 1280 kg | 752 kg | 1008 kg/m ³ | 1447 kg/m ³ | 2077.3 J/(kg K) | 1.67 |
| I_{sp} | Δv_{tot} | P_c | $OF_{nominal}$ | OF_{real} | Total Power Consumption | |
| 317 s | 1.9619 km/s | 8.62 bar | 1.4355 | 0.8 | 84.63 W | |

Table 2.4: Leros 1-b Engine Properties

| Quantity | I_{sp} | Δv_{tot} | Mass | Total Power Consumption |
|----------|----------|------------------|---------|-------------------------|
| 12 | 229 s | 0.2367 km/s | 0.33 kg | 13.64 W |

Table 2.5: MR-111C Properties

For the sizing of the tanks, the material of the tanks of pressurizer is assumed to be titanium, while for the tanks of fuel and oxidizer calculations are carried out both for aluminium and titanium.

| Material | ρ | σ |
|--------------------|------------------------|----------|
| Titanium (Ti6Al4V) | 4430 kg/m ³ | 950 MPa |
| Aluminium (Al7075) | 2810 kg/m ³ | 503 MPa |

Table 2.6: Tank Material Properties

The masses of Fuel and Oxidizer reported in Table 2.3a are certain data [30] that will be used for the comparison of the results of the reverse sizing process.

Sizing Process

With all the data presented in the previous paragraph, it is possible to obtain the masses of fuel and oxidizer starting from the Tsiolkovsky equation:

$$\Delta v = I_{sp} g_0 \ln \left(\frac{m_0}{m_f} \right) \quad (2.1)$$

From this equation it is possible to compute the mass ratio:

$$MR = \frac{m_0}{m_f} = e^{\left(\frac{\Delta v}{I_{sp} g_0} \right)} \quad (2.2)$$

Where the final mass is retrieved knowing the dry mass and taking into account a 20% margin [39].

Computing m_0 from the mass ratio and the final mass it is possible to retrieve the propellant mass with a margin considering residuals (2%), ullage (3%) and loading uncertainty (0.5%):

$$m_{prop} = 1.055 (m_0 - m_f) \quad (2.3)$$

Afterwards, from O/F and m_{prop} in Equations 2.4 and 2.5 the masses of fuel and oxidizer needed in bi-propellant can be obtained:

$$m_f = \frac{m_{prop}}{1 + O/F} \quad (2.4)$$

$$m_o = m_{prop} - m_f \quad (2.5)$$

Once known the Fuel mass needed by the mono-propellant engine, computed in Eq.2.3, the total mass of Fuel is $m_{f_{tot}} = m_{f_{mono}} + m_{f_{bi}}$.

From the densities of the two components the resulting total volume is (adding 10% to account for unusable volume. [35]):

$$V_{prop} = 1.1(V_O + V_F), \quad (2.6)$$

Since Juno utilizes a regulated pressurization system, it is required to size the mass of pressurizing gas and its tank. In order to do so we have assumed a propellant tank pressure, kept constant by the gas, of

$$P_{tank} = P_{chamber} + \Delta P_{inj} + \Delta P_{feed} \quad (2.7)$$

where $P_{chamber}$, the pressure in the combustion chamber, has been taken from Leros-1b data sheet[46], $\Delta P_{inj} = \frac{1}{2} \rho_o v_{feed}^2$ is the total loss in the injection system and $\Delta P_{feed} = 50\text{kPa}$ is the total loss in the feeding system (pipes, valves). Assuming the final pressure in the pressurizing tank $P_{press,f} = P_{tank}$, the initial pressure $P_{press,i} = 10P_{press,f}$ and the temperature of the propellant tanks $T_{tank} = 293K$, the total margined mass of pressurizing gas is:

$$m_{press} = 1.2 \left(\frac{P_{tank} V_{prop}}{RT_{tank}} \frac{\gamma}{1 - \frac{P_{press,f}}{P_{press,i}}} \right) \quad (2.8)$$

and finally the volume of pressurizing gas is computed through the perfect gas law in Equation 2.9.

$$V_{press} = \frac{m_{press} R_{specific} T_{press}}{P_{press,i}} \quad (2.9)$$

The pressurizing gas temperature has been assumed the same of the propellant one; this assumption, and the consequent gaseous helium hypothesis, were made in order to simplify the computation, even if the results would have been different if we had used the liquid helium assumption.

In the end, selected the material on which the tanks are made, we can define the sizing dimensions

$$r_{tank} = \left(\frac{3}{4} \frac{V_{tank}}{\pi} \right)^{\frac{1}{3}} ; \quad t_{tank} = \frac{P_{tank} r_{tank}}{2\sigma} \quad (2.10)$$

$$m_{tank} = \rho_{tank} \frac{4}{3} \pi \left((r_{tank} + t_{tank})^3 - r_{tank}^3 \right)^3 \quad (2.11)$$

where σ and ρ_{tank} are the material yield stress and density.

Results

The actual size and material of the tanks used in the mission are not publicly available, the authors therefore decided to perform the sizing with the likely materials used as well as with two possible values for O/F ratio used in the bi-prop. engine. The consequence is firstly differing values for the tank wall thickness and consequently weight as well as their relative volume. From the given compatible materials from section 2.2.2 the choices for the material are titanium (Ti6A14V) and aluminium (Al7075). For the purposes of this analysis the two values for the O/F ratio are the optimal, in terms of I_{sp} given by [35] and the value provided by the data sheet[46]. The latter, results in fuel and the oxidizer tanks to be in term of radius and volume, similar

| | Mass[kg] | $V_{tank}[l]$ | $t_{tank}[mm]$ | $m_{tank}[kg]$ |
|-------------|----------|---------------|----------------|----------------|
| Fuel | 1208.2 | 329.6 | 0.51 | 3.30 |
| Oxidizer | 788.1 | 299.5 | 0.49 | 3.00 |
| Pressurizer | 8.4 | 213.5 | 0.23 | 1.78 |

Table 2.7: **Sizing Results** with $O/F = 0.8$ and propellant tanks in aluminium (Al7075)

| | Mass[kg] | $V_{tank}[l]$ | $t_{tank}[mm]$ | $m_{tank}[kg]$ |
|-------------|----------|---------------|----------------|----------------|
| Fuel | 951.1 | 259.5 | 0.47 | 2.60 |
| Oxidizer | 1045.1 | 397.3 | 0.54 | 3.98 |
| Pressurizer | 8.0 | 204.0 | 0.23 | 1.70 |

Table 2.8: **Sizing Results** with $O/F = 1.4355$ and propellant tanks in aluminium (Al7075)

| | Mass[kg] | $V_{tank}[l]$ | $t_{tank}[mm]$ | $m_{tank}[kg]$ |
|-------------|----------|---------------|----------------|----------------|
| Fuel | 1208.2 | 329.6 | 0.27 | 2.75 |
| Oxidizer | 788.1 | 299.5 | 0.26 | 2.50 |
| Pressurizer | 8.4 | 213.5 | 0.23 | 1.78 |

Table 2.9: **Sizing Results** with $O/F = 0.8$ and propellant tanks in titanium (Ti6A14V)

Using an O/F ratio of 0.8 the masses of fuel and oxidizer are very close to the nominal masses found on the spacecraft properties (2.3a). Furthermore, this O/F ratio results in propellant tanks of similar dimensions allowing the same assembly to be used in for both fuel and oxidizer. For these reasons the sizing with the optimal O/F ratio of 1.4355 can be discarded.

As for the choice of the tanks material, titanium is more dense than aluminium, but having a much higher structural resistance its choice results in thinner walls that in the end provide lighter and structurally stronger tanks.

Budgets

Considering the mass of pressurizer, tanks and thrusters, as well as the power consumption for the Leros 1-b main engine and the secondary system, the following mass and power budgets for the propulsive subsystem are obtained:

| Mass budget [kg] | Power Budget [W] |
|------------------|------------------|
| 35.08 | 248.31 |

Table 2.10: Mass and power budgets with $O/F = 0.8$ and propellant tanks in Titanium (Ti6A14V)

Chapter 3

TTMTC System

Change Log H3

| | |
|---------|-----------------------------------------------------------------------------------------|
| § 3.2.4 | pp. 22: revised and added comments on the results, in particular the SNR value obtained |
| § 3.3 | pp. 23: The three tables in Appendix have become Tab. 3.1. |
| § 3.3 | pp. 23: Table 3.1: changed values and added missing values |

3.1 TTMTC subsystem overview

The Tracking, Telemetry and Telecommand subsystem was one of the most challenging to design. Its crucial role in providing commands, telemetry and science data, reason why the connection with the Nasa's DSN had to be guaranteed throughout all the different mission phases, results in a set of five different antennas[45][65]:

- Two Low Gain Antennas (LGAs)
- Medium Gain Antenna (MGA)
- Toroidal Low Gain Antenna (TLGA)
- High Gain Antenna (HGA)

All the Juno TTMTC subsystem works at X-Band for all the nominal communications (Command up-link and Telemetry down-link) and for the Tracking (Doppler and ranging). During Gravity Science Orbits at Jupiter, TTMTC subsystem includes also a Ka-Band two-way tracking capability.

3.1.1 Antennas Configuration and Analysis

Since Juno is a spinning earth-pointing spacecraft, all the antennas are aligned to the spinning axis, as it can be seen in Figure 3.1. In the following sections is reported a brief description of each of them. [65] [45]

Low Gain Antennas

In the Juno spacecraft there are two identical LGAs: one faces forward (FLGA) and is mounted near the HGA and the other one is mounted on the aft deck of the spacecraft (ALGA). They are horn-style antennas made of an open ended circular waveguide with choke rings that are crucial to minimize the back-radiation and to provide a circular pattern shape.

The LGAs are used briefly near Earth when the spacecraft is far from its nominal attitude (spacecraft-forward-toward-Earth orientation) for all the initial communications. They provide coverage over the NASA DSN X-band transmit (~ 7.1 GHz) and receive (~ 8.4 GHz) bands with gains > 8.7 dBic and > 7.7 dBic near boresight for the receive and transmit bands, respectively.

Medium Gain Antenna

Also the MGA is a horn-style antenna which is used near Earth but is also operational in case of an emergency even at distant ranges, providing > 18.8 dBic and > 18.1 near boresight for the DSN receive and transmit bands, respectively.

To provide an alternative telecommunications system network path for the spacecraft in the event of a hardware failure, both ports of the polarizer are used to allow both right and left circular polarization.

Toroidal Low Gain Antenna

The TLGA is mainly used when the spacecraft is far from its nominal Earth pointing orientation. This happens during several main engine firings where the spacecraft turns approximately 90 degrees from Earth pointing.

Since Juno is spin stabilized, a conical shaped antenna would not allow for a telecommunication's signal lock, hence a torus shaped radiation pattern is required. The antenna that would give this pattern is the dipole, but it has a limited peak gain of ~ 2.2 dB that is not enough for the great distances between Earth and Jupiter.

For this reason, the chosen dipole geometry is the biconical antenna: this configuration is preferred because it expands the bandwidth of the dipole of about 3 octaves, it has a more robust geometry which allows for an easier fabrication and it is also possible to expand the gain of the standard dipole by increasing the aperture of the bicone antenna by increases of the cone diameters and height.

Other goals had to be met in the development of the TLGA, such as sidelobes and line losses.

To minimize sidelobes the choice has been to use corrugations for horn antennas: this approach lowered the sidelobes but it also lowered the directivity of the antenna by a small amount, still resulting in an adequate solution.

To minimize transmission line losses a rectangular to coaxial waveguide transition was developed. This transition was matched to the corrugated horn and it achieved better than 20 dB return loss over the entire band from 7 GHz to 9 GHz, providing a good result.

Other factors played a significant role in the design of the TLGA, such as the charge, thermal and launch environments.

High Gain Antenna

The HGA is the main mean of communication with Earth during Juno's scientific orbits. This antenna needed to maximise the gain due to the great distances involved and also due to the limited power supply of the spacecraft transmitter (25 W).

An important constraint on the functioning of the antenna is given by the three-arm solar array employed to facilitate the power generation: this arrangement limits the pointing of the antenna main beam to just ± 0.25 degrees. Another mission of the HGA is to provide the Ka-Band link between Juno and the DSN ground station during a gravity science experiment: with the attitude control limitation the Ka-Band beam would, on average, be pointed in a way that would lead to insufficient gain.

In order to maximise the gain both at X and Ka-Band the Juno team decided to shape the main reflector and subreflectors of the HGA adding subtle perturbations to the canonical geometries in order to have the phase fields as uniform as possible: this provided a good solution to optimizing the gains.

Other significant challenges such as the high radiation and high temperature environment were overcome using a material capable of releasing the charge accumulation (a carbon loaded Germanium Kapton) and a thermal blanket over the aperture of the antenna. Figure 3.2 shows the activity of each antenna during the different mission phases.

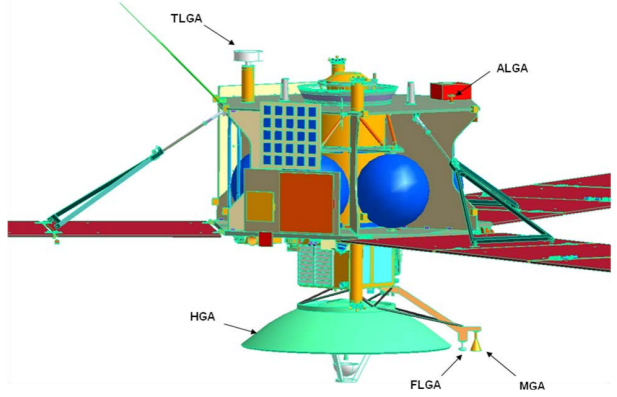


Figure 3.1: Placement of antennas on Juno spacecraft.
Credits:[45]

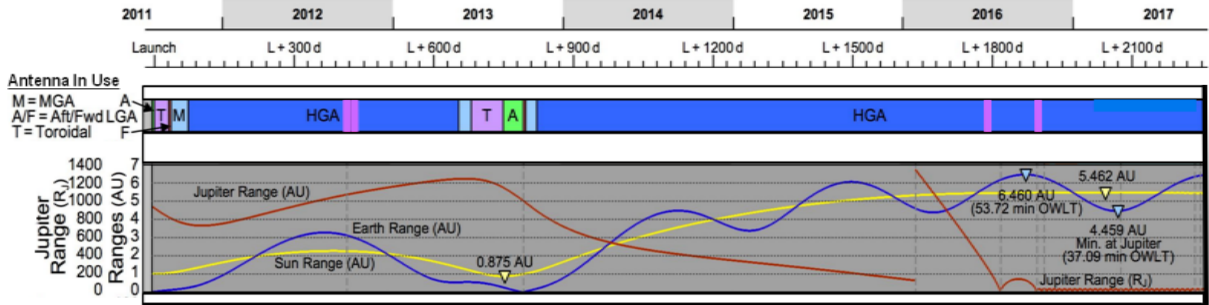


Figure 3.2: Activity of Antennas throughout the mission. Credits: Ref [65]

3.1.2 Ground Stations

The Ground Station selected is the NASA DSN, a network of antennas at three deep space communications facilities that are located approximately 120 degrees apart around the world.[45] The three antennas are placed one at Goldstone, California, another near Madrid, and the last one near Canberra. These three locations allow to have a constant coverage of the spacecraft while Earth rotates. Each site is composed by one large antenna (70m diameter) and a set of 34m-diameter antennas. The larger one is used mainly during DSM and the JOI, but also when the spacecraft enters in safe mode. During the nominal operations the spacecraft's communications are established with the 34-m antennas.

Since there was the risk of a small visibility gap during the separation from the launch vehicle, ESA stations of Perth and New Norcia provide support with acquisition and tracking of the spacecraft downlink signal.

In addition, as Ka-band is used for the Gravity Science investigation, at every perijove Juno needs to be in view of Goldstone, as is the only DSN antenna capable of Ka-Band uplink.

3.1.3 TTMTC subsystem architecture

In the following, an overview of Juno's TTMTC subsystem is given. A detailed diagram is given in Figure 3.3 [45].

The baseline components for Juno's TTMTC s/s are taken from other missions, mainly the Mars Exploration Rover, meaning that they were proven on previous interplanetary missions. The heritage components include its main X-band signal processing pipeline inside the vault as well as the the antenna architecture on the outside. The signal processing components are redundant, ensuring sufficient error tolerance. The main components are the two Small Deep Space Transponders (SDST). Those process the incoming and generate the outgoing signals. The primary SDST is also capable of transmitting Ka-band signals as backup for Gravity Science. It is referred to as SDST X/X/Ka while the other one is called SDST X/X.

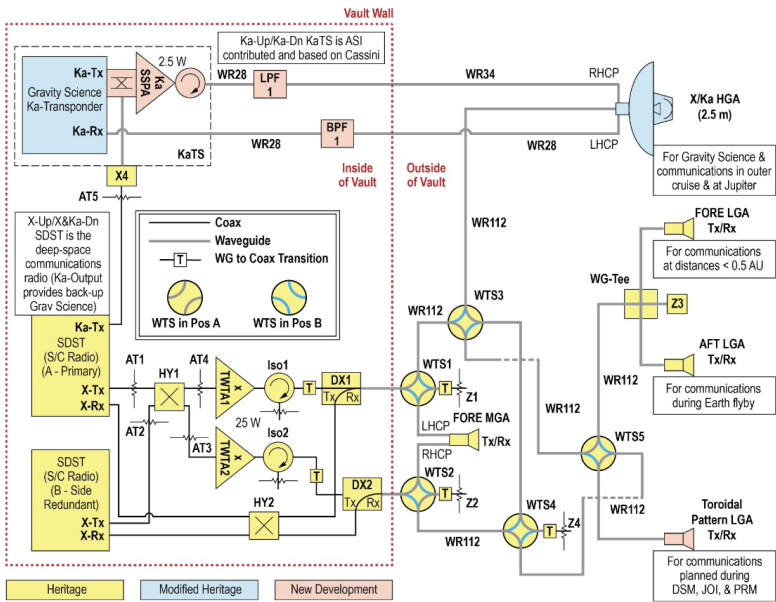


Figure 3.3: Juno's TTMTC architecture. Everything inside the red line is placed inside Juno's vault, which protects its electronics from radiation. Yellow components are taken from MER without modification, blue ones are modified, and red ones are newly added. [45]

As the antenna gain will be higher with Ka-band compared to X-band – and because this configuration is only used for Gravity Science which does not require high data rates – lower power output is required for the Ka-band signal and therefore a low-weight SSPA was sufficient compared to the heavier TWTAs used in the X-band chain. After the KaTS, the signal passes to filters and then into the antenna. Note, that the Tx and Rx signal of the Ka-band architecture only uses wave guides to propagate the signals.

3.2 Reverse sizing

The worst case scenario is taken at a range of 6.2 au meaning an assumption of a non co-planar superior conjunction. The TTMTC communication reverse sizing is done as follows, two cases analysed is the minimum telemetry data rate and increased data rate for science data D/L. The U/L sizing is performed using the same worst case but considering a different command data rate.

3.2.1 Frequency Band selection

The selection of the frequency band for the TTMTC subsystem is primarily determined by the International Telecommunications Union (ITU). The ITU allocates specific portions of the frequency spectrum for various

The Tx signals from the SDSTs are split by a Hybrid element (depending on if the primary or the redundant part is being used) and subsequently go into a 25 W TWTA – which also has a redundant counterpart). This was chosen over a Solid State Amplifier because the power output of TWTA is usually higher, which justified the typically higher weight. Diplexers connect the amplifier chain of the Tx part and the Rx inputs of the SDSTs on the inside of the vault to the antenna architecture on the outside. At this point the wiring system switches from coaxial cables to wave guides and an elaborate system of switches routes the signals to the corresponding antennas. These make sure, that both both amplifier chains and both SDSTs can access all antennas.

Newly built or modified components are the HGA and the Toroidal Pattern LGA as well as the Ka-band components. The Ka-band architecture consists of the Ka-band Translator (KaTS) which is built up of a Ka-band transponder and an amplification circuit. Its main component is a 2.5 W Solid State Power Amplifier (SSPA).

communication purposes, including deep-space missions like Juno. Juno falls under Category B of the ITU's allocation scheme, which is designated for spacecraft operating at distances greater than 2 million kilometers from Earth.

Between the possible choices for the frequency band, X-Band has been selected for communications and navigation, as offers a relatively wide bandwidth compared to other frequency bands, allowing for the transmission of large amounts of data, and also minimize the attenuation due to Earth's atmosphere and interplanetary plasma. Ka-band is used together with X-Band for improved Doppler measurement performance in Gravity Science investigation.

Once selected the frequency band, the up-link frequency (7153 MHz for X-Band and 25-34 GHz for Ka-Band) and the down-link frequency (8404 MHz for X-Band and 32 GHz for Ka-Band) and for Ka-Band are selected inside the range imposed by ITU.

3.2.2 Antenna selection

The choice of antenna is made keeping in mind the distances involved. These require a narrow beam width as well as high gain making a parabolic reflector the preferred option. A narrow beam width does however put constraints on the ACS. Another constraint put into place by the narrow beam width is the orientation of the spacecraft during transmission.

The antenna is placed on the front deck, pointing in the same direction as the solar arrays. This makes it possible to transmit data to earth while generating power at the same time as the Earth will appear in angular proximity to the sun when observed from Jupiter. It is placed along Juno's rotation axis to stay still when Juno is rotating.

3.2.3 Link Budget

The link budget is used to determine the received power to be used to determine the required transmitter power needed.

Data

The TTMTC system has the capability of sending a large variety of data rates, 20 in total. The Juno spacecraft has been sized to have a local storage of $data = 256 \text{ MB} = 2048 \text{ Mbit}$. The D/L ground station contact time was assumed to be 8h. Multiple such contacts were performed per orbit instead of one big transmission to allow greater flexibility in scheduling data transfers. Assuming a single ground station pass $T_{TX} = 8 \text{ h}$ was assumed meaning a science data rate of 70 kbit/s. The closest possible is then $R_{data} = 100 \text{ kbit/s}$ accounting for 18 kbit/s of TM.[45] Data rates for the U/L is difficult to acquire, a minimum worst case $R_{data} = 200 \text{ kbit/s}$ is therefore assumed.

Encoding Without encoding the data sent would be easily susceptible to noise, bit errors would neither be correctable nor identifiable. Achieving an acceptable BER would therefore require unreasonable high transmission power as well as low noise levels. As will be seen later the use of either convolutions or Reed-Solomon encoding is not viable with high data rates. To avoid this, for all high rate data transmission a modern encoding known as turbo encoding is used. The turbo code rate is 1/6 with 8920 bits frame size meaning an encoding index $\alpha_{enc} = 6$. [45] This gives a required $E_B/N_0 = -0.10 \text{ dB}$ for a $BER_{TM-min} = 10^{-6}$ close to the Shannon limit.

Modulation QPSK modulation allows to double the data rate compared to a BPSK system while maintaining the same bandwidth of the signal. Since the radio communication channels are allocated by the Federal Communications Commission, which therefore gives a prescribed maximum bandwidth, the advantage of QPSK over BPSK is the possibility to transmit twice the data rate in a given bandwidth at the same BER [67].

Transmitted power

For the purposes of amplification for TTMTC from Jupiter with a limited power budget, a heavier but more efficient TWTA is preferred. Starting from the DC power of the transmitter aboard the spacecraft, $P_{AMP} = 56 \text{ W}$ and a TWTA efficiency $\mu_{TWTA} = 57\%$ Transmitted power $P_{TX} = \mu_{TWTA} \cdot P_{AMP} = 32 \text{ W}$. Transmitter losses Cable loss is assumed to be -1 dB, $L_{cable} = -1 \text{ dB}$. The power from the ground stations varies greatly depending on the transmission, the ground station and the frequency. For the purposes of this analysis a transmitted power of 20 kW is assumed.

Antenna

Antenna peak gain, parabolic antenna $\mu_{ant} = 0.55$:

$$G_{TX-ant} = 10\log\left(\frac{\pi^2 D_{TX}^2 \mu_{ant}}{\lambda^2}\right) \quad [dB] \quad (3.1)$$

Ground station

For the nominal down link the DSN's 34 m antennas are used. But for increased science data delivery the 70 m antennas are used.[45] The DSN was chosen because it offers high gain antennas and high pointing accuracy, it has been proven to work on numerous deep space missions before Juno, justifying the high operational cost involved. Antenna peak gain:

$$G_{RX-ant} = 10\log\left(\frac{\pi^2 D_{RX}^2 \mu_{ant}}{\lambda^2}\right) \quad [dB] \quad (3.2)$$

Antenna beam width:

$$\Theta_{RX} = 65.3 \frac{\lambda}{D_{RX}} \quad [^\circ] \quad (3.3)$$

For the 34 and 70 meter receiver ground stations, the system temperature is 21 K.

Losses

Free space propagation loss is determined from the worst case when assuming circular orbits and a superior conjunction. This gives a worst case equal to 6.2 au.

$$L_{space} = 20\log\left(\frac{\lambda}{4\pi r_{max}}\right) \quad [dB] \quad (3.4)$$

Atmospheric loss $L_{atm} = -0.1$ dB. Pointing loss, With the pointing accuracy of the 34 m- and 70 m- stations is $\eta = 0.004^\circ$.

Noise

The thermal system noise density

$$N_0 = 10\log(kT_s) \quad [dB] \quad (3.5)$$

Now the final BER can be determined by examining the E_B/N_0

$$E_B/N_0_{final} = P_{RX} - N_0 - 10\log(B) \quad (3.6)$$

A S/C receiver system temperature of 250 K [45] and a ground station receiver temperature of 21 K is used [16].

3.2.4 Results

The final link budget for the received power can be constructed as shown in Table 3.1. Using Equation 3.2 the receiver gain is underestimated by a significant amount for the 70 m ground stations. The value used instead is 74.35 dB taken from the handbook [16]. The results for the D/L with the minimum required data rate of 18 kbit/s to the 34 m ground station at a range of 6.2 au and the ones of the D/L to the 70 m ground stations for SD and TM transmission of 100 kbit/s are shown in table 3.1, together with the uplink link budget.

The figures of merit of the sizing are the E_B/N_0 and the SNR, these quantities have to match the required performances allowing the receiver to have the capability of translating and tracking the signal, distinguishing it from the noise. From table 3.1 it is possible to see that the E_B/N_0 obtained satisfies the required one with a margin higher than 3 dB, while the SNR, in the D/L cases, is far lower than the minimum allowed.

One of the possible causes why the SNR reaches non compatible values with the constraints provided, could be addressed by the lack of correct information about the type of Carrier Phase Modulation. To compute the Carrier Modulation Index Reduction, the team assumed a standard value of $\beta = 78^\circ$ [35], resulting in high modulation losses that could have significantly reduced the SNR of the carrier with respect to the real mission one.

Another factor that can affect the value of the SNR is related to the Bandwidth. In the sizing the value of B has been computed starting from the Data Rate considering the type of Modulation (QPSK) and Encoding and how they influence it. In Juno's mission, a Turbo encoding with $\alpha_{enc} = 6$ is applied to the signal, which combined with the effect of QPSK modulation results in an increase of the effective data rate, and thus the bandwidth, by a factor of 3. In the actual mission B is computed considering several other different factors that the authors have neglected in the computations, such as a roll-off factor depending on the filter used for modulation.

In conclusion, the results obtained, particularly the SNR values, are not suitable for a real-mission application and it would be necessary a more in-depth analysis of modulation in order to obtain correct results.

3.3 Input Data and Results Table

| Link Parameter Inputs | | | |
|--------------------------------|------------------|------------------|------------------|
| | Minimum Downlink | Maximum Downlink | Uplink |
| Range | 6.2 au, 927.5 Gm | 6.2 au, 927.5 Gm | 6.2 au, 927.5 Gm |
| DataRate | 18 kbit/s | 100 kbit/s | 200 kbit/s |
| Encoding | Turbo | Turbo | Turbo |
| Modulation | QPSK | QPSK | QPSK |
| Ground station | DSN 34 m | DSN 70 m | DSN 70 m |
| Attitude pointing | Earth pointing | Earth pointing | Earth pointing |
| Transmitter parameters | | | |
| Transmitter power [W] | 56 | 56 | 20000 |
| Transmitter efficiency [%] | 57 | 57 | - |
| Transmitter circuit loss [dB] | -1 | -1 | -1 |
| Antenna Gain [dB] | 44.25 | 44.25 | 74.35 |
| Transmitted power output [dBW] | 15.12 | 15.12 | 43.01 |
| Antenna beam width [°] | 0.9322 | 0.9322 | 0.0333 |
| EIRP [dBW] | 58.37 | 58.37 | 116.36 |
| Path parameters | | | |
| Space Losses [dB] | -290.3 | -290.3 | -290.3 |
| Atmospheric attenuation [dB] | -0.1 | -0.1 | -0.1 |
| Receiver parameters | | | |
| Receiver Gain [dB] | 66.93 | 74.35 | 44.25 |
| Receiver Beam Width [°] | 0.0685 | 0.0333 | 0.9322 |
| Receiver Pointing Losses [dB] | -0.0409 | -0.174 | -0.000167 |
| Received Power [dBW] | -165.1 | -157.6 | -131.1 |
| System noise temperature [K] | 21 | 21 | 250 |
| System noise density [dB] | -215.4 | -215.4 | -204.6 |
| Channel performance | | | |
| Bandwidth [kHz] | 27 | 15 | 300 |
| Output E_B/N_0 [dB] | 2.931 | 2.9756 | 15.79 |
| Required E_B/N_0 [dB][45] | -0.1 | -0.1 | 9.6 |
| E_B/N_0 Margin [dB] | 3.031 | 3.0756 | 6.19 |
| Maximum BER [dB] | 10^{-6} | 10^{-6} | 10^{-6} |
| Output SNR [dB] | 2.9306 | 2.976 | 15.79 |
| SNR minimum [dB] | 10 | 10 | 10 |
| SNR margin [dB] | -7.069 | -7.0244 | 5.79 |

Table 3.1: Link parameters for the different scenarios: Minimum/Maximum Downlink and Uplink

Chapter 4

Attitude Determination and Control System

4.1 AOCS architecture

The attitude and orbit control subsystem (AOCS) is a functional chain of the satellite that encompasses the attitude and orbit sensors, the attitude estimation, attitude and orbit control algorithms and actuators.

The essential tasks that the subsystem needs to perform are:

- **Attitude and Orbit Determination:** to retrieve the current spacecraft's state vector and the spacecraft's attitude at any instant throughout the mission.
- **Guidance, Navigation & Control:** to carry out all the manoeuvres as specified by the mission requirements. It needs also to ensure the necessary capability to execute orbital control manoeuvres as determined by mission analysis.
- **Safe Mode:** to autonomously achieve and maintain, in the event of major anomalies, a safe pointing attitude that guarantees spacecraft's vital functions, until the anomaly is corrected.

Juno contains the following instruments to determine and control its attitude and orbit:

- 12 hydrazine thrusters, as the solar panels can not provide enough electrical power to drive reaction wheels or any other electrical driven actuators. In addition, hydrazine guarantees high stability over time.
- 2 autonomous Star Trackers, which can operate in spinning mode.
- 2 Inertial Measurement Units, which are composed by 3 gyroscopes and 3 accelerometers each.
- 2 Spinning Sun Sensors, each one composed by a fine Sun Sensor and a pulse Sun Sensor. It is a redundant system consisting of one optical head per redundant electronic channel, which have been accurately implemented to work at high distance from the Sun.
- 2 Magnetometer Fluxgate Sensors. Their primary task is to measure Jupiter's Magnetic Field, which is one of the main goals of the mission. It could also be used for attitude determination once in orbit around Jupiter.

4.1.1 Selection of the Actuators

Juno uses full 3-axis control, because its mission profile requires it to point in arbitrary directions, to perform its science objectives. Therefore, Juno has 12 hydrazine RCS thrusters with a nominal thrust which can vary from 1.3 N to 4.5 N, placed on 4 towers: 2 on the front and 2 on the aft deck. Because the core structure of Juno is relatively thin, the tower configuration was chosen to increase the thrusters' lever arms and therefore their torque.

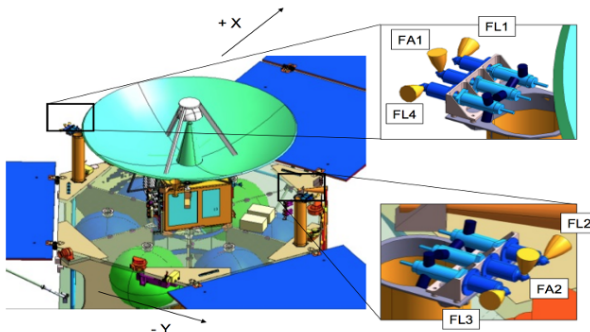


Figure 4.1: Juno's RCS-thrusters location [63].

There are 3 thrusters on each tower, two are placed in lateral direction opposite-facing and one in axial direction. This symmetry allows for balanced thrust coupling, which minimises the translational forces exerted on the spacecraft when changing the attitude. They are canted at an angle of 10° outward for the axial thrusters, and 5° outward and 12.5° upward for the lateral thrusters. Even though this slightly reduces their efficiency and thrust in the nominal direction, the canting was necessary to not pollute the scientific instruments and solar panels with exhaust plumes. Fig. 4.1 shows the thruster positioning on the spacecraft[49].

| | |
|----------------|------------------------------------------------|
| Actuator Model | RCS Thrusters MR-111C 4N |
| Mass Budget | 0.33 Kg Valve: 8.25 W |
| Power Budget | Valve Heater: 1.54 W Cat.Bed Heater: 3.85 W |

Table 4.1: Single RCS Thruster Specifications.

Juno's thrusters are its only actuators. They were chosen as opposed to reaction wheels or a CMG because the spacecraft has high angular momentum in its base configuration due to the spin-stabilization. Therefore reaction wheels would have been too heavy, and energy consumption too high or turning rates would have been too low. Magnetic torquers were not chosen, because Juno has a highly sensitive magnetometer on its solar array which would have been affected negatively.

4.1.2 Selection of the Attitude Sensors

Juno uses a diverse set of different sensors to determine its attitude. Tab. 4.2 contains specifications of the main sensors.

| Sensor | Model | Accuracy | Mass Budget | Power Budget |
|--------------|--------------------------|--------------------------------------------------|-------------|--------------|
| Star tracker | AA-STR | 0.013° (in pitch/yaw directions) | 2.6 Kg | 5.6 W |
| Sun sensor | Fine Spinning Sun Sensor | 0.1° for FOV 0° - 40° 0.25° for FOV 40° - 64° | 0.71 Kg | 0.4 W |
| IMU | Scalable SIRU | Drift Rate: 0.001 °/hr | 7.1 Kg | max 43 W |

Table 4.2: Attitude determination sensor specifications.

To ensure proper functioning despite potential failures, the spacecraft incorporates redundancy in its IMUs, star trackers, sun sensors, and guidance computers.

Star trackers Juno uses a custom variation of Leonardo's AA-STR as its two star trackers. They use an update rate of 4s. Star trackers offer high precision – which was necessary for Juno's high telecom and science pointing requirements –, and thanks to the so-called TDI (Time Delayed Integration) technology, which compensates for motion blur, they can perform accurate attitude determination with rotation rates of up to 10 RPM [37]. Since a Star Tracker is capable to retrieve the attitude of the spacecraft alone, they are used in Operational Mode as primary source for attitude determination. Nevertheless, due to its small field of view, the impossibility to work when the Sun is in its field of view, and the slowness of the data acquisition (1-10 Hz), it is necessary to have also other sensors on-board.

IMU Juno uses 2 IMUs as most spacecraft do because they are fast and precise. Since they can only measure angular rates and not absolute angles, they tend to accumulate drift errors, which is why they are used in combination with other sensors. The IMUs are activated during Jupiter flybys to determine anomalies and measure the gravitational field. During the operational phase, the IMU is typically reserved for the most precision-demanding spacecraft attitude maneuvers, particularly those occurring at perijove. This is because the IMU guarantees very high precision in both measurement and attitude determination. Typically in all the other phases IMU is off, as it consumes significant electric power [25]. Since it was not possible to find the exact configuration of the IMUs used in reality, the team assumed that Juno used HRG-based IMUs, as they were already used by Cassini mission, so they have been already tested in an harsh radiation environment [51].

Sun sensors Juno employs two Fine Spinning Sun Sensors to determine the direction of the Sun in the spacecraft body frame. While sun sensors are valuable for estimating the sun direction, they alone can not provide a full three-axis attitude estimation. For this purpose, at least one additional independent source of attitude information is required, such as the Star Tracker. The Sun Sensors are used in the Juno spacecraft primarily in Safe Mode to ensure proper Sun pointing for the solar panels, and to guarantee the correct attitude until new commands are sent from ground. In the Operational Mode, the attitude is typically retrieved through the Star Trackers, and the two Sun Sensors are used as backup in case of failures.

4.1.3 Stabilization

Juno uses spin stabilization as a fuel and energy saving method of keeping a constant attitude. To save weight and complexity, all of Juno's instruments are fixed to its side. Spinning allows all of the instruments to sweep over Jupiter regularly to perform their measurements. The rates are 1 RPM for regular cruise and 2 RPM for performing science. The latter rate is higher to increase stability and allowance for each instrument to perform twice as many measurements. In case of firing of Juno's main engine, the spin rate is increased to 5 RPM in order to improve stability even further. Traditional attitude actuators, as reaction wheels or CMGs (Control Moment

Gyro), require several Watts of power that, in Juno's case, would increase the stand-by power consumption too much, since Juno is solar-powered. Given that, spin stabilization was a more suitable alternative.

This type of stabilization brings some drawbacks:

- A complete stabilization is possible only in deep space (cruise mode) due to the absence of perturbations and it depends on the spin rate of the spacecraft.
- It is difficult to change the spin axis and to overcome the gyroscopic resistance.
- The spin axis inertia moment must be the largest, otherwise the stability is not guaranteed.

4.2 Control modes

Juno is designed in order to operate in several different modes throughout its mission:

- **Safe Mode:** Juno has two types of Safe Mode, depending on whether the attitude knowledge is retained or not. If it is known, the spacecraft pointing (whether Sun or Earth) is not changed. Despite, if the attitude knowledge is lost, Juno's solar panels would be pointed to the Sun, describing a cone of 2° . A Safe Mode is required in case of major anomalies, in which the spacecraft has to achieve the correct pointing to assure the right spin rate and to ensure the vital functions. Safe Mode has to be performed autonomously due to the fact that the transition has to be performed as soon as possible in order to prevent any risk of mission lost, and the distance from Earth does not allow for a swift intervention.
- **Orbit Control Modes:** During the Main Engine manoeuvres Juno leaves its nominal attitude pointing the HGA (High gain antenna) off-Earth in order to align itself to the burn attitude. In burn mode the spin velocity is increased to 5 RPM in order to better stabilize the spacecraft during the burn.
- **Operational Modes:** The followings are the modes necessary to fulfill mission targets, such as scientific observations or specific required pointing. Juno has two principal operational modes (Figure 4.2):
 - **MWR attitude:** the nadir pointing of the rotational plane has to be assured in order to allow the MWR (Microwave radiometer) to acquire datas. Three different types of MWR can be detected, according to the angle between Juno spin vector and the orbit normal. In particular, in the MWR attitude the spin vector and the normal are aligned, in the MWR-Tilt the angle is 14° , and in the MWR-Xtrk the angle is 90° , since Juno's spin vector is aligned with Jupiter pole axis;
 - **Gravity Science attitude:** the HGA Earth pointing is required in order to correctly measure the influence of the gravity field on Juno, and to establish a stable link with the Ground Station to transmit the data acquired.

- **RADIOMETER PASS**: No Gravity Science Radiometer antennas aligned with nadir
- **GRAVITY PASS**: No Radiometry HGA aligned with Earth

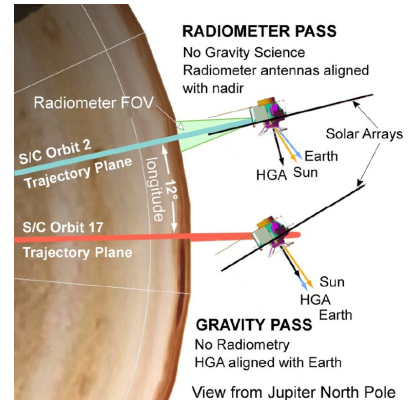


Figure 4.2: Attitude in Operational Mode

- **Transfer Mode:** During cruise phase to Jupiter, Juno enters the transfer mode in which the HGA is pointed to the Earth for communications and the spin velocity is set to 1 RPM for stabilization. During Earth fly-by and just after the launch, due to thermal reasoning, the pointing is "off-sun".

| Control Mode | Actuators | Sensors |
|---------------------|--------------------|--------------------------------------------|
| Safe Mode | RCS (12 thrusters) | Sun Sensors & Star Trackers |
| Orbit Control Modes | RCS (12 thrusters) | IMU |
| Operational Modes | RCS (12 thrusters) | Star Trackers (Sun Sensors for redundancy) |
| Transfer Mode | RCS (12 thrusters) | Sun Sensors & Star Trackers |

Table 4.3: Actuators and Sensors suite selection according to mode

4.3 Pointing budget

A pointing budget breakdown for Juno is given in Tab. 4.4. It includes the maximum performance error per s/s per mode. The knowledge error is not given in the table as it is trivial for most s/s. Except for the payload no specific knowledge of the attitude is necessary except that which is necessary to fulfill the pointing requirements. This means the knowledge should be at least as precise as the performance. The scientific instruments require knowledge, that is more precise, than the performance. Because Juno is rotating, each instrument sweeps over large parts of Jupiter so the required pointing precision is limited, while the instruments need to know precisely, which parts of Jupiter they are observing at each time. The most precise instrument (after JunoCam, which is mainly used for publicity and therefore excluded here) is the magnetometer, which needs to know its attitude to get Jupiter's magnetic field vector. However, it has its own star trackers and therefore means of attitude estimation already built in and is therefore excluded from this budget. The second most precise instrument is JIRAM, with an imaging precision of about 0.1° judging from its data [62] and Juno's distance from Jupiter. Therefore this is assumed as absolute knowledge error. The main constraint for Juno's rate – which is present in all phases equally – is that Juno cannot be pointed away from the sun for longer than the time the batteries can supply it with power. With JOI as the longest burn and the assumption, that the s/c has to perform a 180° turn twice, this leads to a minimum turning rate of $0.1^\circ/\text{s}$.

The APE for the TTMTTC s/s is driven by the HGA. It was assumed as half of the HPBW. During cruise and JOI, the HGA is not pointed at the earth when the s/c is in Orbit Control Mode. Then the omnidirectional LGAs are used to send tones, so no pointing is required. The propulsion system's APE was estimated by looking at the relative Δv errors of the burns in the first DSM and of an RCS correction manoeuvre [49]. The APE was chosen to result in a vectorial error of the same order of magnitude. In the gravity science mode, Juno's HGA drove the pointing budget as it had to constantly point at earth to measure Juno's position and velocity. In MWR mode, the rotational plane had to be aligned with Jupiter. The resolution of the MWR was estimated from its data [63] and given the distance to Jupiter during fly-by, an APE could be computed. For the EPS the pointing error was chosen such that solar array power production would not fall below 99 % due to facing away from the sun. This number was chosen because of Juno's great distance to the sun and therefore the importance of running the solar cells with high efficiency. The only mode where TCS has specific pointing requirements is shortly after launch and during the earth fly-by where Juno's has to point away from the sun for thermal reasons. It was assumed, that a surface whose normal vector is supposed to be perpendicular to the sun vector should not be visible by more than 5 % to prevent excessive heat-up.

This leads to an overall APE of 0.11° (imposed by the propulsion system in orbit control mode) and an overall AKE of 0.1° (imposed by JIRAM during the science phase). An APE of 0.11° is achievable with Juno's given RCS configuration. The precision requirements are coarse enough, that the thrusters' minimum impulse bit in combination with Juno's spin stabilisation can fulfill it. Looking at tab. 4.2, the AKE requirements are fulfilled with the star trackers leaving margin to the assumed AKE by a factor of 10.

| Subsystem | General | | Cruise | | Science | |
|-------------|-----------|---------------|--------------------|-----------------|----------|--|
| | Safe Mode | Transfer Mode | Orbit Control Mode | Gravity Science | MWR Mode | |
| TTMTTC | 0.35 | 0.35 | — | 0.35 | 0.35 | |
| Propulsion | — | — | 0.11 | 0.23 | 0.23 | |
| Science P/L | — | — | — | 0.35 | 0.7 | |
| EPS | 8 | 8 | — | 8 | 8 | |
| TCS | — | 3 | — | — | — | |

Table 4.4: Juno's pointing budget. The table shows the absolute performance error in degrees split into phases and modes.

4.4 Reverse sizing

To justify the spacecraft AOCS system a reverse sizing is performed. This is done in order to size the attitude control actuators and propellant amount considering the magnitude, traverse time and number of slew manoeuvres, stabilization burns and budget attitude control under effects of drift and perturbation torques.

4.4.1 Model of the Disturbances

The main perturbations during cruise phase and Jupiter approach were solar radiation pressure and torque due to misalignment of the thrusters. This is quite obvious, as during the cruise phase the spacecraft is not orbiting around a planet, but it is in a heliocentric orbit.

To model the disturbances affecting Juno's spacecraft in orbit around Jupiter, the team assumed a circular orbit with radius equal to perijove radius ($1.1 R_j$). In this way, it is possible to perform the control not only in the worst case scenario, where the values of the disturbances are the highest, but also by considering the part of the orbit where the slews occur in the real mission, which is some hours before and after the Perijove. Indeed, even if it could have been a good assumption to consider a circularization of the orbit with an average value, the choice didn't seem to be the more appropriate due to the high values of the eccentricity and of the distances involved. Considering the Jupiter's planetary constants, and referencing to the formula given during the lessons, the team modeled the perturbations affecting Juno's attitude. The Atmospheric Drag was negligible with respect to the other perturbations, while the Solar Radiation Pressure in the order of 10^{-7} . The two most affecting perturbations are the torque associated to the Gravity Gradient (10^{-4}) and the torque due to Jupiter's strong magnetic field (10^{-3}).

In light of the challenges associated with modeling the perturbations induced by Jupiter's moons, the team has made the decision to disregard their effects on Juno's spacecraft attitude and orbit.

4.4.2 Attitude actuator sizing

According to the description of Juno orbit plane geometry at each perijove [40], it is possible to reconstruct the number and the types of the slews performed to switch from one type of attitude, described in section 4.2, to another.

Indicating with θ the angle between Juno spin axis before and after the slew, it is possible to determine the time for the slew maneuvers considering the lowest value of force which can be given by the thruster (to have the lowest possible angular rate during the slew) [1]. By multiplying the resulting time for the corresponding number of slews, it is possible to retrieve the total time propellant mass for each type of slew:

$$m_{fuel} = \frac{t_{tot}F}{I_{sp}g_0} \quad (4.1)$$

The results are the following:

| Type of slew | Number | θ [°] | Mass of fuel [kg] |
|-----------------------|--------|--------------|-------------------|
| From GRAV to MWR | 3 | 4 | 0.0071 |
| From MWR to MWR-Tilt | 1 | 14 | 0.0044 |
| From MWR-Tilt to GRAV | 3 | 18 | 0.0150 |
| From MWR-Xtrk to GRAV | 4 | 90 | 0.0447 |

4.4.3 Orbital Control

The same thrusters utilized for executing slew maneuvers are also employed during the Science Orbits to maneuver the spacecraft under the effects of the primary disturbances (section 4.4.1). To approximate the hydrazine consumption by these thrusters, the team implemented the control process specifically for the MWR orbit, utilizing the results to estimate the total fuel mass required for all other Science Orbits. In the MWR orbit, Juno must align its spin vector (\underline{z}_b) with the orbit's normal and spin at 2 RPM [40]. Therefore, the desired angular velocity that the control needs to maintain is:

$$\omega_d = \{0, 0, 2 \text{ RPM}\}^T \quad (4.2)$$

The attitude error is computed as:

$$\mathbf{A}_e = \mathbf{A}_{B/N} \mathbf{A}_d \quad (4.3)$$

where $\mathbf{A}_{B/N}$ is Juno's attitude and \mathbf{A}_d is the desired attitude.

To obtain the torque provided by the thruster, a simple "bang-bang" type controller has been implemented:

$$\underline{M}_c = -\underline{T} sgn(\underline{S}) \quad (4.4)$$

Where the parameter \underline{S} is the tracking control obtained through the Lyapunov control function:

$$\underline{S} = - \left[-k_1 \underline{\omega}_e - k_2 \left(\mathbf{A}_e^T - \mathbf{A}_e \right)^V + \underline{\omega} \mathbf{I} \underline{\omega} + \mathbf{I} (\mathbf{A}_e \dot{\omega}_d - [\omega_e] \mathbf{A}_e \omega_d) \right] \quad (4.5)$$

with:

$$\underline{\omega}_e = \underline{\omega} - \mathbf{A}_e \underline{\omega}_d \quad (4.6)$$

The torques of the thrusters are given by:

$$\underline{T} = \underline{F} \cdot \underline{l} \quad (4.7)$$

where \underline{l} is the distance vector between the thruster couples and \underline{F} is a function of the \underline{S} parameter and it is obtained through a Schmidt-Trigger logic:

$$\underline{F} = \begin{cases} F_{\text{thruster}} & \text{if } |S_i| > S_{\text{threshold}} \\ 0 & \text{if } |S_i| \leq S_{\text{threshold}} \end{cases} \quad i = x, y, z$$

where $S_{\text{threshold}}$ is the value of the \underline{S} parameter for which the thrusters get turned on or off and F_{thruster} is kept to its minimum value of $1.3N$ to avoid overconsumption of fuel.

The team implemented two different control processes for two different situations that will be further explained in the next sections.

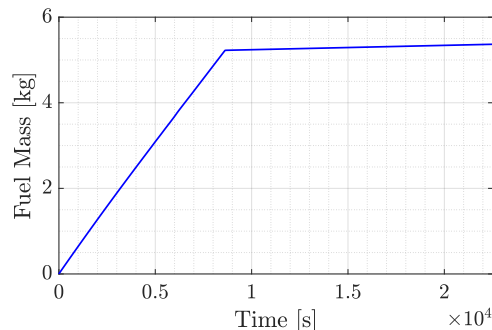
Spacecraft stabilization after GRAV to MWR slew manoeuvre

The first implemented control strategy is designed to bring Juno from a generic attitude and angular velocity to the desired 2 RPM rotation after the GRAV to MWR slew manoeuvre. The initial conditions are retrieved by the angular rate of the spacecraft during the slew manoeuvre:

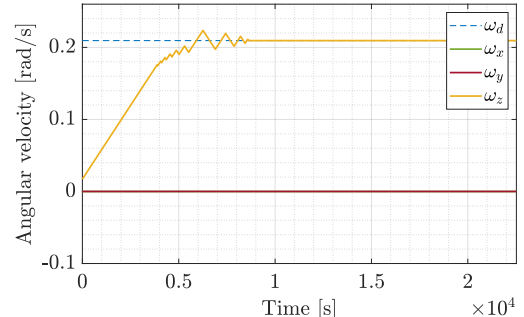
$$\underline{\omega}_0 = \{6 \cdot 10^{-4}, 9 \cdot 10^{-4}, 1.72 \cdot 10^{-2}\}^T \text{ [rad/s]} \quad (4.8)$$

The parameters of the control have been set to $k_1 = 20$, $k_2 = 0.4$ and $S_{\text{threshold}} = 3 \cdot 10^{-5}$.

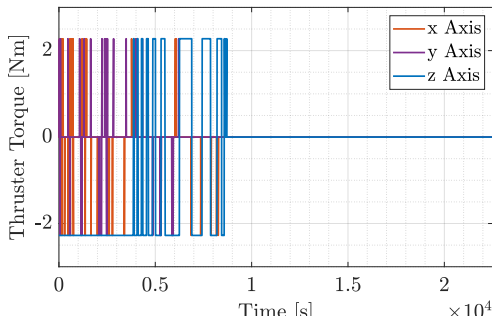
The following plots show the obtained results for the first control strategy:



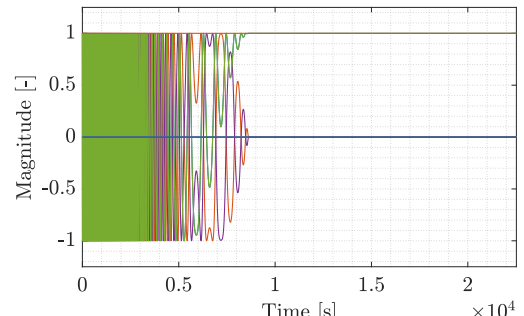
(a) Used fuel mass during control



(b) Angular Velocity



(c) Thruster Activity



(d) Attitude error

Figure 4.3: Spacecraft Stabilization after slew manoeuvre

The total mass of fuel used for the stabilization after one slew amounts to:

$$m_{f_{stab}} = 5.23\text{kg} \quad (4.9)$$

MWR attitude control

The second control strategy has been implemented to ensure proper orientation during one MWR orbit, under the effect of the external disturbances, using the same control logic explained in section 4.4.3. Particular focus was put on determining the number of thruster pulses per orbit to correct the attitude.

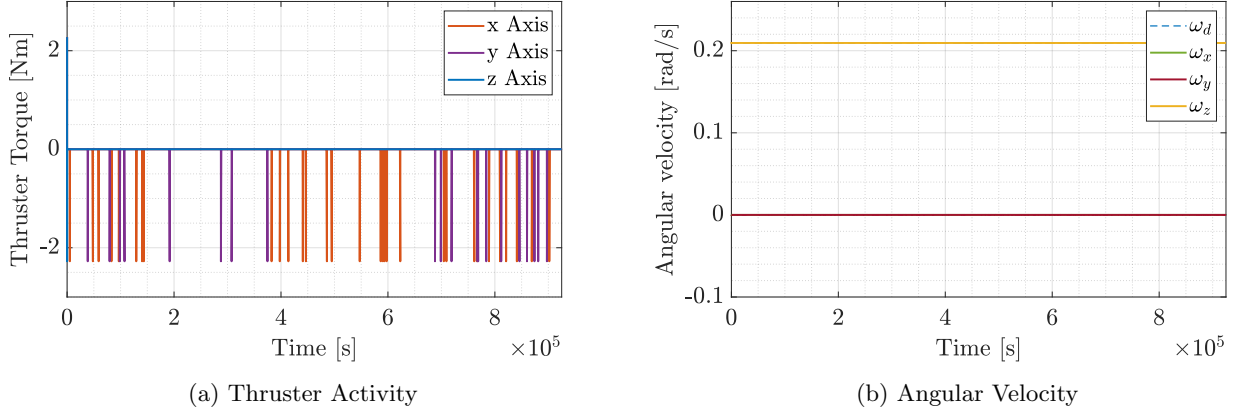


Figure 4.4: Spacecraft Attitude Control

As can be seen in fig. 4.4a, the total number of pulses per orbit is $N_{pulses} = 54$. By considering an average time of activation of $t_{pulse} = 0.5\text{s}$ it was possible to retrieve the total mass of hydrazine needed to control the spacecraft during a Science Orbit:

$$m_{f_{contr}} = \frac{N_{pulses} t_{pulse} F_{thruster}}{I_{sp} g_0} = 0.0156\text{kg} \quad (4.10)$$

4.4.4 Final comments

In order to calculate the total mass of fuel consumed by Juno both the slews and the control of the spin rate of the spacecraft along the 36 orbits have been considered. Furthermore, as already indicated, the evaluation of the disturbances have been computed by assuming circular orbits with a radius equal to the perijove.

Once the results are available through the procedure indicated in the previous sections, the total mass of consumed fuel is computed by considering 11 slew manoeuvre stabilizations and 36 orbital attitude controls. By considering an additional margin of 50%, the final mass budget is the following:

| Control | Mass of fuel [kg] | Mass of fuel with margin [kg] |
|--------------------------|-------------------|-------------------------------|
| Slew Manoeuvres | 0.0711 | 0.1067 |
| Stabilization after Slew | 57.53 | 86.295 |
| Attitude Control | 0.562 | 0.842 |
| Total Mass of Fuel | 57.6167 | 87.244 |

In conclusion, the total amount of mass of fuel is 87.244kg , which is a reasonable value compared to the 221.13kg which have been evaluated in the sizing of the Propulsion Subsystem for the RCS Thrusters.

Chapter 5

Thermal Control System

5.1 TCS Architecture and Design Rationale

Juno has to operate across a wide range of environment passing from Earth to Jupiter and therefore the Thermal Control System (TCS) has to ensure the survivability of all the temperature sensible subsystems, payloads and sensors, in every external condition.

To fulfill the objectives, Juno's TCS employs both passive elements, such as MLI blankets and louvers, and active components consisting of heaters[27]. Additionally, elements that are external to Juno's main body, such as HGA, MAG and other sensors, has to be individually blanketed and heated to maintain their corresponding temperature limits.

5.1.1 TCS Main Components

In the following paragraphs, a more precise description of Juno's TCS will be presented, as well as its design rationale.

Radiation Vault: The Radiation Vault is an insulated 200 kg cube made of Titanium (with a thickness of about 1 cm) inside the spacecraft that contains most of the electronic devices and computers (Figure 5.1). Since the spacecraft is exposed to about 20 million rads of radiation during the Science Orbits around Jupiter, vault's main goal is to reduce the radiation exposure by about 800 times, ensuring proper integrity and functioning of all the components stored inside it.

Due to the high heat production of the electronics inside the radiation vault, the TCS' main concern is cooling. Furthermore, a copper thermal doubler is used to distribute the thermal loads effectively across Juno's structure and it will be further discussed in the next sections.

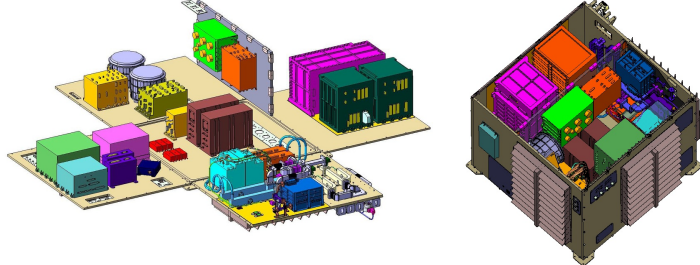


Figure 5.1: Juno's Radiation Vault [29]

Multi-layer Insulation: Multilayer Insulation (MLI) blankets offer a lightweight insulation system with high thermal resistance in vacuum. Typically consisting of 10 to 30 layers of aluminized Kapton sheets, each around $6.35\text{ }\mu\text{m}$ thick, these blankets are separated by a low thermal conducting material net, such as Dacron, to prevent layer-to-layer conductivity. Additionally, the outermost layer of the MLI blanket, typically $25.4\text{ }\mu\text{m}$ to $50.8\text{ }\mu\text{m}$ thick, is composed of aluminized Kapton to mitigate degradation resulting from exposure to space throughout the mission. In Juno mission all the radiation vault is insulated using MLI blankets, as the propulsion module. All the sensors and scientific instruments placed outside of the main deck are insulated separately using MLI blankets as well. Furthermore, the High Gain Antenna (HGA) dish is shielded by a Germanium-Kapton blanket (which ensure RF signal transmission [50]) since, while Juno is close to the Sun (up to $\sim 1.4\text{ AU}$), it is used as a thermal shield. All the remaining external structure, excluding the front and aft deck and specific component placement areas, is insulated with MLI.

The choice to use MLI blankets in Juno spacecraft is their extremely lightweight and effectiveness in reducing heat loss to the cold space, or preventing excessive heating of the surroundings from an internal component with heat dissipation.

Heaters: Electric heaters play a crucial role in maintaining spacecraft equipment temperatures within precise limits. In the Juno spacecraft, critical components such as the attitude sensors and the propulsion module, especially the pressurized tanks (Hydrazine) and the thrusters' catalyst bed, require to be heated. Unlike the Li-Ion batteries, these components are placed outside of the insulated vault and need strict operative temperature ranges for optimal functionality. Consequently, heaters are indispensable to ensure their proper operation.

The decision to utilize Film Heaters is driven by their simplicity; they consist of electrical resistance filaments sandwiched between two layers of Kapton [18]. Additionally, heaters offer the advantage of precise control over heating power. However, it is important to note that the drawback of employing heaters is their power consumption, which is particularly critical in the Juno mission.

Passively Controlled Thermal Louvers: Juno uses electronic-free thermal louvers for the thermal control of the spacecraft: this solution is a crucial advantage for Juno mission, where the only power supply is given by the solar panels and its availability is limited due to the great distance from the Sun [53]. A passive thermal louver is a device made of movable panels that, by opening or closing, regulate the spacecraft's body exposure to the external heat sources. The panels are moved by precise tailored metallic coiled springs which expand or contract depending on the temperature.

This design choice ensures that the onboard power resources remain allocated primarily for the scientific instruments and data collection, rather than thermal regulation.

Another advantage of louvers is their inherent simplicity which augments the robustness and reliability of Juno's TCS. By avoiding complex electronic, the louvers minimize risks of malfunctions or performance degradation, providing higher duration. Furthermore, the high adaptability of louvers to different operational scenarios is another great reason behind their choice. Juno's wide range of orbits and payload operations, besides its critical environmental conditions, necessitate a thermal control solution capable of satisfying different thermal loads without requiring continuous intervention from ground control. For this reason, louvers are attached to the sides of the vault to vary the surface's absorbed and reflected as well as emitted light content accordingly [18].

For these reasons, the choice of passively controlled thermal louvers for Juno's TCS represents a thoughtful choice that provides high power efficiency, reliability, and adaptability, which are essential for the mission.

Positioning of the TCS components

In Table 7.2, a schematic overview of the positioning of the different TCS components is provided:

| Component | Position | Rationale |
|-----------------|---------------------------------------------------------------------------------------------------------|------------------------------------------------------------------------------------------------------------------------------------------------------------------|
| MLI blankets | Radiation Vault and entire s/c surface, sensible areas like sensors, HGA antenna and propulsion module. | To give proper thermal insulation to the whole surface. More sensible devices like sensors, antennas and the propulsion module require an individual insulation. |
| Passive Louvers | External Radiators and Radiation Vault | Placed over radiative surfaces, opening or closing based on the required temperature ranges to be satisfied. |
| Heaters | Hydrazine tanks, thrusters catalyst bed, sensors, batteries | To ensure proper temperature for the propulsion subsystem and more sensible devices like batteries, sensors and actuators. |
| Thermal Doubler | Radiation vault | To optimize the heat transfer from inside the vault to the external radiators. |

Table 5.1: TCS architecture positioning

5.1.2 Peculiar Solutions

A brief analysis of the peculiar solutions used in the Thermal Management of the mission will now be presented such as the thermal doubler and ceramic components for the thermal management of the magnetometer.

Copper Thermal Doubler for Thermal Management: A thermal doubler is a device which serves as an interface component designed to augment thermal conductivity and distribute thermal loads effectively across the spacecraft's structure. The choice of this device for the TCS architecture of Juno has been made to meet the critical thermal requirements of the mission, while also ensuring the integrity of the mechanical interface [64]. This device is particularly crucial for the titanium vault which contains the electronics devices. It is in fact

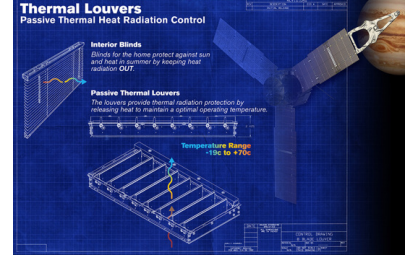


Figure 5.2: Juno's Thermal louvers scheme [53]

crucial to mitigate the undesirable thermal effects induced by the titanium vault, which are enlarged by Jupiter's extreme radiation environment. By using a copper thermal doubler, the thermal management system spreads thermal loads uniformly across the radiator surface, resulting in a reduced effective thermal resistance encountered within the vault wall. This approach ensures efficient heat transfer from the telecommunication equipment to the external radiators, and it also preserves the structural integrity of the spacecraft's TCS, which is a critical aspect for operational stability in the harsh environmental conditions of Juno's mission.

The thermal doubler enhances heat dissipation efficiency, preserves mechanical interface flatness and reinforces the structural integrity of critical spacecraft components. All these aspects are crucial and help facilitating the TCS success in Jupiter's high radiation environment.

Ceramic Component for Magnetometer System Another interesting choice in Juno's TCS is the utilization of a ceramic component (carbon fiber-reinforced silicon carbide , C/SiC) for the sensor carrier of the magnetometer system [52].

While the primary function of the sensor carrier is of magnetic field research purposes, its material selection is directly linked to thermal management considerations, due to Jupiter's hostile radiation environment which necessitates the adoption of very resilient components from a thermal point of view.

The C/SiC material, used in the sensor carrier, ensures a proper solution to these challenges with its high thermal resistance, coupled with low density and excellent temperature resistance, which enable the carrier to sustain the extreme thermal fluctuations encountered during Juno's mission. By ensuring efficient heat dissipation and minimizing the dimensional changes due to temperature variations, the sensor carrier maintains optimal performance and structural integrity, which are all critical aspects for accurate magnetic field measurements during the mission.

5.2 Heat Sources along the mission phases

Being an interplanetary mission to the outer solar system, Juno encounters a variety of thermal environments during its operative life. Table 5.2 delineates the internal and external sources responsible for Juno's heating throughout different phases. While the basic on-board electronics like OBDH, ADCS and the telecommunication system are active in every phase, the components dissipating most power – the scientific instruments – are turned off during the cruise phase and only partially on for testing during the earth fly-by. One of the biggest factor contributing to the heat variation is the incoming solar flux. Close to earth it is 15 times larger than close to Jupiter.

| Phase | Heat sources | |
|------------------|--------------------------------|---------------------------------|
| | Internal | External |
| Earth fly-by | OBDH, ADCS, TTMTC, Instruments | Sun, Earth Albedo, Earth IR |
| Eclipse (EFB) | OBDH, ADCS, TTMTC, Instruments | Earth IR |
| Cruise | OBDH, ADCS, TTMTC | Sun |
| Jupiter approach | OBDH, ADCS, TTMTC, Instruments | Sun |
| Science orbit | OBDH, ADCS, TTMTC, Instruments | Sun, Jupiter Albedo, Jupiter IR |

Table 5.2: Heat sources encountered by Juno in its various phases.

Table 5.3a shows the power dissipated by Juno's internal electrical components. It has been assembled looking into the generated internal power flux of the components in use during the spacecrafts operations. It was assumed that all eight of Juno's instruments require about as much power as JIRAM, which dissipates 16.7 W.

Table 5.3b shows the temperature limits for the sensitive components used in order to size the TCS. Because JIRAM has an IR camera, that has to be operated at very low temperatures, its temperature range is not compatible with the other components. For this reason, its temperature is controlled separately. For the other components, note, how the li-ion batteries dictate the allowed temperature range inside the s/c.

These extreme changes in thermal environment as well as the tight temperature requirements imposed by the batteries require sophisticated and flexible thermal control. Juno achieves this by using its louvers, to change surface reflectivity and emittance according to phase. Additionally, MLI blankets are used to decouple the components, e.g. the propellant tanks, as much as possible from the Juno's environment.

| s/s | Component | Heating [W] | Equipment | | T limits [°C] | |
|---------------------|------------------------------|-------------|----------------------|------|---------------|------|
| | | | | | Low | High |
| Processing | RAD750 processor | 10.0 | Data processing unit | -20 | +50 | |
| | Command & data handling | 10.0 | Li-ion batteries | +10 | +30 | |
| | Power & data distribution | 10.0 | Solar panels | -165 | +130 | |
| Scientific Payloads | Electronics of 8 instruments | 133.6 | Star tracker | -30 | +60 | |
| | Star tracker (2 times) | 25.2 | Sun sensor | -30 | +50 | |
| | Sun sensor (2 times) | 0.4 | IMU | -10 | +60 | |
| ADS | IMU | 43.0 | TTMTC electronics | -20 | +50 | |
| | TWTA | 31.0 | Tanks | 0 | +40 | |
| | SSA | 2.5 | Propellants | +7 | +35 | |
| TTMTC | Transponders | 20.0 | Science electronics | -10 | +45 | |
| | Payload + IMU OFF (WCC) | 152.1 | MAG | -20 | +60 | |
| | Payload + IMU ON (WHC) | 285.7 | JIRAM IR camera | — | -153 | |
| Total | Margined | 357.1 | JADE | -10 | +40 | |

(a) Estimated internal heat generation in the electronics vault.

(b) Temperature limits for sensitive components compiled from [35] and the available specifications sheets.

Table 5.3: Internal Heat Generation and Temperature Ranges for Juno's components

5.3 Reverse sizing

In the following section a preliminary reverse sizing of the TCS is performed, identifying at first glance the worst hot case and the worst cold case and then computing mass and power budget of the components (MLI, louvers, heaters). A single node analysis is performed modeling the spacecraft as an equivalent sphere in order to find the overall spacecraft temperature. A more accurate analysis would have been the multinodal one, since in reality Juno's sensors and subsystems are individually controlled and exposed to heat sources.

The initial data used for sizing, presented in Table 5.4, includes information on the effective radiators' emissivity, which varies within the range of 0.14 to 0.74, due to Juno's equipped louvers. Additionally, the most restrictive operative temperature interval for the Thermal Control System (TCS) sizing has been determined based on component temperature limits as outlined in Table 5.3b.

| Environment | | | Spacecraft | |
|-----------------------|-------------------------|--------------------------|--------------|----------------------|
| q_0 | 1367.5 W/m ² | Solar Flux at 1 AU | A_{tot} | 52.66 m ² |
| T_{Earth} | 290 K | Earth's mean Temperature | A_{cross} | 13.17 m ² |
| R_{Earth} | 6378 km | Earth's Radius | r_{sphere} | 2.05 m |
| a | 0.36 | Albedo Factor | T_{max} | 303.15 K |
| ε_{Earth} | 0.7 | Earth's Emissivity | T_{min} | 283.15 K |
| T_{space} | 3 K | Temperature Deep Space | Q_{intWHC} | 357.1 W |
| r_{flyby} | 6938 km | Radius Earth Fly-By | Q_{intWCC} | 152.1 W |
| σ | $5.68 \cdot 10^{-8}$ | Boltzmann's Constant | | |

Table 5.4: Initial Data used for the sizing of TCS

5.3.1 Worst cases

A brief explanation of the rationale behind the choosing of the two analyzed cases is reported in the following.

Worst Hot Case: The critical analysis for the WHC focused its attention on the Earth Fly-by and on the post-launch phase since they are the two phases in which the solar flux, due to the proximity to the sun, is the highest. The other sources of heat have been considered resulting on the EFB (before the eclipse zone) as the WHC, since the most of the instruments are turned on for testing and the proximity to the Earth surface (560 km) make the IR flux and the Albedo flux higher with respect to the parking orbit phase.

In order to perform the reverse sizing of the WHC, all the instruments have been considered turned on and the HGA shielding effect on the radiation vault has been neglected.

Worst Cold Case: The two critical phases analyzed to choose the WCC were the Eclipse phase during the EFB and the End of the Cruise (EoC), just before the Jupiter approach. In the first mentioned, the team considered the maximum Internal Generated Power (IGP) (in order to be consistent with the previous case) and the IR heat flux, since the Solar and the Albedo heat fluxes were nulls. Regarding the EoC phase the IGP were instead considered the lowest (all instruments turned off) and the only external heat flux was the solar one at 5AU (the distance to Jupiter at this point is still too high to consider IR and Albedo fluxes). The resulting total Heat in the two cases are $Q_{\text{eclipse}} = 369.53 \text{ W}$ and $Q_{\text{EoC}} = 156.82 \text{ W}$. According to them, the WCC chosen by the team is the End of Cruise phase with all the instruments considered off.

5.3.2 Sizing MLI

The sizing of TCS starts from the evaluation of the emissivity and absorvivity of the MLI. Since there were no information available regarding Juno's MLI, the team assumed the number of inner layers $N_{\text{layers}} = 17$, each one composed by a 6.35 μm thick aluminized Kapton sheet, spaced 0.25 mm apart from the next layer through a Dacron polyester net. The values of emissivity ε for each layer is retrieved from [6]: $\varepsilon_{\text{Kapton}} = 0.34$

Then the heat resistance of each layer, assuming only radiation between the layers, can be determined:

$$R_{\text{MLI}} = \frac{1}{\varepsilon_{\text{Kapton}}} + \frac{1}{\varepsilon_{\text{Kapton}}} - 1 \quad (5.1)$$

In anticipation of the extreme conditions encountered during Juno's mission and the consequent degradation which the outermost layer will be subjected, the team selected a thicker layer (50.8 μm) of aluminized Kapton ($\varepsilon_{\text{ext}} = 0.55$, $\alpha_{\text{ext}} = 0.34$). To provide protection during installation and handling, also the innermost layer is thicker (25.4 μm , $\varepsilon_{\text{int}} = 0.45$). Then the thermal resistance of the outer and inner layer R_{ext} are determined through Equation 5.1, considering ε_{ext} and ε_{int} respectively instead of $\varepsilon_{\text{Kapton}}$.

The equivalent ε and α are:

$$\varepsilon_{\text{eq}} = \frac{1}{R_{\text{int}} + R_{\text{MLI}} \cdot N_{\text{layers}} + R_{\text{ext}}} = 0.011 \quad \alpha_{\text{eq}} = \frac{\varepsilon_{\text{eq}} \cdot \alpha_{\text{ext}}}{\varepsilon_{\text{ext}}} = 0.0068 \quad (5.2)$$

The results obtained are compatible with the typical value of MLI blankets used in space applications [38]. The overall thickness of the MLI blanket is 0.48 cm, considering a total of 19 layers.

5.3.3 Hot Case

The team initially tried the possibility of having a completely passive TCS computing the resultant $T_{s/c}$ coming from the energy balance in the, defined above, worst case, without applying louvers.

In order to compute the energy balance, the different heat fluxes have to be defined:

$$q_{\text{sun}} = q_0 \left(\frac{r_{\text{Earth}}}{r_{s/c_{\text{WHC}}}} \right)^2 ; \quad q_{\text{albedo}} = q_{\text{sun}} a \left(\frac{R_{\text{Planet}}}{R_{\text{orbit}}} \right)^2 ; \quad q_{\text{IR,pl}} = \sigma \varepsilon_{\text{Earth}} T_{\text{pl}}^4 \left(\frac{R_{\text{Planet}}}{R_{\text{orbit}}} \right)^2 \quad (5.3)$$

and the View Factor between the Earth and the Spacecraft (for Sun-s/c $F = 1$ due to the great distance among them) is computed:

$$F_{E-s/c} = \frac{1}{2} \left(1 - \frac{\sqrt{\left(\frac{r_{\text{flyby}} - R_E}{r_{\text{flyby}}} \right)^2 + 2 \frac{r_{\text{flyby}} - R_E}{r_{\text{flyby}}}}}{1 + \frac{r_{\text{flyby}} - R_E}{r_{\text{flyby}}}} \right) \quad (5.4)$$

from which the total external Q absorbed by the spacecraft are:

$$Q_{\text{sun}} = A_{\text{cross}} \alpha_{\text{eq}} q_{\text{sun}} ; \quad Q_{\text{albedo}} = A_{\text{cross}} F_{E-s/c} \alpha_{\text{eq}} q_{\text{albedo}} ; \quad Q_{\text{IR,pl}} = A_{\text{cross}} F_{E-s/c} \varepsilon_{\text{eq}} q_{\text{IR,pl}} \quad (5.5)$$

to which $Q_{int_{WHC}}$ (Table 5.4), defined as the total internal power plus a 25% margin, must be added. The margin has been selected due to the high dissipation that will occur when Juno is in the proximity of the Earth, as the Solar Panels produce around 14 kW. The resulting $T_{s/c}$ is:

$$T_{s/c_{WHC}} = \sqrt[4]{\frac{Q_{int_{WHC}} + Q_{sun} + Q_{albedo} + Q_{IR,pl}}{\sigma \varepsilon_{eq} A_{tot}} + T_{space}^4} = 350.17 \text{ K} \quad (5.6)$$

that is higher than the maximum admissible temperature T_{max} , reported in Table 5.4.

Since the temperature is outside the payload-imposed temperature, the team size the minimum louvers area needed in order to obtain an acceptable temperature. The area is computed starting from Eq 5.7, imposing as $T_{s/c}$ the maximum temperature T_{max} :

$$A_{rad} = \frac{Q_{sun} + Q_{albedo} + Q_{IR,pl} + Q_{int_{WHC}} - \sigma \varepsilon_{eq} A_{tot} T_{s/c}^4}{\sigma (\varepsilon_{rad} - \varepsilon_{eq}) T_{s/c}^4} = 0.6199 \text{ m}^2 \quad (5.7)$$

The area of the radiators is feasible with the real one. In fact, Juno is equipped with 4 louvers [53], each one with a surface of 0.16 m², for a total area of 0.64 m² [54].

5.3.4 Cold Case

As the team has done in the WHC case, $T_{s/c}$ is computed in the WCC considering the heat fluxes affecting the spacecraft. Since the distance from Jupiter is yet too high, $q_{albedo} = q_{IR,Ju} = 0$, while $q_{sun_{min}} = 0.0369 \cdot q_0$ (considering Jupiter corrective factor of 3.69%). The WCC internal power $Q_{int_{WCC}}$ (Table 5.4) is defined as the total internal power without the contribute of the instruments that, as stated in Section 5.3.1 are considered off. From which, with the procedure utilized in the previous section:

$$T_{s/c_{WCC}} = \sqrt[4]{\frac{Q_{int_{min}} + Q_{sun_{min}}}{\sigma \varepsilon_{eq} (A_{tot} - A_{rad}) + \sigma \varepsilon_{rad_{min}} A_{rad}} + T_{space}^4} = 253.46 \text{ K} \quad (5.8)$$

which is lower than T_{min} (Table 5.4).

In order to maintain thermal control of Juno, even within the WCC, the utilization of an active control device becomes essential. To size the necessary power (Q_{heater}) required from the Heater to sustain the spacecraft at the designated temperature (T_{min}), a new energy balance has been performed, considering as:

$$Q_{heater} = \sigma \varepsilon_{eq} (A_{tot} - A_{rad}) T_{min}^4 + \sigma \varepsilon_{rad_{min}} T_{min}^4 - Q_{int_{min}} - Q_{sun_{min}} = 86.15 \text{ W} \quad (5.9)$$

Applying a required 25% margin and considering a power density of 5 W/cm²[43], the team obtained:

$$Q_{heater} = 107.69 \text{ W} ; A_{heater} = 21.54 \text{ cm}^2 \quad (5.10)$$

5.3.5 Mass, Power, and Data Budgets

Table 5.5 provides the mass and power allocations for the Thermal Control System, including passive and active components. Mass calculations for Multi-Layer Insulation (MLI) are based on standard layer density[38], while Louvers and Heaters masses are sourced from data-sheets[43][54]. All masses are margined by a factor of 1.2.

| | MLI | Louvers | Heaters | Budget |
|-----------|-------|---------|---------|---------------|
| Mass [kg] | 31.23 | 5.16 | 0.113 | 42.74 |
| Power [W] | - | - | 107.69 | 107.69 |

Table 5.5: TCS Mass and Power Budget

For the data rate, a resolution of 8 bit per measurement was assumed. That results in a temperature precision of 0.3 °C in the range from -20 °C to 50 °C. If Juno has 20 temperature sensors (6 in the vault, 1 for each instrument, and one for each propellant tank), that are read 3 times per minute, that gives a data rate of 1 B/s. Assuming this data is sent 5 times per orbit (every 10 days), a total of 864 kB have to be stored. Both data rate and stored data are far less than 1% of the total and therefore negligible.

Chapter 6

Electric Power System

6.1 EPS Architecture and Design Rationale

Juno is the first solar-powered probe to be sent to Jupiter. Previous missions relied on Radioisotope Thermal Generators (RTGs) for their Electric Power Subsystem (EPS). However, due to a shortage of plutonium in the United States and the high costs associated with it, designing an alternative power source became essential [57]. The only available solution was the use of solar arrays, despite the fact that the available solar power at Jupiter is only about 3.9% of that at Earth. The following section analyzes the adopted EPS architecture, including both primary and secondary energy sources, according to mission phases and power budget needed and discusses the rationale behind the choices made.

6.1.1 Primary Source: Solar Arrays

The design of the solar arrays was extremely challenging because they have to supply the required power from the s/s (shown in Table 6.1) throughout the mission. The main problems that the design team had to facing were:

- Generate enough power even with low intensity sunlight (3.9% of the sunlight at Earth)
- Work efficiently in LILT (Low Intensity Low Temperature). The LILT effect is the phenomenon attributed to the fact that the low solar intensity and degradation due to Jupiter's harsh radiation environment decrease the cells efficiency while the low operating temperatures increase it and so, a combination of these two conditions can cause anomalous performances degradation [11].

In order to solve the first driver, two strategies were adopted: the first one consisted in maximizing the solar cells area, while the second one consisted in maximizing their efficiency. As a result, a $\sim 50 \text{ m}^2$ cell area was designed, resulting in three $9 \text{ m} \times 2.7 \text{ m}$ arrays divided in 11 solar panels (4 on each panel except for the one having the MAG at its tip (Figure 6.1)). The selected cells are the multi-junction cells ($\text{GaInP}_2/\text{GaAs}/\text{Ge}$) that allows to reach a 30% of efficiency under Jupiter environmental conditions. This type was preferred over the mono crystalline silicon cells due to their high efficiency, obtained by utilizing a broader light spectrum [7], and resistance to degradation caused by radiations.

A further optimization of the power generated is achieved by designing the mission avoiding Jupiter's eclipses, reducing radiation exposure, and ensuring that all scientific measurements are taken with the solar panels facing the sun with a maximum angle of incidence of 9.7° .

Facing the second problem, Juno team performed specialized testing under LILT conditions, observing that some cells exhibited significant efficiency reduction, while others produced under the same process did not. Consequently, each cell was individually tested using an innovative procedure; those demonstrating degradation effects were discarded [13].

As the spacecraft travels farther from the sun, the decreased solar intensity results in a reduction of available current, so that more cell strings are needed to provide the required power. The issue was solved during the design phase by implementing three different string lengths to supply the required voltages across various distances from the Sun. The selection of string lengths was based on voltage and power set points for three distinct distance ranges from the Sun:

- Long strings for the Inner Cruise (Sun distance from 0.85 AU to 1.9 AU)
- Medium strings for the Middle Cruise (Sun distance from 1.8 AU to 3.75 AU)
- Short strings for the Outer Cruise and Science Phase (Sun distance from 3.75 AU to 5.5 AU)

Each panel is generally made by strings of the same length grouped into circuits. They are switched as necessary to support the bus loads based on the spacecraft's load and the battery's state of charge [13].

In order to safeguard the cells from incident UV radiation during the early mission and charged particles in Jupiter's orbit, the cover glass was coated with an anti-reflective coating and a layer of Indium Tin Oxide (ITO).

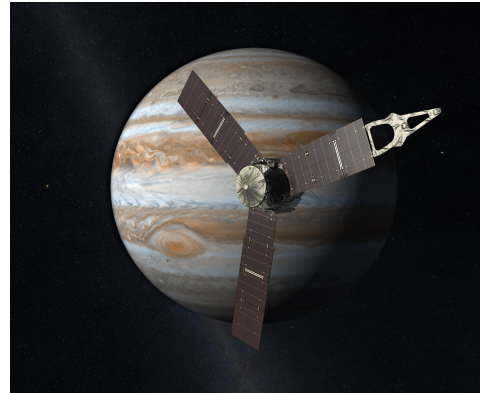


Figure 6.1: Juno's Solar Arrays and MAG-boom.

In summary, Juno's Electric Power Subsystem (EPS) has successfully achieved a total power generation capacity of 464.5 W at Jupiter with an expected power generated of 420.4 W at the EoM [13]. This result aligns with the mission's stringent power requirements (Table 6.1) and is a direct outcome of the innovative architectural and design choices detailed in the preceding sections.

6.1.2 Secondary Source: Li-ion Batteries

The secondary power source for the Juno mission is a set of two Li-ion batteries stored inside the Radiation Vault with a capacity of 55 Ah each, which are used when Juno is not exposed to sunlight. This happens during the 2 DSMs, and most importantly during Earth Fly-by.

For missions to outer planets, Li-ion batteries are usually preferred to the competing technologies, such as $Ag-Zn$, $Ni - H_2$ and $Ni - Cd$ batteries [55]. In fact, they provide higher energy density and higher specific energy, and they can also withstand higher temperature excursions due to the possession of non-aqueous based electrolytes. Furthermore, Li-ion batteries have great life characteristics, both in terms of cycle and calendar life.

The chemistry used for Juno's Li-ion batteries is the so called "heritage" chemistry [56], which was also used in a variety of other interplanetary missions. It consists of a mesocarbon microbeads (MCMB) anode, a $LiNi_xCo_{1-x}O_2$ (NCO) cathode and a low-temperature ternary all-carbonate-based electrolyte. The MCMB anode provides a stable structure for lithium-ion intercalation, which is essential to achieve high energy density and rechargeability. The NCO cathode provides high capacity and stable cycling, which allows the battery to have consistent power delivery over extended periods, critical for long missions like Juno's. Additionally, the electrolyte was chosen for its ability to remain stable and conductive even at low temperatures, a critical requirement for the cold space environment that Juno operates in.

The heritage Li-ion chemistry has demonstrated exceptional durability and robustness, making it a reliable choice for Juno. These factors collectively contribute to the longevity and reliability of the EPS, ensuring that Juno can maintain operations despite the challenging conditions encountered around Jupiter.

In conclusion, Li-ion batteries with their peculiar heritage chemistry were chosen for their high energy density, reliability, ability to endure numerous charge-discharge cycles and to withstand various temperature fluctuations encountered at Jupiter's harsh environmental conditions. The placement of the batteries need to be close to the biggest consumers of power to reduce the mass of cables required. Being located inside the radiation vault has the added benefit of simplifying the TCS design.

6.1.3 Power Distribution

The Power Distribution and Drive Unit (PDDU) plays a crucial role in managing and monitoring the spacecraft's EPS with a Direct Energy Transfer (DET) regulation method.

The PDDU ensures efficient power distribution from the solar arrays to the various subsystems, it regulates the spacecraft's power bus and facilitates controlled power distribution to support Juno's scientific objectives and operational needs in the challenging environment around Jupiter. The PDDU is also responsible for managing the state of charge (SOC) of the batteries.

Juno's PDDU is able to switch between three types of solar array strings (see Section 6.1.1), this adaptability is critical as it allows Juno to optimize power generation throughout the various phases of its mission.

As for the choice of the Direct Energy Transfer (DET) for the Juno mission, it is justified by its higher efficiency – crucial for a mission like Juno which has a very limited power supply –, reliability and mass and cost savings aspects which are suitable for long duration missions.

Since there was no available information on the type of bus regulation, the authors assumed an unregulated bus voltage because of its reduced complexity and weight saving aspects: having less components means reducing the probability of failures and this aspect is vital for long missions. The operational point is therefore lead by the loads requirement (including the batteries). Since the voltage is fixed at 28 V any power surplus is dissipated as heat within the array, which removes the need for shunt regulation and shunt radiators. This approach is effective across the wide range of solar distances (0.85–5.44 AU) and temperatures (-140 °C to +85 °C) encountered during the mission. The team assumed this type of bus regulation because it is well-suited for long duration missions (~ 5 years).

6.2 Power Budget

In Table 6.1 is reported the power budget supplied per phase per each subsystem. All the requested power have been estimated by referring to previous papers and data-sheets, and mainly to previous sizing computed. For

each phase the worst case (the most power-demanding) has been considered.

| | CRUISE | | | | SCIENCE | | | | SAFE |
|--------------------|---------------|--------------|---------------|---------------|--------------|---------------|--------------|---------------|-------------------|
| | Inner | EFB | Outer | JOI | MWR | | GRAV | | MODE |
| | | | | | Orbit | Pj | Orbit | Pj | |
| Propulsion | 84.63 | - | 84.63 | 84.63 | - | 13.84 | - | 13.84 | - |
| Biprop Main Engine | 84.63 | - | 84.63 | 84.63 | - | - | - | - | - |
| Monoprop Thrusters | - | - | - | - | - | 13.84 | - | 13.84 | - |
| TTMTC | 70 | 70 | 70 | 70 | 116.6 | - | 116.6 | 116.6 | 70 |
| X-band TWTA | 70 | 70 | 70 | 70 | 70 | - | 70 | 70 | 70 |
| Ka-band TWTA | - | - | - | - | 46.6 | - | 46.6 | 46.6 | - |
| ADCS | 12.2 | 44 | 12.2 | 44 | 12.2 | 12.2 | 12.2 | 12.2 | 2 |
| Star Trackers | 11.2 | - | 11.2 | - | 11.2 | 11.2 | 11.2 | 11.2 | - |
| Sun Sensors | 1 | 1 | 1 | 1 | 1 | 1 | 1 | 1 | 2 |
| IMUs | - | 43 | - | 43 | - | - | - | - | - |
| TCS | 100 | 160 | 130 | 180 | 140 | 140 | 140 | 140 | 70 – 150 |
| Heaters | 100 | 160 | 130 | 180 | 140 | 140 | 140 | 140 | 70 – 150* |
| EPS | 10 | 10 | 10 | 10 | 10 | 10 | 10 | 10 | 10 |
| PDU | 10 | 10 | 10 | 10 | 10 | 10 | 10 | 10 | 10 |
| OBDH | 20 | 20 | 20 | 20 | 20 | 20 | 20 | 20 | 20 |
| C&DH | 10 | 10 | 10 | 10 | 10 | 10 | 10 | 10 | 10 |
| RAD750 processor | 10 | 10 | 10 | 10 | 10 | 10 | 10 | 10 | 10 |
| Payload | - | 74.5 | - | - | 74.3 | 124.4 | 41.7 | 91.8 | - |
| JEDI | - | 9.7 | - | - | 9.7 | 9.7 | 9.7 | 9.7 | - |
| MAG | - | 19 | - | - | 17.8 | 19 | 17.8 | 19 | - |
| WAVES | - | 9.6 | - | - | 5.2 | 9.6 | 5.2 | 9.6 | - |
| JADE | - | - | - | - | 9.0 | 17.3 | 9.0 | 17.3 | - |
| MWR | - | - | - | - | 32.6 | 32.6 | - | - | - |
| UVS | - | 11.8 | - | - | - | 11.8 | - | 11.8 | - |
| Juno CAM | - | 6.0 | - | - | - | 6.0 | - | 6.0 | - |
| JIRAM | - | 18.4 | - | - | - | 18.4 | - | 18.4 | - |
| TOTAL | 296.83 | 378.5 | 326.83 | 408.63 | 373.1 | 320.44 | 340.5 | 404.44 | 172 – 252* |

Table 6.1: Power Budget [W] for each phase of Juno’s mission. *Depends on the where Juno enters in Safe Mode

Here we briefly explain the main assumptions done in the power budget. For the Propulsion subsystem budget, for both the Main Engine and the Thrusters has been considered only the power requested to activate the valves (and to heat the catalyst bed for the thrusters). The value for thrusters is referred to one unit.

In TTMTC power budget it is important to highlight that during perijove passes there are no communications with ground, as due to the extremely harsh environment the whole system is off. This is not valid during perijove passes of Gravity Science Orbits, where X-band and Ka-band translators and power amplifiers are used [15].

Regarding the ADCS, since during cruise, Juno is in All-Stellar mode, both the Star Trackers are on, and even a Sun Sensor to guarantee the correct pointing of the solar panels. During the most critical manoeuvres IMU replaces Star Trackers for attitude determination. In Safe Mode, where precise attitude control is not required, only Sun Sensors are used for rough pointing of the solar panels.

Regarding TCS, the obtained value in the previous sizing isn’t suitable with reality due to the assumptions made for sizing. In fact, when modeling the spacecraft as an equivalent sphere, the power required by heaters isn’t accurately calculated, as it doesn’t consider the need for dedicated heaters for each sensor, tank and instrument which are placed outside the main deck. Indeed the value estimated in [57] for heaters exceeds 150 W in the worst case scenario (JOI). Based on this, since no information is available, the team estimated the potential power requirements for each phase. Earth Fly-By, where Juno is partially in eclipse, represents the second most power-demanding phase for TCS. Then, since during the Science Phase the distance to the Sun is far larger than

the one during cruise, the power demand for TCS will be higher. Considering these factors, the team derived the power budget for TCS in each phase.

It's important to note that the power budget for each phase is less than the available power, even at the End of Mission (EOM), with a considerable margin in each phase. This is crucial for addressing any potential emergencies that may occur throughout the mission.

6.3 Reverse Sizing

6.3.1 Solar Arrays

Close to the sun, the temperature in the solar cells is higher and therefore the voltage lower. To apply the voltage, necessary to charge the batteries in all phases of the mission, a few long strings of solar cells are used in the beginning while they are gradually augmented by shorter strings in parallel during later phases. Because the solar irradiation close to earth is high, these few long strings suffice, while the lower temperature at Jupiter allow short strings to apply sufficient voltage to charge the batteries. The corresponding solar cell and battery chart can be seen in fig. 6.2. [13]

Juno uses DET due to time and budget constraints in the design of the EPS. Furthermore, the electronics and line losses of power point tracking are larger than the simple architecture of DET, allowing for a more efficient usage of the limited solar power near Jupiter. [13]

Given the power requirement P_d and the solar array line efficiency X_d , the necessary solar array power can be computed using

$$P_{sa} = \frac{P_d}{X_d}. \quad (6.1)$$

The power requirement P_d is not the same for all phases. It was assumed, that the power demand for the cruise phase is lower than in the beginning and near Jupiter. Note how the charging of the battery is not included in this power demand. This is because Juno's orbit is specifically designed to not encounter eclipses. The available specific power of the solar arrays near Jupiter at EOL is given by

$$p_{EOL} = \cos \alpha \cdot d_{EOL} \cdot \varepsilon \cdot I_0 \quad (6.2)$$

with the angle between solar array normal and sun vector α , the degradation factor at EOL d_{EOL} , the solar arrays efficiency ε and the solar irradiation at Jupiter I_0 . Because Juno has three kinds of solar cell string lengths – each satisfying the power demand at a different point in the mission – this specific power has to be computed at 1.9 AU and 3.8 AU as well. Assuming the worst case of a degradation similar to EOL, only I_0 has to be changed in Equation 6.2. The two specific powers are called $p_{1.9\text{ AU}}$ and $p_{3.8\text{ AU}}$.

The following equation is used to compute the number of cells in series per string

$$N_{series} = \left\lceil \frac{V_{sys}}{V_{sa}} \right\rceil. \quad (6.3)$$

V_{sys} is the voltage necessary to charge the batteries and V_{sa} is the voltage of one solar cell. This value is temperature dependent so N_{series} has to be computed at three distances: At earth ($N_{series, long}$), at 1.8 AU ($N_{series, mid}$), and at 3.7 AU ($N_{series, short}$).

To find the number of strings and with that also the number of solar cells, the necessary solar cell area has to be computed. Again, this has to be done for the three different string lengths using

$$A_{sa, EOL} = P_{sa}/p_{EOL}. \quad (6.4)$$

The power requirement P_{sa} and the specific power produced by the solar arrays p_{EOL} have to be exchanged for their corresponding counterparts in other phases of the mission. The results for the intermediate lengths are called $A_{sa, 1.9\text{ AU}}$ and $A_{sa, 3.8\text{ AU}}$.

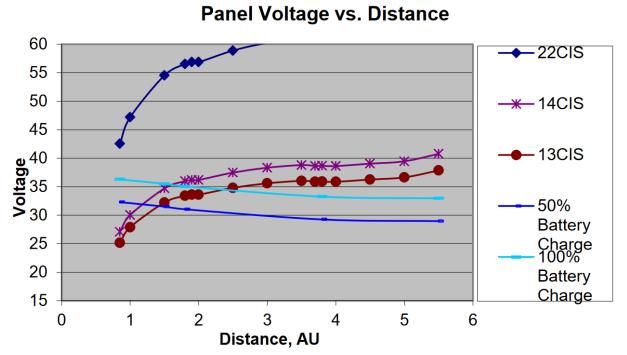


Figure 6.2: Cell and Battery voltages at different distances [13]

From this, the number of strings can be computed starting with the long strings using

$$N_{parallel,long} = \left\lceil \frac{A_{sa,1.9\text{ AU}}}{N_{series,long} \cdot A_{cell}} \right\rceil \quad (6.5)$$

where A_{cell} is the area of a single solar cell. This gives the number of long strings necessary to meet the power demand at 1.9 AU. The mid strings follow in a similar fashion. Note however, that the long strings add to the power production so they have to be subtracted from the result

$$N_{parallel,mid} = \left\lceil \frac{A_{sa,3.8\text{ AU}}}{N_{series,mid} \cdot A_{cell}} \right\rceil - N_{parallel,long}. \quad (6.6)$$

The number of short strings are computed in an analog way

$$N_{parallel,short} = \left\lceil \frac{A_{sa,EOL}}{N_{series,short} \cdot A_{cell}} \right\rceil - N_{parallel,long} - N_{parallel,mid}. \quad (6.7)$$

Finally the total number of solar cells (N_{sa}) is just the sum of cells in all strings and the total effective area and the weight can be computed from:

$$A_{sa} = N_{sa} \cdot A_{cell} \quad ; \quad m_{sa} = A_{sa} \cdot \rho_{sa} \quad (6.8)$$

with the area density given as sum of the densities of the cells and the aluminium structure underneath

$$\rho_{sa} = \rho_{cells} + \rho_{al} \cdot t_{al}. \quad (6.9)$$

Inputs, Results, and Interpretation

The maximum power demand assumed for the early mission phases and everything at Jupiter until EOL was $P_{d,1.9\text{ AU}} = P_{d,EOL} = 420\text{ W}$ [13]. For the outer cruise a maximum power budget of $P_{d,3.8\text{ AU}} = 300\text{ W}$ was assumed. As Juno does not use power point tracking, but instead relies on constant voltage DET, a typical value of $X_d = 0.85$ was used for the computations. The degradation was assumed to be constant at its EOL value as a worst case estimate $d_{EOL} = 0.90$ [13].

A condensed overview of the remaining inputs is given in Table 6.2a, while the results are listed in Table 6.2b.

| Quantity | Value | Quantity | Value | Reference |
|-----------------------------|------------------------|----------------------|---------------------|-------------------|
| α [13] | 9.7° | $N_{series,long}$ | 22 | 22 |
| ε [59] | 0.243 | $N_{series,mid}$ | 14 | 14 |
| $I_{1.9\text{ AU}}$ | 376 W/m ² | $N_{series,short}$ | 13 | 13 |
| $I_{3.8\text{ AU}}$ | 94 W/m ² | $N_{parallel,long}$ | 107 | 114 |
| $I_{1.9\text{ AU}}$ | 50.5 W/m ² | $N_{parallel,mid}$ | 367 | 369 |
| V_{sys} [13] | 33 V | $N_{parallel,short}$ | 869 | 848 |
| $V_{sa,1\text{ AU}}$ [13] | 1.53 V | N_{sa} | 18789 | 18698 |
| $V_{sa,1.8\text{ AU}}$ [13] | 2.4 V | A_{sa} | 48.9 m ² | 50 m ² |
| $V_{sa,3.7\text{ AU}}$ [13] | 2.56 V | m_{sa} | 341.4 kg | 340 kg |
| A_{cell} [59] | 26 cm ² | | | |
| ρ_{cells} [59] | 0.84 kg/m ² | | | |
| ρ_{al} | 123 kg/m ³ | | | |
| t_{al} | 5 cm | | | |

Table 6.2: (a) The remaining inputs to the reverse sizing. (b) The results of the reverse sizing. The reference values are the ones actually used on Juno. They were taken from [13].

As can be seen in the table, the reverse sizing results are close to the setup that was actually flown on Juno. This implies that the solar cell data as well as the assumed topology, powers, and other components were correct. Note how the number of parallel strings computed and therefore the total number of solar cells are less than the minimum computed here in the reverse sizing. This could be due to area constraints on the real solar panels or due to assumptions made for the sizing that were too strict. As the relative error is less than 0.5 %, this is not investigated further. The difference in actual and computed solar array area can be attributed to the spacing between the cells, which was not included in the reverse sizing.

6.3.2 Batteries

The batteries need to be sized properly to ensure enough stored energy capacity to cover peaks in demand and periods without the primary energy source. This determines mass, volume and the configuration of the accumulators. With proven success on many previous flown missions, the MCMB-NCO Li-ion cells produced by Yardney were chosen for the mission. Assuming a cell capacity $C_{cell} = 8 \text{ Ah}$, a cell voltage $V_{cell} = 3.6 \text{ V}$, and a system voltage $V_{sys} = 33 \text{ V}$ means that 10 cells in series are required, resulting in a real system voltage $V_{real} = 36 \text{ V}$.

The spacecraft does not experience periodic eclipses during its mission. Consequently, the battery sizing is based on the maximum energy demand encountered during any mission phase. The science pointing of the MWR and GRAV science orbits allows partial illumination of the solar panels and therefore alleviate the batteries despite the long duration and high power demand. This leaves the JOI burn as the sizing case.

Typical values for the Depth of Discharge (DoD) of Li-ion batteries range between 50% to 60%, due to the low amount of cycles, the DoD has been set to 50%.

The power drawn during the JOI, from Table 6.1 is 409 W. A 60% margin is applied as supported by [10] for conceptual design stages. The sizing case duration is 1 h and 35 min¹ for a 35 min engine burn and time attitude change.

A preliminary, non refined, analysis has been performed resulting in a battery system capacity $C_{real_{NF}} = 33.8 \text{ Ah}$, which is not an accurate result comparing it to the real values stated in Section 6.3.2.

Therefore, a more accurate analysis has been performed considering the single cell performance and the required series and parallel string number. The resulting battery system Capacity $C_{real} = 48 \text{ Ah}$ is a reasonable value, with respect to the 55 Ah of the actual mission, considering the assumptions made. The ultimate results are shown in Table 6.3, each battery pack having a mass $M_{bat} = 12.4 \text{ kg}$ and taking up a volume $V_{bat} = 6.91 \text{ dm}^3$ using specific energy and specific density respectively from Table 6.3.

6.3.3 Mass, Power, Volume and Data Budgets

Using the results from section 6.3.2 and 6.3.1 an estimated mass power, volume and data budget can be constructed:

| Budget | Solar arrays | Batteries | PDU | Cables | Total |
|---------------------------|--------------|-----------|------|--------|--------------|
| Mass [kg] | 341.4 | 24.8 | 2.0 | 100.0 | 505.9 |
| Power [W] | 0.0 | 0.0 | 10.0 | 0.0 | 10.0 |
| Volume [dm ³] | — | 13.8 | 2.0 | 11.2 | 27.0 |
| Data [kB/s] | 0.0 | 0.0 | 1.0 | 0.0 | 1.0 |

Table 6.4: Mass, power, volume and data budgets for Juno's EPS. The solar arrays are excluded from the volume budget because they are mounted externally and therefore do not take up space inside the main body. The data budget does not include possible electrical data collected by the payloads as they have their own power regulation that is not part of the main EPS system. The cable mass was assumed to be 20 % of the total EPS mass, which amounts to 3 % of total s/c mass (a reasonable value), as an early stage assumption [35].

¹Assuming a attitude change magnitude of 180 deg at an angular velocity 0.1 deg/s performed twice

Chapter 7

CONF & OBDH System

7.1 Configuration

The overall spacecraft configuration is dictated by several requirements that in the design phase imposed particular choices. The main requirements for Juno were [35]:

- **Spin Stability:** The spacecraft needs to spin around the axis identified by the High Gain Antenna (HGA).
- **Spin Axis Alignment:** During the launch phase the spin axis has to be kept aligned in order to avoid deviations.
- **Solar Arrays Positioning:** Due to their large surface area, their position has to be strategically designed in order to enhance the spin stability; an undeployed configuration must be considered to allow for insertion into the launch module.
- **Payload and Sensors Positioning:** It has to be guaranteed the clearness of the scientific instruments and Sensors Field of View (FOV) and pointing.
- **Thrusters Positioning:** They have to be strategically placed in order to avoid the exhaust plume interference with payload and sensors, ensuring the complete three-axis control.
- **Tanks Positioning:** The tanks have to be balanced with respect to the Center of Mass (CM) at any propellant level.
- **Spacing for Subsystems:** Adequate space had to be provided for the proper functioning of all spacecraft subsystems.

7.1.1 Structural Design

Juno's structure has been carefully designed in order to satisfy the requirements expressed above.

The spin stability requirements imposed to have the HGA, identified with the $+z$ body axis, and the major moment of inertia axis, aligned. Furthermore the solar arrays have to be positioned in the spacecraft's X-Y plane to improve angular momentum and optimize stabilization and arrays sun pointing with the constraint of HGA's earth pointing (see Figure A.1a).

Juno's main body features a composite hexagonal structure with a diameter and height both measuring 3.5 m.

Two Main Bulkhead Decks are directly connected to the main body providing the subsystems a flat mounting surface and interconnections. The decks are essential in order to facilitate the thermal management and for a secure attachment of the sensors and instruments (see Figure A.1d and Figure A.4b).

Above the forward deck is mounted the Radiation Vault that ensures the protection to the sensitive electronic components from the challenging Jupiter environment and radiations. It is 1 cm thick and weights approximately 200 kg. Inside the vault, critical components such as the flight computer, power distribution unit, and data storage devices are shielded from the harmful effects of high-energy particles. The radiation vault is positioned right under the HGA in order to exploit it as a thermal shield during the most critical phases of the mission.

7.1.2 Launcher Interface and Launch Configuration

Juno has been launched inside the Atlas V551 two-stage launch vehicle. The spacecraft is enclosed in the Atlas V 5-meter, 20.7-meter long payload fairing (PLF), which is a shell made of two pieces that encapsulates the s/c and the Centaur upper stage booster [2].

Inside there is an all-aluminum forward load reactor (FLR), which centers the PLF around the Centaur upper stage engine and holds the launch vehicle adapter. The FLR also ensures vehicle structural stability and payload shear loading [4].

At launch, Juno's solar arrays are folded around the main body (see Figure Juno A.2), ensuring a compact configuration able to fit in the PLF. The solar arrays began their three minutes long deployment about five minutes after separation (see Figure A.3) which was achieved 54 minutes after launch.

7.1.3 Subsystems Configuration

In this section a brief description of the solutions utilized for Juno's subsystems will be provided.

EPS: As said before the arrays assembly has to be positioned in the X-Y spacecraft's plane in order to better stabilize the spinning. Batteries are mounted on the forward deck in the proximity of the major electronic components and sensors. This solution allows to reduce the length and weight of the electric cables required. The PDDU is located inside the radiation vault to protect the sensible components from the radiations coming from Jupiter.

Propulsion Subsystem: [48] The Main Engine is placed on the Aft deck along the spacecraft z-axis (axis of rotation), this allows the thrust direction to be independent from the rotation of Juno. It has been chosen a single engine, reducing complexity and space required on the decks, to avoid the generation of angular momentum and subsequent process due to a non-perfect thrust alignment.

The 12 RCS thrusters are configured as 4 Rocket Engine Modules on towers with 3 thrusters each. They allow for translation and rotation about all three axes with balanced thrust coupling. The towers are placed along the z-axis with two pointing in the s/c's forward and two in the aft direction; the placement of the towers all serves to increase the angular momentum that can be applied in the x and y directions. On each tower, three thrusters are mounted with two of them pointing lateral (positive and negative x-direction) allowing, thanks to Juno rotation, thrust generation along every x-y plane direction, as well as one pointing axially outward (see Figure A.1e). Additionally, the thrusters must be placed further from the scientific instruments and the solar arrays, reducing possible disturbances due to exhaust plumes.

The propellant tanks (6 in total, 4 for fuel and 2 for oxidizer) are mounted directly on the main body of the spacecraft; they have a spherical shape due to the lower inert mass that this configuration allow. They are placed symmetrically with respect to Juno spin axis in such a way that the centre of mass is aligned to it throughout the mission. The higher mass increases the inertia moment further stabilizing the rotation.

TTMTC Subsystem: [45] The HGA is the TTMTC subsystem component mainly driving the overall space-craft configuration. It requires accurate Earth pointing throughout the mission to ensure communications and data transmission with ground. Aligning its beam to the z-inertia-axis allows to solve this driver saving in propellant required for Attitude Control. An important constraint on the functioning of the antenna is given by the solar arrays employed to facilitate the power generation: this arrangement limits the pointing of the antenna main beam to just +/- 0.25 degrees. The HGA is located above the radiation vault in order to exploit its dish as a thermal shield for the radiation vault (see Figure A.1d).

Next to the HGA, always aligned to the spin axis due to the same Earth pointing requirement, are located the MGA and the FLGA, while on the Aft deck (direction -z) is positioned the ALGA (Figure A.1c).

On the Aft deck is located also the Toroidal-LGA, required for communications while the pointing is off-Earth.

The HGA is located above the radiation vault in order to exploit its dish as a thermal shield for the radiation vault where the TTMTC electronic components such as the TWTAs and the SDSTs are located in order to protect them from the radiations.

AOCS: [41] The main requirement regarding the sensors is the clearness of their FOV. For this reason, the sun sensors, having a FOV of $0^\circ - 60^\circ$, are positioned on the external side of the Front deck, pointing the z-axis, avoiding the HGA to be in their view. They are placed in this position even if because it is the most stable one, allowing to have the sun always in their FOV (see Figure A.1d).

The two star trackers have been modified in order to works under Juno's spinning mode. They are placed on the Front Deck having a clear field of view and avoiding the exhaust plume of the thrusters.

IMUs are positioned inside the radiation vault as they need to be shielded from radiations.

TCS: Due to the wide range environment Juno has to face, both heating (Heaters) and cooling (Louvers) devices have to be present and well designed.

The louvers are especially needed to radiate the heat in the radiation vault coming from the power consumption of the electronic components, therefore they are located on its side (Figure A.1d) and they automatically open or close themselves as requested. As they are completely passive, they satisfy the low power consumption requirement.

The Heaters are needed to heat the temperature sensible components, especially the propellant tanks, the catalyst bed, the Li-ion batteries and the sensors. Each component has its dedicated heater in order to remain always in the right temperature range.

Additionally, the entire s/c surface, included the radiation vault and the HGA, is covered with a MLI blanket that allows for a complete insulation.

The arrays and most of the payload instruments and sensors are individually thermal regulated as they need.

7.1.4 Payload Configuration

The following table gives an overview of all the scientific instruments positioning according for their specific requirement and field of view. In Appendix .1 is shown the positioning of all the scientific instruments.

| Payload | FOV | Requirements | Positioning |
|---------|-----------------------------------------------------------------------------------------------------------------------------------------------------------------------------------------|-------------------------------------------------------------------------------------------------------------------------------------|--------------------------------------------------------------------------------------------------------------------------------------------------------------------------------------------------------------------------------------------------|
| MWR | 6 peripherally mounted antennas, radiometers, and control/calibration electronics with FOV ranging from 12° to 30° | Clear view of Jupiter's atmosphere; avoid interference from the s/c own emissions; minimize shadows from other components | Body of the s/c facing outward |
| MAG | ASC FOVs of 14° by 20° full-angle rectangular pyramids centered on the +Z axes of the ASC frames; FGM FOV of 1° half-angle cone centered on the +Z axis of the corresponding FGM frames | Minimize magnetic interference from other sensors or s/c subsystems | MAG and sensors mounted on an arm extending from the s/c body |
| GS | No traditional FOV, instrument relies on radio tracking through Doppler's effect | HGA pointing towards Earth to ensure gravity measurements | HGA on top of s/c and radio transponder inside the Radiation vault |
| JADE | 4 sensors (3 electron analyzers, 1 ion mass spectrometer) with FOVs of 360° by 90° for electrons and 270° by 90° for ions | Avoid interference from other instruments and s/c body | Sensors distributed around the s/c to provide complete coverage of the particles' distribution |
| JIRAM | 3.5° by 6.0° for the imager | Must be oriented towards Jupiter's poles to capture the auroral activity, avoiding interference from other instruments and s/c body | Side panel of the s/c body |
| JEDI | 12° by 160° FOV divided between 6 sensors with 26.7° look directions | Avoid interference from other instruments and s/c body, minimize background noise due to the s/c own radiation | Instrument deck. 2 sensors are installed to get a 360° coverage perpendicular to the spacecraft spin axis to get complete pitch angle snapshots. The other sensor is parallel to the spin axis to obtain complete sky-views over one spin period |
| WAVES | - | Reduce interference from other s/c systems | Electric dipole antenna mounted aft on the s/c perpendicular to the spin axis; magnetic search coil parallel to the spin axis; receivers in the electronics vault |
| UVS | 6° by 0.05° FOV perpendicular to the spin axis | Avoid interference from other instruments and s/c body | Side of s/c, between solar arrays |
| JunoCam | 18° by 3.4° FOV in the spin plane | Provide a wide view of Jupiter, avoid as much as possible damage from high-energy particles surrounding the planet | Side of the s/c |

Table 7.1: Payload Positioning Rationale. Data retrieved from [28], [41]

7.2 On Board Data Handling Subsystem

The On-Board Data Handling (OBDH) subsystem is a critical component of Juno's spacecraft design and operation, responsible for managing and processing all data generated and received by the spacecraft. It ensures the efficient collection, storage, and transmission of scientific and engineering data, enabling the spacecraft to perform its mission objectives accurately and reliably.

Due to the harsh radiation environment where Juno operates, all the electronics need to be designed to function in extremely high radiation levels, exceeding 10 Mrads. Additionally, these electronics are encased in a titanium radiation vault, which limits the radiation dose to 25 krads, a level that is manageable for the onboard systems [5].

7.2.1 Architecture and Design Rationale

The overall architecture can be defined as a hybrid architecture, incorporating elements of both centralized and distributed systems. In particular, Juno is based on federated bus architecture, where all the devices and processors communicate with the CPU through a share communication channel called bus.

Regarding the centralized aspects of the system, Juno's OBDH is provided with a Central Processing Unit (CPU), which manages the overall spacecraft operations and executes the commands, and a central data storage (through solid-state recorders SSRs [36]) for all the data collected by sensors and scientific instruments before transmitting back to Earth. This guarantees high reliability, as data monitoring and control is simplified by the fact that all the data traffic passes in a single point.

Instead, regarding the typical characteristics of a distributed architecture, each scientific instrument in Juno's probe has its own dedicated processor, which handles data collection, initial processing, and compression autonomously. This distribution of processing tasks helps to manage the high data throughput and allows instruments to operate semi-independently. In particular, the scientific instruments are connected to the CPU through an RS-422 bus, which guarantees high speed data transfer. Furthermore, all the subsystems communicate through a MIL-STD-1553 bus. In this way, deterministic transmission can be ensured, reducing troubleshooting time. In addition, the distributed processing capability allows the spacecraft to perform many operations autonomously, reducing reliance on real-time commands from Earth due to communication delays, crucial for a deep space mission such as Juno.

7.2.2 Components

The Command and Data Handling (C&DH) system is built on two redundant, single-fault tolerant units. Each C&DH unit features a RAD750 flight processor and cPCI bus connected to 3U cards, with the exception of the DTCI (Data, Telemetry & Command Interface) card which uses a 6U format. The DTCI card contains the interfaces for not only the command and data interfaces to the instruments, but also provides 32 Gbits of science data storage (base 2, at end-of-life). It also provides additional 8 Gbits for EDAC (Error Detection and Correction), used to implement error detection and correction mechanisms, which help ensure the integrity and reliability of stored data by correcting errors caused by radiation and other space-related factors.

This storage capacity has proven sufficient for both minimum and maximum science orbit downlink data needs and can handle representative stress cases that consider data re-transmission and prioritization [33].

CPU

The RAD750 is a radiation-hardened single-board computer produced by BAE Systems Electronics, Intelligence & Support and it is designed for use in the high-radiation environments encountered by satellites and spacecraft.

The RAD750 is characterized by 256 MB of NVM (Non-Volatile Memory) flash memory, that can retain stored information even after power is removed and 128 MB of DRAM (Dynamic Random-Access Memory) local memory, that stores each bit of data in a memory cell. It supports a total instrument throughput of 100 Mbps, which exceeds the requirements for the payload. It has a core clock speed ranging from 110 to 200 MHz and is capable of processing at 266 MIPS or higher [68].

The CPU can be equipped with an extended L2 cache to enhance performance, indeed larger caches provide better hit rates even if they have longer latency [66]. Other main features of the CPU can be retrieved from the data-sheet presented Table 5 in Appendix .2.

Instruments Processors

Juno's scientific instruments have their own processors to enable real-time analysis and autonomous operation, allowing the instruments to make immediate decisions without waiting for commands from Earth. These processors handle error correction and instrument-specific tasks, ensuring data integrity and optimal performance. Additionally, they support efficient data processing and parallel functionality, which maximizes scientific output and enhances overall mission efficiency and redundancy. All the electronics units for each instrument are placed in the radiation vault, as always to minimize the total radiation dose they need to withstand.

In Table 7.2 are briefly described the processors and the Command & Data Unit for Juno's scientific instruments.

| Instrument | C&DH Unit |
|------------|---------------------------------------------------------------------------------------------------------------------------------------------------------------------------------------------------------------------------------------------------------------------------------------------------------------------------------------------------------------------------------------|
| MWR | 8051 microcontroller based system that processes and executes spacecraft commands and telemetry, controls science and housekeeping data provided by MWR |
| JEDI | 3 16-bit 10MIPS processors implemented on RTAX2000 FPGAs |
| JADE | The Instrument Processor Board (IPB) runs the flight software, executes spacecraft commands, and manages data collection, formatting, and transmission. Memory: 128 KB PROM for the boot code; 512 KB EEPROM for Flight Software; 4 MB SRAM used for Code and Data when the software is executing [42] |
| JIRAM | The instrument controller sends science data and telemetry to the spacecraft and receives commands for instrument operations and timing synchronization data from the spacecraft. It also regulates all functions of the instrument, controlling the observation sequences and commanding the various electronics boards |
| UVS | The UVS controller uses an Intel 8-bit 8051 microcontroller implemented in a radiation-hardened FPGA. Memory: 32 kB PROM, 128 kB EEPROM, 32 kB SRAM, and 128 kB of acquisition memory [19] |
| WAVES | The Waves Data Processing Unit (DPU), based on the Y180s core, employs two radiation-tolerant FPGAs for data management, applying digital signal processing techniques, data compression, and interfacing with spacecraft systems. Memory: a 32 kB programmable ROM stores the Y180s boot code, while a 2 MB RAM holds the operating system, applications, and telemetry buffers [34] |
| JunoCam | 1 Actel RTSX FPGA which enables to capture and transmit high-quality images [21] |

Table 7.2: Scientific Instruments Command & Data Handling Unit

The Gravity Science experiments rely on the spacecraft's main C&DH system and the X-band and Ka-band communication systems to measure Doppler shifts in radio signals [58]. Additionally, the MAG instrument relies solely on the main C&DH system, transmitting measurements directly through the RS-422 link.

BUS

The main functions of the spacecraft on-board bus are the acquisition of data from sensors, instruments and all the other subsystems, the transmission to the control computer and the distribution of the time information [17].

Juno's OBDH, due to its hybrid architecture, relies on two different onboard command and control buses: the MIL-STD-1553B bus for the communications between each subsystem and the central computer and the RS-422 bus to exchange data and commands between each scientific instrument and the central computer.

MIL-STD-1553B Bus It is a widely used standard in space systems for multiplexed serial data bus communications. Communication occurs on a single transmission line using time division multiplexing, allowing different units to communicate at distinct times. Optional redundant transmission lines can be incorporated into a 1553 system to enhance fault tolerance. The bus operates at a fixed data rate of 1 Mbit/s and is typically implemented as a dual standby redundant architecture [69].

MIL-STD-1553B bus has been selected mainly for its robustness, which is crucial due to the harsh radiation environment in which Juno operates. In addition, its high accuracy in data transmission, obtained through error-checking mechanisms, enables real-time operational performances. Due to the relatively low-speed data transfer, it has been used only for the crucial communications between the subsystems and the central computer.

RS-422 Bus RS-422 is a serial data bus communication standard that use differential balanced signals, which guarantees reliable point-to-point communications. It is based on twisted-pair wire from transmitters to receivers. In this way reduces the susceptibility to noise and improves the signal integrity for long distances. RS-422 drivers can transmit to up to 10 receivers, guaranteeing high data transfer rates (up to 10 Mb/s).

RS-422 has been selected for the communications between scientific instruments and the central processor for its high-speed data transfer. In fact, scientific instruments need high speed data transfer rates due to the large volume of data they have to transmit, but also because typically they need to perform real-time data processing. This enables to perform autonomous operations, which are crucial due to the distance between Juno and the ground station which implies a communication delay that makes impossible a ground-based control of the operations. In addition, high-speed data transfer allows for more efficient use of onboard storage and downlink opportunities.

7.2.3 Reverse Sizing

For this study, only the components of the service module are sized. The scientific instruments and their data processing are assumed to be given by the scientist and only their final data output has to be accounted for in the OBDH design. This means they are viewed as blackboxes similar to the other components on Juno. This does not include the science data storage, which belongs to the service module and is therefore estimated at the end of this section.

The throughput of Juno's components and instruments is given in Table 7.4. The total throughput per phase is given as the sum of all separate throughputs of active instruments:

$$KIPS_{tot} = \sum_i k_i \times KIPS_i. \quad (7.1)$$

To get the required ROM memory, the number of words for all subsystem codes have to be summed up and multiplied by 32 bit/word, as the RAD750 is a 32 bit processor:

$$ROM = \frac{\sum Code \times 32 \text{ bit/word}}{8000 \text{ bit/kB}}. \quad (7.2)$$

The RAM memory can be computed in a similar way, this time including data and code:

$$RAM = \frac{\sum (Code + Data) \times 32 \text{ bit/word}}{8000 \text{ bit/kB}}. \quad (7.3)$$

The total processor memory is just the sum of ROM and RAM.

Results

Everything mentioned so far gets a safety margin of 400 %.

To determine the operating modes which size the onboard computer system, the most demanding modes are: science collection, maneuvering and communication. Looking at their respective subsystems involved, the most demanding mode in terms of throughput is the maneuvering, in terms of required program storage and memory science collection is the most demanding. The results are shown in Table 7.3, where they are compared to the actual hardware that flew on Juno.

| | Throughput [kIps] | ROM [kb] | RAM [kb] |
|----------|-------------------|----------|----------|
| Sizing | 1133 | 529 | 1131 |
| Margined | 5666 | 2646 | 5656 |
| Real | 266 000 | 256 000 | 128 000 |

Table 7.3: Data Budget for the OBDH subsystem

These results are estimated using the compiled data shown in Table 7.4. Where by comparing the acquisition frequency and the corresponding throughput an estimation for OBDH system requirements can be found. It becomes apparent that the actual hardware in Juno is massively oversized (by a factor of almost 100 for the ROM). Even though the engineers could have used a less capable, cheaper architecture, they chose this processor probably because it was flight proven in previous missions like the *Mars Reconnaissance Rover* or the *Kepler space telescope*. Furthermore, considering the demands on radiation hardening and reliability there was likely no simpler alternative available on the market that fulfilled these requirements.

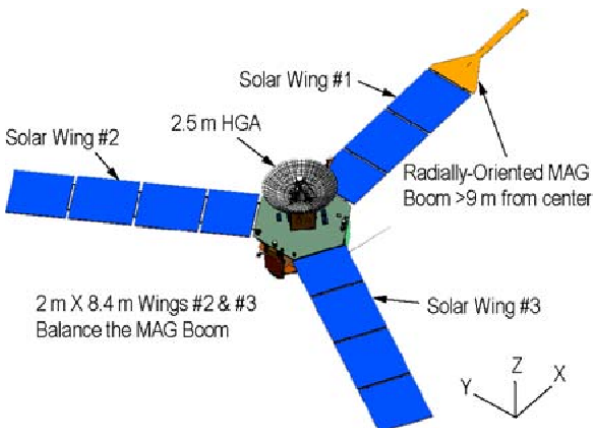
| Component | Number | Code [words] | Data [words] | Through-put [KIPS] | Frequency [Hz] | Acquisition frequency [Hz] | KIPS |
|--------------------------|--------|--------------|--------------|--------------------|----------------|----------------------------|----------|
| ADCs | | | | | | | |
| Thruster control | 12 | 600 | 400 | 1,2 | 2 | 1 | 7,2 |
| Star tracker | 2 | 2000 | 1500 | 2 | 0,01 | 1 | 400 |
| IMU | 2 | 800 | 500 | 9 | 10 | 10 | 18 |
| Sun sensor | 2 | 500 | 100 | 1 | 1 | 1 | 2 |
| Kintematic integration | 1 | 2000 | 200 | 15 | 10 | 10 | 15 |
| Error determination | 1 | 1000 | 100 | 12 | 10 | 10 | 12 |
| Attitude determination | 1 | 15000 | 3500 | 150 | 10 | 10 | 150 |
| Attitude control | 1 | 24000 | 4200 | 60 | 10 | 10 | 60 |
| Complex Ephemeris | 1 | 3500 | 2500 | 4 | 0,5 | 1 | 8 |
| Orbit propegation | 1 | 13000 | 4000 | 20 | 1 | 1 | 20 |
| | Total: | 72300 | 23500 | | | Total: | 692,2 |
| PS | | | | | | | |
| Tank | - | - | - | - | - | - | - |
| Main engine | 1 | 1200 | 1500 | 5 | 0,1 | 0,1 | 5 |
| Tank control valve | 2 | 800 | 1500 | 5 | 0,1 | 0,1 | 10 |
| Tank pressure sensor | 8 | 800 | 1500 | 5 | 0,1 | 0,1 | 40 |
| | Total: | 9200 | 16500 | | | Total: | 55 |
| EPS | | | | | | | |
| Solar panels | 3 | - | - | - | - | - | - |
| Batteries | 2 | - | - | - | - | - | - |
| Cables and harness | 1 | - | - | - | - | - | - |
| Power voltage control | 1 | 1200 | 500 | 5 | 1 | 0,1 | 0,5 |
| Power current control | 1 | 1200 | 500 | 5 | 1 | 0,1 | 0,5 |
| | Total: | 2400 | 1000 | | | Total: | 1 |
| TCS | | | | | | | |
| Heaters | 38 | 800 | 1500 | 3 | 0,1 | 0,1 | 114 |
| | Total: | 30400 | 57000 | | | Total: | 114 |
| TTMTC | | | | | | | |
| X-Band HGA | 1 | - | - | - | - | - | - |
| S-Band HGA | 1 | - | - | - | - | - | - |
| Transponders (Uplink) | 3 | 1000 | 4000 | 7 | 10 | 10 | 21 |
| Transponders (Downlink) | 3 | 1000 | 2500 | 3 | 10 | 10 | 9 |
| | Total: | 6000 | 19500 | | | Total: | 30 |
| SYSTEM | | | | | | | |
| I/O Device Handlers | 1 | 2000 | 700 | 50 | 5 | 1 | 10 |
| Test and diagnostic | 1 | 700 | 400 | 0,5 | 0,1 | 1 | 5 |
| Math utilities | 1 | 1200 | 200 | 0,5 | 0,1 | 1 | 5 |
| Executive | 1 | 3500 | 2000 | 60 | 10 | 10 | 60 |
| Run time kernel | 1 | 8000 | 4000 | 60 | 10 | 10 | 60 |
| Complex autonomy | 1 | 15000 | 10000 | 20 | 10 | 10 | 20 |
| Fault detection monitors | 1 | 4000 | 1000 | 15 | 5 | 1 | 3 |
| Fault correction | 1 | 2000 | 10000 | 5 | 5 | 10 | |
| | Total: | 36400 | 28300 | | | Total: | 163 |
| PAYLOAD | | | | | | | |
| MAG | 2 | 1000 | 2500 | 0,197 | 0,5 | 0,5 | 0,394 |
| JIRAM | 1 | 1000 | 2500 | 2,324 | 0,5 | 0,5 | 2,324 |
| JADE | 1 | 1000 | 2500 | 0,29 | 0,5 | 0,5 | 0,29 |
| MWR | 1 | 1000 | 2500 | 0,723 | 0,5 | 0,5 | 0,723 |
| GS | 1 | | | - | - | - | - |
| JEDI | 1 | 1000 | 2500 | 0,29 | 0,5 | 0,5 | 0,29 |
| WAVES | 1 | 1000 | 2500 | 0,723 | 0,5 | 0,5 | 0,723 |
| UVS | 1 | 1000 | 2500 | 0,29 | 0,5 | 0,5 | 0,29 |
| JUNO CAM | 1 | 1000 | 2500 | 0,723 | 0,5 | 0,5 | 0,723 |
| | Total: | 9000 | 22500 | | | Total: | 5,757 |
| | | | | | | Total through-put: | 1060,957 |

Table 7.4: Reverse Sizing Results

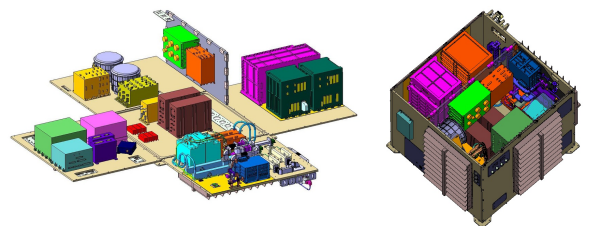
.1 Appendix A: Configuration Figures

In this section are reported all the figures necessary to better understand Juno internal and external configuration.

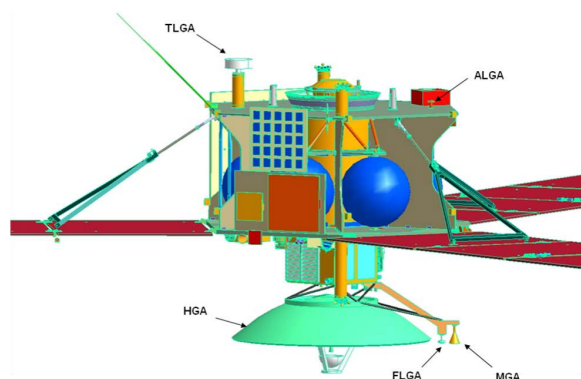
Subsystems



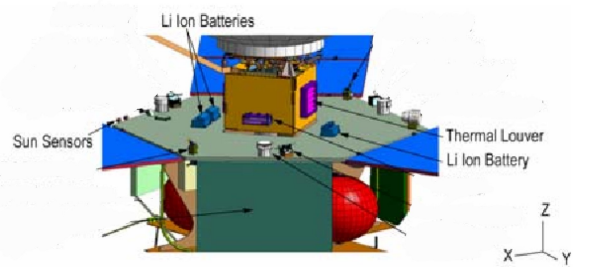
(a) Solar Arrays and HGA assembly



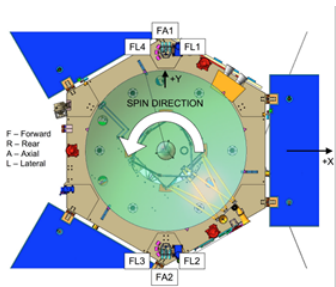
(b) Radiation Vault



(c) Antennas Positioning



(d) Sun Sensors, Batteries, Louvers and Vault Position



(e) Thrusters Positioning

Figure A.1: Subsystems Components Positioning

Launch Configuration and Arrays Deployment

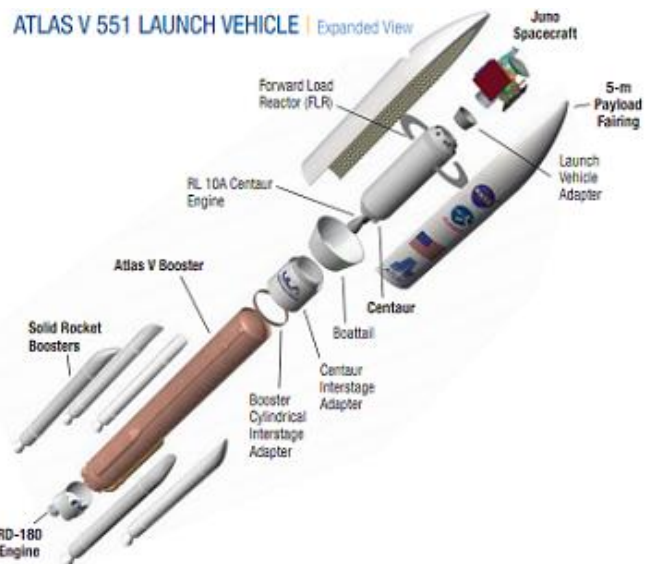


Figure A.2: Juno Launch Configuration

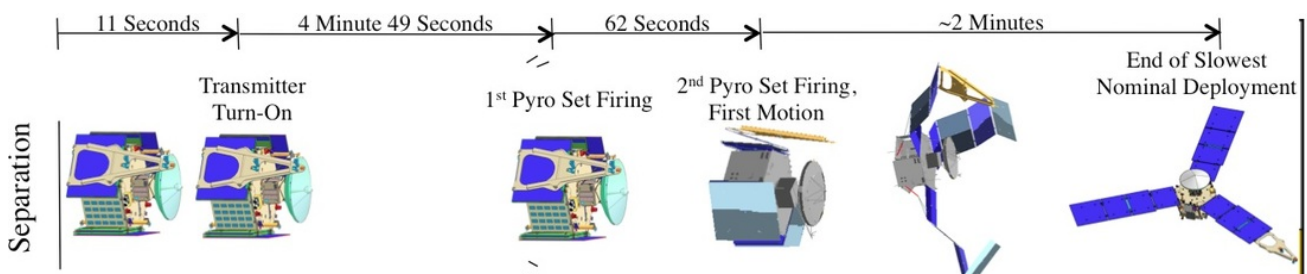
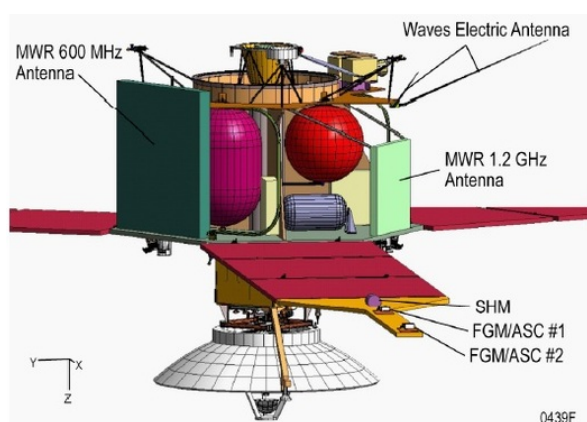
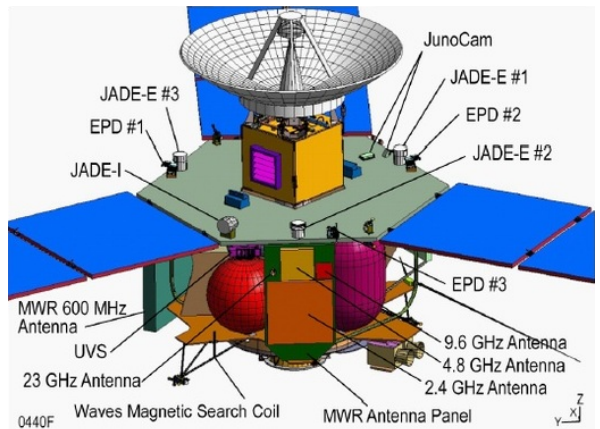


Figure A.3: Arrays Deployment

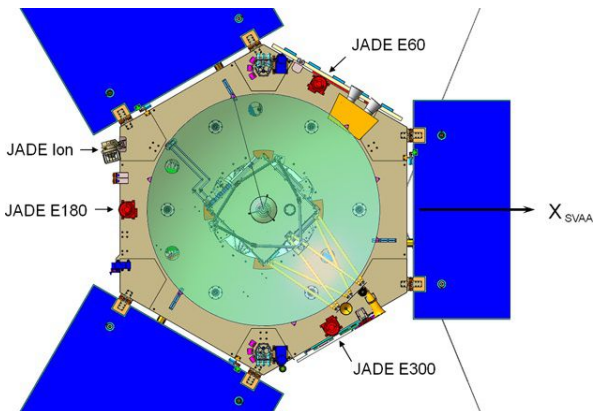
Payload



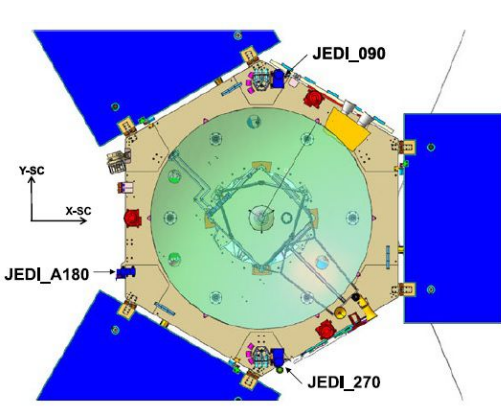
(a) Scientific Instrument Configuration: internal view



(b) Scientific Instrument Configuration: external view



(c) JADE Instrument Configuration

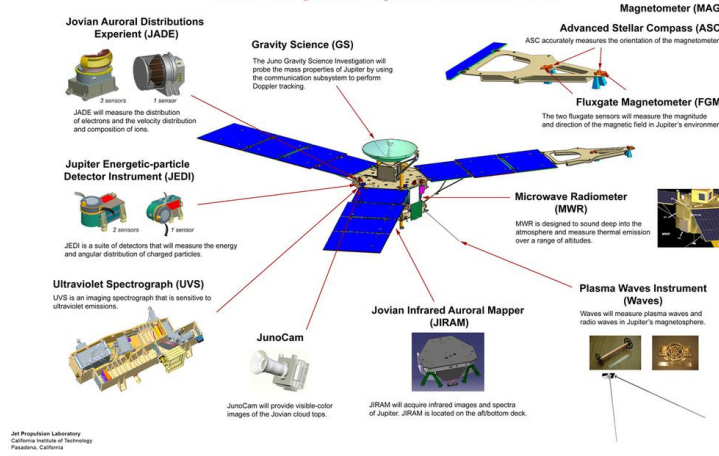


(d) JEDI Instrument Configuration

National Aeronautics and Space Administration



Juno Payload System Overview



(e) Juno Scientific Payload Configuration

Figure A.4: Payload Positioning

.2 Appendix B: RAD750

In this Appendix we reported the data-sheet of the Central Processor Unit (CPU) of Juno's spacecraft retrieved from [5]. It is quite important to notice the extremely high radiation hardness of this particular processor, represented by the high Total Ionizing Dose capable to withstand and the low probability of Single Event Upset (error caused by a single ionized particle hitting the electronic component).

| | |
|----------------------------|-----------------------------------------------------------------------------------|
| Power Supply | 2.5 V |
| Power dissipation | 5 W |
| Temperature range | -55 °C to +125 °C |
| Radiation hardness | Total Ionizing Dose: 200 Krad (Si) SEU: 1E-10 upsets/bit-day Latchup:Immune |
| Mean Time Between Failures | > 4.3M hours |

Table 5: RAD750 processor data-sheet

Bibliography

- [1] URL: <https://satsearch.co/products/aerojet-rocketdyne-mr-111c>.
- [2] National Aeronautics and Space Administration. *Juno Launch Press Kit*. URL: https://www.jpl.nasa.gov/news/press_kits/JunoLaunch.pdf.
- [3] European Space Agency. *Concurrent Design Facility Studies Standard Margin Philosophy Description*. 2017.
- [4] *Atlas V Juno Mission Overview Brochure*. URL: https://www.ulalaunch.com/docs/default-source/news-items/av_juno_mob.pdf.
- [5] BAE SYstems. *RAD750 datasheet*. 2002. URL: https://web.archive.org/web/20090326020946/http://www.aero.org/conferences/mrqw/2002-papers/A_Burcin.pdf.
- [6] Bhandari, Pradeep. “Effective Solar Absorptance of Multilayer Insulation”. In: *SAE International Journal of Aerospace* 4.1 (July 2009), pp. 210–218. DOI: <https://doi.org/10.4271/2009-01-2392>.
- [7] Andreea Boca et al. “A Data-Driven Evaluation of the Viability of Solar Arrays at Saturn”. In: *IEEE Journal of Photovoltaics* 7.4 (2017), pp. 1159–1164. DOI: [10.1109/JPHOTOV.2017.2698499](https://doi.org/10.1109/JPHOTOV.2017.2698499).
- [8] S. J. Bolton et al. *The juno mission - space science reviews*. Nov. 2017. URL: <https://link.springer.com/article/10.1007/s11214-017-0429-6>.
- [9] C.D. Brown. *Elements of Spacecraft Design*. AIAA Education Series. American Institute of Aeronautics & Astronautics, 2002. ISBN: 9781600860515. URL: <https://books.google.it/books?id=mTSSMhcmVbkC>.
- [10] Charles D. Brown. *Elements of spacecraft design / Charles D. Brown*. eng. AIAA education series. Reston, VA: American Institute of Aeronautics and Astronautics, Inc., 2002. ISBN: 1563475243.
- [11] Robert Cataldo. “Spacecraft Power System Considerations for the Far Reaches of the Solar System”. In: *Outer Solar System: Prospective Energy and Material Resources*. Ed. by Viorel Badescu and Kris Zacny. Cham: Springer International Publishing, 2018, pp. 767–790. ISBN: 978-3-319-73845-1. DOI: [10.1007/978-3-319-73845-1_16](https://doi.org/10.1007/978-3-319-73845-1_16). URL: https://doi.org/10.1007/978-3-319-73845-1_16.
- [12] J. E. P. Connerney et al. “The Juno Magnetic Field Investigation”. In: *Space Science Reviews* 213.1 (Nov. 2017), pp. 39–138. ISSN: 1572-9672. DOI: [10.1007/s11214-017-0334-z](https://doi.org/10.1007/s11214-017-0334-z). URL: <https://doi.org/10.1007/s11214-017-0334-z>.
- [13] Stephen F Dawson, Paul Stella, and William McAlpine. “JUNO Photovoltaic Power at Jupiter”. In: *10th International Energy Conversion Engineering Conference*. 2012. DOI: [10.2514/6.2012-3833](https://doi.org/10.2514/6.2012-3833).
- [14] Randy Dodge and Mark A. Boyles. *Key and driving requirements for the Juno Payload of instruments*. 2007. URL: <https://hdl.handle.net/2014/40566>.
- [15] Dodge, Randy and Boyles, Mark A. “Key and driving requirements for the Juno Payload of instruments”. Version V2. In: (2007). DOI: [2014/40566](https://hdl.handle.net/2014/40566). URL: <https://hdl.handle.net/2014/40566>.
- [16] *DSN Telecommunications Link Design Handbook*. Nov. 2000. URL: <https://deepspace.jpl.nasa.gov/dsndocs/810-005/>.
- [17] European Space Agency. *Overview of the spacecraft onboard command and control bus*. URL: https://www.esa.int/Enabling_Support/Space_Engineering_Technology/Onboard_Computers_and_Data_Handling/Overview_of_the_spacecraft_onboard_command_and_control_bus.
- [18] Georg Siebes Gajana C. Birur. “Spacecraft Thermal Control”. In: (2001).
- [19] G. R. Gladstone, S. C. Persyn, J. S. Eterno, et al. “The Ultraviolet Spectrograph on NASA’s Juno Mission”. In: *Space Science Reviews* 213 (2017), pp. 447–473. DOI: [10.1007/s11214-014-0040-z](https://doi.org/10.1007/s11214-014-0040-z).

- [20] *HANDLING AND STORAGE OF NITROGEN TETROXIDE*. May 1963.
- [21] Candice J. Hansen, Michael A. Caplinger, Andrew Ingersoll, et al. “Junocam: Juno’s Outreach Camera”. In: *Space Science Reviews* 213 (2017), pp. 475–506. DOI: 10.1007/s11214-014-0079-x. URL: <https://doi.org/10.1007/s11214-014-0079-x>.
- [22] Elizabeth Howell. *Juno is Powered by the Sun, and That’s a Big Deal — smithsonianmag.com*. <https://www.smithsonianmag.com/air-space-magazine/juno-powered-sun-and-s-big-deal-180959691/>.
- [23] <https://www.jpl.nasa.gov/>. *Juno - Jupiter Missions - NASA Jet Propulsion Laboratory — jpl.nasa.gov*. <https://www.jpl.nasa.gov/missions/juno>.
- [24] Southwestern Research Institute. *Mission Juno Instruments*. 2012. URL: https://web.archive.org/web/20120426062922/http://missionjuno.swri.edu/HTML/junospacecraft_instruments/50.
- [25] J. Connerney, P. Lawton, S. Kotsiaros, M. Herceg. *The Juno Magnetometer (MAG) Standard Product Data*. URL: <https://pds-ppi.igpp.ucla.edu/data/JNO-J-3-FGM-CAL-V1.0/DOCUMENT/SIS-addendum.pdf>.
- [26] Jennie R. Johannessen, Thomas A. Pavlak, and John J. Bordi. *Initial Jupiter Orbit Insertion and Period Reduction Maneuver Plans for Juno*. Version V1. 2017. DOI: 2014/47555. URL: <https://hdl.handle.net/2014/47555>.
- [27] JPL. *Juno Press Kit*. URL: https://www.jpl.nasa.gov/news/press_kits/juno/spacecraft/ (visited on 05/03/2024).
- [28] *JUNO MAG Instrument Kernel*. Accessed: 2024-05-26. URL: https://naif.jpl.nasa.gov/pub/naif/JUNO/kernels/ik/juno_mag_v03.ti.
- [29] *Juno Mission*. Accessed: May 9, 2024. URL: <https://spaceflight101.com/juno/>.
- [30] *Juno Mission to Jupiter - eoPortal — eoportal.org*. <https://www.eoportal.org/satellite-missions/juno>.
- [31] *Juno Mission Trajectory Design 2013; Juno — spaceflight101.com*. <https://spaceflight101.com/juno/juno-mission-trajectory-design/>.
- [32] *Jupiter orbit insertion press kit*. URL: https://www.jpl.nasa.gov/news/press_kits/juno.
- [33] Bill Kurth. “Juno Spacecraft Description”. In: (2012).
- [34] W. S. Kurth, G. B. Hospodarsky, D. L. Kirchner, et al. “The Juno Waves Investigation”. In: *Space Science Reviews* 213 (2017), pp. 347–392. DOI: 10.1007/s11214-017-0396-y.
- [35] Michèle Lavagna. *Lecture notes in Space Systems and Spacecraft Operations*. Politecnico di Milano - Aerospace Science & Technology Dept. 2024.
- [36] LaVallee, David and Mauk, Barry and Haggerty, Dennis and Schlemm, Charles and Paranicas, Chris. “Science planning and commanding for Jupiter”. In: *2017 IEEE Aerospace Conference*. 2017. DOI: 10.1109/AERO.2017.7943982.
- [37] Leonardo. *SATCAT - A-STR*. URL: <https://www.satcatalog.com/component/a-str/>.
- [38] M.M. Finckenor, D. Dooling. *Multilayer Insulation Material Guidelines*. NASA, 1999. URL: <https://ntrs.nasa.gov/api/citations/19990047691/downloads/19990047691.pdf>.
- [39] *Margin philosophy for science assessment studies*. 1. European Space Research and Technology Centre. June 2012.
- [40] Stuart Stephens Marty Brennan. “Juno attitude and Orbit Geometry”. In: (2017-05-31).
- [41] Steve Matousek. “The Juno New Frontiers Mission”. In: *International Astronautical Congress*. 2005. URL: <https://hdl.handle.net/2014/37654>.
- [42] D. J. McComas, N. Alexander, F. Allegrini, et al. “The Jovian Auroral Distributions Experiment (JADE) on the Juno Mission to Jupiter”. In: *Space Science Reviews* 213 (2017), pp. 547–643. DOI: 10.1007/s11214-013-9990-9.
- [43] Minco. *Satellite All-Polyimide Thermofoil™ Heaters*. URL: <https://www.minco.com/catalog/?catalogpage=product&cid=satellite-heaters&id=HAP6731>.
- [44] *Mission Juno — missionjuno.swri.edu*. <https://www.missionjuno.swri.edu/>.

- [45] Ryan Mukai et al. “DESCANSO Design and Performance Summary Series Article 16: Juno Telecommunications”. In: *Jet Propulsion Laboratory, California Institute of Technology* (2017). Revision A: Addition of Operations from Early Cruise through First Months of Operation, Five Science Orbits (Sept. 2012–May 2017).
- [46] Nammo Space UK LEROS 1b apogee engine Nammo — nammo.com. <https://www.nammo.com/product/nammo-space-leros-1b-apogee-engine/>.
- [47] Rick Nybakken. “The Juno mission to Jupiter — A pre-launch update”. In: *2011 Aerospace Conference*. 2011, pp. 1–8. DOI: 10.1109/AERO.2011.5747272.
- [48] Thomas A. Pavlak et al. “Maneuver Design for the Juno Mission: Inner Cruise”. In: *AIAA 2014-4149. Session: Flight Dynamics Operations and Spacecraft Autonomy*. 2014. DOI: <https://doi.org/10.2514/6.2014-4149>.
- [49] Thomas A. Pavlak et al. *Maneuver design for the Juno mission: inner cruise*. Version V2. 2014. DOI: 2014/45626. URL: <https://hdl.handle.net/2014/45626>.
- [50] M.P. Petkov and J.D. Vacchione. URL: https://www.ngdc.noaa.gov/stp/satellite/anomaly/2010_sctc/docs/3-2_MPetkok.pdf (visited on 05/03/2024).
- [51] S.A.Jerebets. “Gyro Evaluation for the Mission to Jupiter”. In: (). URL: <https://ieeexplore.ieee.org/stamp/stamp.jsp?tp=&arnumber=4161538>.
- [52] SGL Carbon. *SGL Group ceramic component reaches Jupiter’s orbit in Juno spacecraft*. URL: <https://www.sglcarbon.com/en/newsroom/news/press-report/sgl-group-ceramic-component-reaches-jupiters-orbit-in-juno-spacecraft/>.
- [53] Sierra Nevada Corporation. *Sierra Nevada Corporation Helps Juno Keep Cool and Science On*. URL: <https://www.sncorp.com/news-archive/sierra-nevada-corporation-helps-juno-keep-cool-and-science-on/>.
- [54] Sierra Nevada Corporation. *Spaceflight Hardware Catalog*. URL: https://satsearch.s3.eu-central-1.amazonaws.com/datasheets/satsearch_datasheet_m6tevz_sierra-space_all-products.pdf?X-Amz-Algorithm=AWS4-HMAC-SHA256&X-Amz-Credential=AKIAJLB7IRZ54RAMS36Q%2F20240506%2Feu-central-1%2Fs3%2Faws4_request&X-Amz-Date=20240506T150858Z&X-Amz-Expires=86400&X-Amz-Signature=91fc7c08b896368426862ce65b79553d78562f6626c3ad0777a731b9c71cefca&X-Amz-SignedHeaders=host.
- [55] Marshall Smart et al. “Performance Testing of Yardney Li-Ion Cells and Batteries in Support of Future NASA Missions”. In: *7th International Energy Conversion Engineering Conference*. DOI: 10.2514/6.2009-4626. URL: <https://arc.aiaa.org/doi/abs/10.2514/6.2009-4626>.
- [56] Marshall C. Smart et al. “The use of lithium-ion batteries for JPL’s Mars missions”. In: *Electrochimica Acta* 268 (2018), pp. 27–40. ISSN: 0013-4686. DOI: <https://doi.org/10.1016/j.electacta.2018.02.020>. URL: <https://www.sciencedirect.com/science/article/pii/S0013468618303025>.
- [57] SolarQuotes. *NASA Chose Solar Power Over Nuclear for Juno Space Probe*. URL: <https://www.solarquotes.com.au/blog/nasa-chose-solar-power-nuclear-juno-space-probe/>.
- [58] Spaceflight101. *Juno Instrument Overview*. <https://spaceflight101.com/juno/instrument-overview/>. 2024.
- [59] Spectrolab. *28.3% Ultra Triple Junction (UTJ) Solar Cells*. URL: <https://www.spectrolab.com/DataSheets/TNJCell/utj3.pdf> (visited on 05/16/2024).
- [60] Stuart K. Stephens. “The Juno mission to Jupiter: Lessons from cruise and plans for orbital operations and science return”. In: *2015 IEEE Aerospace Conference*. 2015, pp. 1–20. DOI: 10.1109/AERO.2015.7118972.
- [61] George P. Sutton and Oscar Biblarz. *Rocket Propulsion Elements*. 9th. Wiley, 2016.
- [62] JPL SwRI. *Juno’s View of Jupiter’s Southern Lights*. URL: <https://www.nasa.gov/image-article/junos-view-of-jupiters-southern-lights/> (visited on 04/24/2024).
- [63] JPL SwRI. *PIA22177: Slices of Jupiter’s Great Red Spot*. URL: <https://photojournal.jpl.nasa.gov/catalog/PIA22177> (visited on 04/24/2024).
- [64] Tech Briefs. *Development of a Precision Thermal Doubler for Deep Space*. URL: <https://www.techbriefs.com/component/content/article/23415-npo47296>.

- [65] Joseph D. Vacchione et al. *Telecommunications antennas for the Juno Mission to Jupiter*. Version V1. 2012. DOI: 2014/45005. URL: <https://hdl.handle.net/2014/45005>.
- [66] Wikipedia. *CPU Cache*. URL: https://en.wikipedia.org/wiki/CPU_cache#Multi-level_caches.
- [67] Wikipedia. *Phase-shift keying*. URL: https://en.wikipedia.org/wiki/Phase-shift_keying (visited on 04/05/2024).
- [68] Wikipedia. *RAD750*. URL: <https://en.wikipedia.org/wiki/RAD750>.
- [69] Wikipedia contributors. *MIL-STD-1553*. 2024. URL: <https://en.wikipedia.org/wiki/MIL-STD-1553>.